

Micro-scale vaccine bioprocessing of a  
Japanese Encephalitis Virus Vaccine

Michael David Hughson

University College London

Engineering Doctorate in Biochemical  
Engineering & Bioprocess Leadership

I, Michael David Hughson confirm that the work presented in this thesis is my own.

Where information has been derived from other sources, I confirm that this has been indicated in the thesis.



---

# 1 Abstract

---

Japanese Encephalitis (JE) is the most common form of viral encephalitis in the world, caused by the Japanese Encephalitis virus (JEV), it is responsible for around 10,000 deaths a year whilst many more are left with long term neurological sequelae and disability. This work sought to use small-scale development techniques alongside high-throughput methodologies to explore and develop selected processing techniques. Formaldehyde inactivation of JEV was characterised and optimised through the use of Design of Experiments screening techniques where temperature, time and formaldehyde concentration were found to be key factors in antigen loss. Glycine and to a lesser extent sorbitol were found to have positive effects as stabilisers during inactivation at different stages of the process. Four anion exchange resins were screened at micro-scale, with the help of an ELISA method evaluated for high-throughput screening, for their potential to replace sucrose gradient purification as the principle purification step of the process. Although Q Sepharose FF was eventually chosen for scale-up studies, the transition of method and recovery rates from batch bind micro-plate studies to 1 mL column scale proved difficult. Yet it was observed that pre-treatment of feed with formaldehyde and glycine could increase JEV antigen recovery rates in flow-through mode chromatography, thought to be due to enhanced stability of the virus particles.

# Valneva Scotland Ltd

---

## Statement of Involvement and Contribution

Valneva Scotland Ltd provided support in the following areas throughout the duration of the project;

1. Determination of the project scope, goal and objectives
2. Financial support for the duration of the project for bench fees, travel, consumables, equipment and student stipend
3. Provision of raw materials inclusive of but not limited to;

JEV WWSB, Vero WCB, anti JEV polyclonal antisera

4. Analytical methodology and manufacturing process documentation
5. Training and support in analytical and process methods
6. Scientific / technical overview and direction

Valneva Scotland accepts no liability for the content of this document, or for the consequences of any actions taken on the basis of the information provided,

Any views or opinions presented in this document are solely those of the author and of University College London and do not necessarily represent those of the company.

# Acknowledgements

---

My time as part of UCL Biochemical Engineering has been the most interesting, rewarding and fulfilling experience of my life. Indeed, I am unlikely to experience anything like it again, which, granted, has its bonuses as well as its many saddening drawbacks. Being a doctoral researcher in central London in a fantastic department at a top institution is an unparalleled opportunity, the challenge and enjoyment of which can scarcely be conveyed by words. Yet, the journey is nothing without the love, support, friendship and guidance of those around you, many of whom share in these trials and tribulations. I doubt any person could survive the endeavour without such warmth by their side, in fact why would one choose to? I honestly believe they are the real reason for these undertakings.

First and foremost thank you to my family, Mum, Andrew, Leanora and Steven. Never doubting, always encouraging, I owe you so much. Dad, every important decision of mine is made thinking of you. You know I love you all dearly, but I don't say it near as often as I should.

Thanks to my long suffering (Leith)housemates Matt and Chris whose loyalty, affection, understanding and humour could cure all ills.

Thank you Tarit, I am honoured to be the first of what I envisage to be many beneficiaries of your counsel (though still somewhat surprised you took on more after being burdened with me). Your knowledge, encouragement, praises and pushing got me through. Thank you Nigel for never being too busy even though I knew you were; the SS Biochem Eng is certainly in safe hands with you at the helm. Thanks to rest of UCL Biochemical Engineering for making it such a great place to spend the years, Gareth, Brian, Ludmila, Hayley, Jana, Paula & Nick and to the rest of the academic, technical and admin guys as well as to those that have moved on, like Andy & Nav.

Much gratitude to the wonderful people at Valneva from my time there, in Livingston: Clare, David, Kirtsen, Ann Louise, Kirsty, Tony, Matt, Peter; and in Vienna: Michi, Mario, Robert, Barbara, Ola, Heidi, Martin. Donald, I have long had visions of you sat at your computer reading my emails only to suddenly shout 'Another bloody conference?!', so thank you so much for your help and support over the years, it was well appreciated.

To the forgotten year, especially Amelia, everything was always better after a drink and a chat with you, Miguel for 'leaving it out' and my desk neighbour Spyros for passively spurring me on through guilt. Thanks to Del for that unforgettable time in the Mexican Jacuzzi, and to JP who pretended he wasn't watching. Many thanks Chatel, but when I finally meet St Peter at the pearly gates I'm hoping he'll send me back to Earth for a few years to make up for all the time I spent waiting for you around the ACBE. To Sara my Lab A buddy and heiress, so much shared and long may it continue.

Thanks Vineyard and Mammalian especially Rich, Lourdes and the Hartham road heroes of brewing and cinema (not you Minaj). To the Regenmed crew Kate, Vish, Owen, Giulia and others, thank-you. Thanks also to Colonades for hosting my many travesties, Kate, Chris & Fer especially. And To the other guys from my MSc., Peter, Tom, Hugh and Martyn, just be thankful you got out when you did...

Val for lessons learned, Ed for foxtail fantasies, Shiers for guilty gardening, Pat for many massages and Ant for Amsterdamage. And Emily I'll never forget your valuable support, patience and encouragement at the start.

From when the slippery slope into Academia started those many years ago in my Portsmouth days: Paul, Jen, James, Rob, Alex, Mary, Terri. Not forgetting the Finnish brethren Joona, Juho and Juuso – *Mitä on ja mitä ei.*

Thank you North London for being my home, Guerilla Science & Bright Club for incredible Public Engagement opportunities, e minha nova família LECC no Rio (*fica na moral!*).

Finally thank you to the EPSRC and to Valneva for the funding and for this unique opportunity to start my career.

Thank you all immeasurably.

# 2 Contents

---

## **2.1 Chapters and sections**

1	Abstract.....	3
	Valneva Scotland Ltd .....	4
	Acknowledgements .....	5
2	Contents.....	8
2.1	Chapters and sections .....	8
2.2	List of abbreviations .....	14
2.3	List of Figures.....	16
2.4	List of tables .....	24
3	Introduction .....	25
3.1	Vaccine bioprocessing .....	25
3.1.1	Early history of vaccines .....	25
3.1.2	Types of vaccines .....	26
3.2	Japanese Encephalitis .....	28
3.2.1	Epidemiology.....	28
3.2.2	JEV – structure and replication .....	29
3.2.3	JE Vaccines .....	33



3.3	Vaccine bioprocessing with application to JE vaccines .....	33
3.3.1	Upstream & the Vero cell line.....	33
3.3.2	Downstream processing.....	34
3.3.3	Viral inactivation in vaccine production .....	39
3.4	Microscale process development.....	46
3.5	Project aims and objectives .....	47
3.5.1	Formaldehyde inactivation of JEV.....	48
3.5.2	Purification of JEV .....	49
3.5.3	Overarching challenges and objectives .....	49
4	Materials and Methods.....	52
4.1	Working viral seed and cell banks.....	52
4.2	JEV production and test material .....	52
4.2.1	Cell culture .....	52
4.2.2	Viral infection and concentration of harvest pool .....	52
4.2.3	Protamine Sulphate treatment .....	53
4.2.4	Storage of test material .....	53
4.2.5	Purified JEV .....	53
4.3	Inactivation experiments .....	54
4.4	Shear experiment.....	54
4.5	Chromatography resin selection & optimisation.....	55

4.5.1	PreDicator Plates (G.E. Healthcare)	55
4.5.2	ÄKTA method	56
4.5.3	Buffer exchange for AKTA chromatography	57
4.6	Analytical techniques	57
4.6.1	Plaque assay (viral infectivity plaque titre determination)	57
4.6.2	Thermo Scientific Pierce BCA Protein Assay	58
4.6.3	Life Technologies Picogreen assay	58
4.6.4	SDS-PAGE and SilverQuest™ staining	59
4.6.5	Immunoassays	59
4.6.6	Zeta potential and dynamic light scattering	62
4.6.7	Nanoparticle tracking analysis	62
4.6.8	Amino acid sequencing	63
4.6.9	Liquid Chromatography-Mass Spectrometry protein identification	63
4.7	Design of Experiments	64
5	Formaldehyde inactivation of Japanese Encephalitis virus	65
5.1	Inactivation Results	67
5.1.1	Formaldehyde treatment of purified JEV	69
5.1.2	Formaldehyde treatment of harvest material	73
5.1.3	Interpretation of DoE results	83
5.2	Formaldehyde treatment discussion	91

5.3	Inactivation summary .....	93
6	Microscale investigation of chromatography resins for JEV purification .....	95
6.1	PreDictor plate resin screening for binding conditions .....	96
6.2	Elution studies on CA and QSFF single resin plates .....	106
6.3	Microscale investigation discussion .....	113
6.3.1	Choosing Q Sepharose FF .....	113
6.3.2	HTS JEV process development and assays .....	114
6.3.3	Microscale investigation summary .....	117
7	Chromatography scale-up of Japanese Encephalitis virus capture and elute .....	118
7.1	Initial Scale-up.....	118
7.2	Antigen Monitoring using Western Blots .....	124
7.3	Consequence of removing the second wash step .....	127
7.4	The impact of cross-linking the virus with formaldehyde treatment .....	130
7.5	Flow-through mode operation and pre-treatment optimisation .....	134
7.6	Scale-up discussion .....	139
7.6.1	From plates to the column.....	139
7.6.2	JEV stability, binding and interaction .....	140
7.6.3	The eluted protein .....	142
7.6.4	Bound versus unbound .....	143
7.6.5	Scale-up summary .....	147

8	Conclusions and Future work .....	148
8.1	Conclusions.....	148
8.1.1	JEV processing .....	148
8.1.2	Process development using small scale high-throughput techniques.....	149
8.1.3	Retrospective process characterisation and development.....	150
8.2	Future work .....	150
8.2.1	Further JEV process investigation .....	150
8.2.2	Impurity characterisation .....	152
8.2.3	Other processes and the future vaccines.....	152
9	References.....	154
10	Appendix .....	170
10.1	Cell passage data .....	170
10.2	Viral harvest titres .....	171
10.3	Example batch process analytics.....	172
10.4	Typical BCA assay standard curve generated with BSA .....	173
10.5	Typical Quant-iT PicoGreen standard curve with dsDNAs .....	174
10.6	Protamine sulphate measured by BCA assay.....	175
10.7	Design summary for fractional 2-level factorial on purified JEV from DX8...	176
10.8	Design evaluation for fractional 2-level factorial on purified JEV from DX8.	177

10.9	Conditions and antigen data for fractional 2-level factorial on purified JEV from DX8.....	180
10.10	DX8 design summary for inactivation of harvest material.....	181
10.11	DX8 design evaluation for harvest material experiment.....	182
10.12	All conditions and data for fractional 2-level factorial on JEV harvest material from DX8.....	184
10.13	BSA and glycine AKTA control runs.....	185
10.14	Outsourced sequencing results.....	187
10.14.1	Sequencing attempt 1 - 5 amino acids.....	187
10.14.2	Sequencing attempt 2 – 10 amino acids.....	188

## **2.2 List of abbreviations**

abs	absorbance
ACBE	Advanced Centre for Biochemical Engineering
AEX	anion exchange
ANOVA	analysis of variance
AU	absorbance units
BCA	bicinchoninic acid
BSA	bovine serum albumin
CA	Capto adhere
CEX	cation exchange
cHP	concentrated pooled harvest material
CQ	Capto Q
CV	column volume
Da	Dalton
DEAE	diethylaminoethyl
DLS	dynamic light scattering
dsDNA	double stranded DNA
DX8	Design Expert 8
ELISA	enzyme-linked immuno-sorbent assay
GRAS	generally recognised as safe
HAS	human serum albumin
hcDNA	host cell DNA
HP	pooled JEV harvest material
HTS	high throughput screening
IEX	ion exchange
JE	Japanese Encephalitis
JE-PIV	Japanese Encephalitis purified inactivated vaccine
JEV	Japanese Encephalitis virus
kDa	kilo Dalton
LC-MS	liquid chromatography - mass spectrometry
LDS	lithium dodecyl sulphate

LOD	limit of detection
LRV	log reduction value
mAb	monoclonal antibody
MCB	master cell bank
mELISA	modified enzyme-linked immuno-sorbent assay
MOI	multiplicity of infection
MVSB	master viral seed bank
MWCO	molecular weight cut-off
NaMe	sodium metabisulphite
ORF	open reading frame
PAGE	polyacrylamide gel electrophoresis
PBS	phosphate buffered saline
PCR	polymerase chain reaction
PDI	polydispersity index
pfu/mL	plaque forming units per millilitre
PS	protamine sulphate
PST	protamine sulphate treated material
QbD	Quality by Design
qPCR	quantitative PCR
QSFF	Q Sepharose Fast Flow
SDS	sodium dodecyl sulphate
SGC	sucrose gradient centrifugation
UCL	University College London
UF	ultrafiltration
v/v	volume per volume (%)
w/v	weight per volume (%)
WB	western blot
WCB	working cell bank
WVSB	working viral seed bank

## 2.3 List of Figures

Figure 3.1 – Image showing the structure of *Flaviviruses*. The E-protein dimers (red) sit on top of the membrane and are anchored in position by the membrane proteins (purple). The nucleocapsid is represented here by the yellowish structure. Image actually shows West Nile virus and is copyrighted to Russell Knightley Media..... 32

Figure 3.2 – Inactivation kinetics of purified Japanese Encephalitis virus treated with 0.05% formalin for 10 days at 22°C, for final use as a vaccine. This figure was produced using data from the literature (Srivastava et al., 2001); plaque forming units (pfu) were counted by direct assay onto cultured Vero cells..... 45

Figure 3.3- Flow schematic of a typical Japanese Encephalitis purified inactivated vaccine (JE-PIV) manufacturing process adapted from the literature (Okuda et al., 1975; Pyo Hong et al., 2001; Srivastava et al., 2001) Steps highlighted in red indicate those identified for investigation as part of this project. Sucrose gradient centrifugation is labour intensive, variable and not amenable to scale-up and anion chromatography is evaluated as a potential alternative. Characterisation of the formaldehyde inactivation step leads to greater process understanding and suggestions for improvement and potential re-location. .... 51

Figure 5.1 – Antigen concentration response Half-Normal probability plot from formaldehyde inactivation experiment with purified JEV. The factors highlighted, with their coded terms evident, are those deemed to be statistically significant as they deviate from the normal distribution as defined by the software. The factors are split into two colours according to the overall effect of switching to their higher level, orange for positive (more antigen) and blue for negative (less antigen). Note that due to the design the following interactions are aliased: DG is aliased to CF and AB; and AD is aliased to BG and EFH. DG and AD were highlighted because they are the most likely to be responsible for significant effects as one or both of the terms had already been singled out as such. .... 72



Figure 5.2 – Details of samples still found to contain active JEV particles. The + and – symbols correspond to the high (+1) and low (-1) values for each factor, respectively, as detailed in Table 5.2. Error bars are based on standard deviation across 2 plaque assay plates. .... 77

Figure 5.3 – Antigen concentration response Half-Normal probability plot from formaldehyde inactivation experiment with JEV harvest material. As in Figure 5.1, the factors highlighted, with their coded terms evident, are those deemed to be statistically significant as they deviate from the normal distribution as defined by the software. The factors are split into two colours according to the overall effect of switching to their higher level, orange for positive (more antigen) and blue for negative (less antigen). Note that due to the design the positive EF interaction is aliased to AD. .... 79

Figure 5.4 – Dynamic light scattering response Half-Normal probability plot from formaldehyde inactivation experiment with JEV harvest material. As with the two previous figures, the factors highlighted, with their coded terms evident, are those deemed to be statistically significant as they deviate from the normal distribution as defined by the software. The factors are split into two colours according to the overall effect of switching to their higher level, orange for positive (average particle size increases) and blue for negative (average particle size decreases). Note that due to the design the positive AC interaction is aliased to BE and EF is aliased to AD. .... 82

Figure 5.5 – ELISA antigen data of JEV harvest material, with and without 0.02% formaldehyde and glycine at different concentrations over 96 hours at 20°C. Key: HP = harvest pool, F = 0.02% formaldehyde, G = glycine. .... 85

Figure 5.6 – ELISA data showing the effect of glycine during formaldehyde treatment at different stages of the JEV purification process. Key: st exp = start of the experiment, cHP = concentrated harvest pool, PST = protamine sulphate treated

material, F = 0.02% formaldehyde, G = 0.5% glycine, S = 5% sucrose. Samples 1 to 7 underwent the incubation at 20°C for 96 hours, sample 1 was a control with no formaldehyde or stabilisers added..... 88

Figure 5.7 – Antigen recovery data from non- and formaldehyde treated harvest material exposed to high and low shear in an ultra scale down shear device. Key: NT = non-treated, FT = Formaldehyde treated, Lo = 1000 rpm, Hi = 6000 rpm.... 90

Figure 6.1 – colour contour plots demonstrating amount of protein bound to each anion exchange resin on the GE PreDicator screening plate for varying loading NaCl concentrations (0, 20, 40 and 60 mM) and pHs (7.5, 8.0 and 8.5), when challenged with PST diluted with appropriate buffer. Figures generated using Matlab R2012b (8.0.0.783). ..... 99

Figure 6.2 – colour contour plots showing the change in absorbance ( $\Delta$  abs) across observed ranges of pH (7.5, 8.0 and 8.5) and NaCl concentrations (0, 20, 40 and 60 mM) for each anion exchange resin of the GE PreDicator screening plate when challenged with PST diluted with appropriate buffer.  $\Delta$  abs was elucidated from modified ELISA testing of the feed and flow-through and subtracting one from the other for each well of the resin screening plate.  $\Delta$  abs colour scale goes from least JEV binding in blue to most JEV binding in red. Figures generated using Matlab R2012b (8.0.0.783)..... 102

Figure 6.3 – silver stained SDS-PAGE (A) and corresponding western blot (B) analysis of selected samples from screening plate study (NaCl concentration in mM and pH). Samples loaded from stated resin and conditions are feed (F), flow-through (FT) and wash (W). Arrow indicates location of E-protein (~51 kDa) band giving positive signal in western blot for antibodies raised against JEV. .... 105

Figure 6.4 – total protein data obtained from QSFF and CA single resin plates challenged with PST diluted with appropriate buffer. Comparison of protein bound

to each resin at different pHs (A). Protein content of eluted fractions for QSFF (B), washes and CA eluted protein content were below the limit of detection. Error bars based on standard deviation of analytical samples as follows: Feed in A and B, n=96; pHs in A, n=32; flow-throughs in B each pH n=32; NaCl elution concentrations in B each pH, n=4..... 108

Figure 6.5 – modified ELISA absorbance data for the load and elute fractions of Q Sepharose FF (A) and Capto Adhere (B) single resin plates challenged with PST diluted with appropriate buffer. Error bars based on standard deviation of analytical samples as follows: Feed in A and B, n=96; flow-throughs in A and B each pH n=32; NaCl elution concentrations in A and B each pH, n=4..... 110

Figure 6.6 – SDS-PAGE analysis of fractions from load and elute of Q Sepharose Fast Flow single resin plate at pH 8.6. Lanes loaded as follows: Novex Mark 12 protein unstained protein standard (M), feed (F), flow-through (FT), wash (W) and NaCl elution concentration (100 – 800 mM). F, FT, W and 100 mM samples were all taken from the same corresponding well. .... 112

Figure 7.1 – PST JEV process material buffer exchanged into 50 mM Tris pH 8.6 loaded onto 1 mL Q Sepharose FF pre-packed column, equilibrated with the same buffer, at 1 mL/min. Chromatogram of U.V. absorbance against volume (A) and corresponding silver stained SDS-PAGE analysis of selected fractions (B and C) where M = Novex Sharp unstained protein standard, SM = start material (pre-buffer exchange) and F = feed. All buffers steps shown in A also included 50 mM Tris pH 8.6. .... 121

Figure 7.2 – Protein (A) and antigen (B) content of feed and elution pool relating to the AKTA run in Figure 7.1, the elution pool specifically relates to lanes 10-12 in Figure 7.1.C. The error bars arise from the standard deviation between analytical samples, n=3. .... 123

Figure 7.3 – PST JEV process material buffer exchanged into 50 mM Tris pH 8.3 loaded onto 1 mL Q Sepharose FF pre-packed column, equilibrated with the same buffer, at 1 mL/min. Chromatogram of U.V. absorbance against volume (A) and corresponding silver stained SDS-PAGE analysis (B and C) and Western blots (D and E) of selected fractions where M = Mark 12 unstained protein standard (B and C) or Novex Sharp pre-stained protein standard (E), F = feed, EP = elution pool and DEP = diluted elution pool. All buffers steps shown in A also included 50 mM Tris pH 8.3. .... 126

Figure 7.4 – PST JEV process material buffer exchanged into 50 mM Tris pH 8.3 loaded onto 1 mL Q Sepharose FF pre-packed column, equilibrated with the same buffer, at 1 mL/min. Chromatogram of U.V. absorbance against volume (A) and corresponding silver stained SDS-PAGE analysis (B) and Western blot (C) of selected fractions where M = Mark 12 unstained protein standard, EP = elution pool, F = feed, and SM = start material. All buffers steps shown in A also included 50 mM Tris pH 8.3 ..... 129

Figure 7.5 – U.V absorbance of non-treated PST feed and formaldehyde and glycine treated PST feed loaded onto 1 mL Q Sepharose FF (A) with corresponding silver stained SDS-PAGE analysis (B and D) and Western blots (C and E) of selected fractions where M = Mark 12 unstained protein standard (B and D) or Novex Sharp pre-stained protein standard (C and E), F = feed, and SM = start material. Non-treated fractions can be seen in B and C with formaldehyde and glycine treated fractions in D and E. All buffers steps shown in A also included 50 mM Tris pH 8.3. .... 133

Figure 7.6 - U.V absorbance of non-treated PST feed and formaldehyde and glycine treated feed applied to a 1 mL Q Sepharose FF at 1ml/min equilibrated with 50 mM Tris pH 8.3 (A) with corresponding silver stained SDS-PAGE analysis (B and D) and Western blots (C and E) of selected fractions where M = Novex Sharp

unstained (B and D) or pre-stained (C and E) protein standard and F = feed. Non-treated fractions can be seen in B and C with formaldehyde and glycine treated fractions in D and E. All buffer steps in A also contained 50 mM Tris pH 8.3..... 136

Figure 7.7 – Average JEV antigen recovery from flow-through chromatography mode of non-treated feeds and PST feeds pre-treated with formaldehyde and glycine and applied to a 1 mL Q Sepharose FF pre-packed column at 1 mL/mL for 6 different AKTA chromatography runs. Loading, equilibration and wash buffer was 50 mM Tris pH 8.3. Error bars represent standard deviation between results from separate chromatography runs, n=3..... 138

Figure 7.8 – Average ratios of bound to unbound peak areas (elution peak area over loading peak area) of AKTA runs from feeds which were stored overnight in Tris loading buffer at 4°C and feed maintained at pH 8.3. Feeds generated from PST JEV process material by either buffer exchanging into or diluting with the Tris buffer in use for a particular experiment. .... 145

Figure 10.1 – Accumulated passage data for Vero cells grown at laboratory scale in T150 tissue culture flasks with L-glutamine, serum and antimycotic supplemented media. Error bars are based on standard deviation of results, where it was impossible to show negative error on the log scale of the primary axis (for passages 3 to 7 and 9), the minimum measured cells/mL value was used. N number for each passage (P): P0 =15, P1 = 14, P2 = 12, P3 = 9, P4 = 9, P5 = 5, P6 = 3. P7 = 4, P8 = 3, P9 = 2..... 170

Figure 10.2 – Average plaque assay derived viral titres for each of the four harvest points at 3, 5, 7 and 9 days post infection of the Vero cell cultures at laboratory-scale production of JEV. Error bars based on standard deviation thus only maximum error can be plotted on a logarithmic scale, n=5. .... 171

Figure 10.3 – Process analytics for a batch after pooling the harvest (HP), concentrating the harvest (cHP) and treating it with protamine sulphate to remove hcDNA. The antigen content data overlaps the total protein and dsDNA data because it is plotted on the secondary axis. Error bars are of standard deviation of samples within their respective assays (n=3). .....	172
Figure 10.4 – BCA assay standard curve generated with bovine serum albumin (BSA). Error bars represent standard deviation of absorbance reading for dilution of the BSA reference standard, n=4. ....	173
Figure 10.5 – Quant-iT PicoGreen assay standard curve generated with the supplied bacteriophage-λ DNA. Excited at 483 nm and read at 525 nm, the error bars represent the standard deviation of measured emissions for each dilutions of the reference standard, n=3.....	174
Figure 10.6 – U.V. absorbance chromatograms 5 mL each of 1 mg/mL BSA, 1% glycine and 1 mg/mL BSA with 1% glycine, all run in 50 mM tris pH 8.3 on a pre- packed 1 mL Q Sepharose Fast Flow column. 1% glycine on its own does not shown any significant U.V. absorbance and when added to 1mg/mL BSA it does not change the elution profile. Insert shows the load and start of the elution peak with the absorbance scale increased 100 fold to distinguish between the U.V. traces. ....	185
Figure 10.7 – Protein concentration determined by BCA assay relating to fractions and samples from the AKTA run described in Figure 10.6. The diluted samples were diluted with equal part PBS. Error bars are based on standard deviation of experimental samples, n=3.....	186
Figure 10.8 – Report from 1 <sup>st</sup> sequencing attempt of 5 amino acid sequence results for excised ~55 kDa gel from eluted fractions of a typical AKTA run.....	187

Figure 10.9 – Report from 2<sup>nd</sup> sequencing attempt of 10 amino acid sequence results  
for excised ~55 kDa gel from eluted fractions of a typical AKTA run..... 188

## **2.4 List of tables**

Table 3.1 – Different types of vaccines in production which each method to illicit an immune response for providing future immunity in the recipient, with descriptions and examples, adapted from (Josefsberg and Buckland, 2012). .....	28
Table 3.2 – Summary of selected formaldehyde inactivation procedures performed on Japanese Encephalitis virus for use as a vaccine. Conditions are quoted as they appear in the publications, N.B formalin = 37 – 41% w/v formaldehyde in water. *Best performing stabiliser of the four tested.....	43
Table 5.1 – factors for 2-level fractional factorial experiment with purified JEV, together with their respective coded terms and value at each level. ....	70
Table 5.2 – factors for 2-level fractional factorial experiment with JEV harvest material, together with their respective coded terms and value at each level. ....	74
Table 6.1 – Resin characteristics adapted from Ion Exchange columns and Media selection guide (GE Healthcare, 2011).....	97
Table 7.1 – Antigen content and recovery data based on ELISA for treated and non-treated feed. Error based on standard deviation within ELISA assay.....	132



# 3 Introduction

---

## ***3.1 Vaccine bioprocessing***

The driver for much of what we see in vaccine development is made on the basis of quality, safety and efficacy. While most countries have implemented a vaccination policy since as early as the 1900's, the manufacturing processes of these vaccines were simplistic and poorly characterised due to technology limitations of the age. The true function and mechanism of action was unknown for many early vaccines and the excipients used were equally obscure. However, these early vaccines became established and as the regulation and indeed regulatory agencies were created, many of these vaccines, excipients and manufacturing processes were grandfathered in. What was known is the interplay between the product and the process and how changes in manufacture can directly affect the quality, safety and efficacy of a vaccine. Such that changes to the process can often require regulatory approval. Much of vaccine bioprocess development is then focused on two main tranches. The first is the development of new processes and products against disease targets; the second to increase process understanding of existing vaccines. It is to this end that the tools of microscale development have been employed to Japanese Encephalitis virus vaccine production. As discussed below, some of the first Japanese encephalitis (JE) vaccines produced in the 1950s were produced in mouse brains and evolved into primary cell derived production. Yet much of the downstream processing remained unchanged during this process update. Thus, this thesis seeks to increase process understanding of JEV production and to explore new process options such as chromatography.

### **3.1.1 Early history of vaccines**

Vaccines can be traced back to the end of the 18<sup>th</sup> century when cowpox pus was used to inoculate against smallpox in humans. A century later bacterial vaccines were

available against cholera and anthrax when it was established that 'weakened', through heat or otherwise, cultures could be used to provide immunity without harming the individual being administered. By the start of the last century a whole-cell inactivated bacterial vaccine was licensed against pertussis for the prevention of whooping cough, which was soon followed by formalin inactivated toxoid vaccines against tetanus and diphtheria in the 1930s (Josefsberg and Buckland, 2012).

### 3.1.2 **Types of vaccines**

Unknowingly at the time, when Edward Jenner began immunising people against smallpox using pus from the bovine variant of the disease, this was the first attenuated live virus vaccine – so called because the strain used as a vaccine was replication incompetent in humans. This is just one of many different types of vaccines that are able to induce protective immunity in humans, broadly speaking the main types are: whole cell or virus vaccines, of which they can also be attenuated, inactivated or both, DNA vaccines and vaccines of antigenic components from a pathogen (Josefsberg and Buckland, 2012), these are summarised in Table 3.1.

The first group of vaccines, whole organism, whether live, inactivated, attenuated or a combination thereof, could be considered the traditional type of vaccine. The focus of this research is in fact targeted towards a whole inactivated virus vaccine, discussed in detail below. Vaccines can be attenuated through multiple passages and expression through non-human hosts, for example, or otherwise adapted so as not to pose a threat to humans. Inactivation, in turn, is performed to damage or weaken the pathogen to such an extent with the same aim. Yet despite these two attributes, the whole organism must be presented to the immune system in such a state that will still confer immunity against wild type (or other protective targets) variants of the disease encountered. Inactivation is covered in more detail below in section 3.3.3. Early chick embryo produced influenza vaccines are examples of live attenuated vaccines. The polio vaccine is another example of an inactivated vaccine.

DNA vaccines, seen as a promising treatment against many forms of cancer, essentially involve reprogramming the recipient's cells to produce specific antigens by transfecting them with the required gene and promoter. DNA vaccines offer easier manufacture than the more traditional vaccines, can be tailored towards a specific immune response (T-cell mediated or antibody) and are safer as no pathogenic organisms are handled. However, although pre-clinical results were promising, the first generation of DNA vaccines demonstrated disappointing potency overall (Liu, 2003). Trials and development of subsequent generations are on-going such as for HPV induced cervical cancer (Poláková et al., 2010) and multiple sclerosis (Stüve et al., 2007).

Other antigenic components of pathogens can be used as vaccines to confer immunity, such as proteins (e.g. inactivated tetanus and diphtheria toxoid vaccines), polysaccharide conjugates (e.g. the *Pneumococcal* vaccine) and virus-like particles (e.g. the human papillomavirus vaccines). Virus-like particles can be produced in recombinant yeast and purified after homogenisation and though downstream processing is more complicated, they have the advantage of being safer to produce and administer because processing of pathogenic organisms is not required and no nucleic acids are administered to the patient. Additionally, the next generation of antigenic targets such as these could more easily be identified using reverse vaccinology (Josefsberg and Buckland, 2012). This is a process by which genome analysis is used to identify the most conserved immunogenic epitopes across strains of pathogens, which can be screened not only as vaccine candidates but also for suitability to large-scale manufacture.

Type of vaccine	Description	Example vaccines
Live attenuated	The organism, viral or bacterial, has been weakened to the point of being unable to cause disease.	Viruses: Measles, mumps, rubella, rotavirus; bacteria: typhoid, tuberculosis.
Inactivated	The disease-causing agent has been killed or inactivated with chemicals, heat or radiation to prevent it from replicating or causing disease.	Japanese Encephalitis, influenza, rabies, hepatitis A.
Subunit	A component of the pathogen of the pathogen is synthesized or purified; e.g. surface antigens and polysaccharides. Can be used in conjugate vaccines	Virus Like Particles: hepatitis B, human papillomavirus; pneumococcal, typhoid.
Toxoid	Toxoids, e.g. proteins, from the pathogen are produced and inactivated. Have been combined amongst themselves and with other subunits (see above).	Tetanus, anthrax and diphtheria.
DNA	Plasmid containing gene(s) coding for an antigen target are used to inoculate so that the recipient produces the it themselves.	None licensed.

Table 3.1 – Different types of vaccines in production which each method to illicit an immune response for providing future immunity in the recipient, with descriptions and examples, adapted from (Josefsberg and Buckland, 2012).

## 3.2 Japanese Encephalitis

### 3.2.1 Epidemiology

Japanese Encephalitis (JE) is caused by the Japanese Encephalitis virus (JEV) an arthropod borne *Flavivirus*, and it is the most common form of viral encephalitis in Asia, There are an estimated 50,000 cases of the disease every year, of which around 10,000 are fatal and approximately 15,000 result in long term neurological sequelae. Fortunately only 1 in 250-500 of those individuals infected with JEV develop any form of symptoms of the disease (Erlanger et al., 2009; WHO, 2006). As with many such

diseases, efforts are underway to efficiently produce safe and effective vaccines to Japanese Encephalitis (JE), mostly in the form of purified and attenuated inactivated whole virus vaccines (Mackenzie et al., 2004).

JEV is transmitted between animals by *Culex* mosquitoes, *Culex tritaeniorrhynchus* being the most important in terms of human infection due to breeding in stagnant rice paddies. Birds are seen as the host for the natural life cycle whereas domestic pigs hosts for the virus amplifying cycle. Humans are regarded as terminal hosts, with those infected living primarily in rural areas in close proximity to swine (Solomon, 2000).

Outbreaks of JE were first reported in Japan in the 1870s and the disease has since spread to most of China, South Asia, Southeast Asia, East Asia, the Indian subcontinent, the Pacific Rim and some regions of northern Australia. It is estimated that a total of 3 billion people may be at risk (Erlanger et al., 2009). Major epidemics occur in endemic regions approximately every 10 years (Solomon, 2000).

### 3.2.2 JEV – structure and replication

JEV is of the genus *Flavivirus* in the family *Flaviviridae*, one of 70 members in the family. *Flaviviruses* are enveloped virions of approximately 500 Å (Mukhopadhyay et al., 2005), JEV, specifically, is around 50 nm (Sumiyoshi et al., 1987). The glycoprotein envelope surrounds the nucleocapsid which itself contains an 11 kb single stranded positive sense RNA genome. This genome contains an open reading frame (ORF) of 10.3 nucleotides equivalent to 3432 amino acid residues (Sumiyoshi et al., 1987).

All *Flavivirus* genomes are similar, the ORF codes for a single polyprotein cleaved during maturation, by viral and host cell proteases, into 3 structural proteins and 7 non-structural proteins (Chambers et al., 1990). The 3 structural proteins are: capsid (C), membrane (M, though expressed as prM, the precursor to M) and envelope (E). E and prM are glycoproteins containing two transmembrane helices. Prior to cleavage to form M, prM is thought to act as a folding and assembly chaperone to E (Mukhopadhyay et al., 2005). The 7 non-structural proteins are NS1, NS2A, NS2B, NS3, NS4A, NS4B and

NS5. The largest of which, NS1, NS3 and NS5, are also the most highly conserved within the *Flavivirus* genus. NS2A, NS2B, NS4A and NS4B are smaller, hydrophobic proteins. *Flavivirus* ORF encoding reads as follows: 5'-C-prM(M)-E-NS1-NS2A-NS2B-NS3-NS4A-NS4B-NS5-3' (Chambers et al., 1990).

The glycoprotein mentioned above is the envelope protein or E-protein, it consists of 3 domains (I, II and III) and forms the viral envelope as 90 homodimers arranged in 30 rafts each of 3 sets of dimers in a 'herringbone' formation parallel to the surface of the lipid bi-layer (Lindenbach et al., 2007; Mukhopadhyay et al., 2005). This envelope structure is anchored in position by the membrane proteins or M-protein that attach the E-proteins to the lipid bi-layer; this *Flavivirus* structure is represented by West Nile virus in Figure 3.1. E-protein domain I forms a  $\beta$ -barrel; domain II, the largest of the 3, runs along the surface of the membrane between the transmembrane regions of the homodimer subunits and has a fusion peptide at its end to mediate entry into host cells (see below); domain III contains an immunoglobulin like-fold, is involved in receptor binding and is the dominant target for neutralising antibodies (Lindenbach et al., 2007; Mukhopadhyay et al., 2005; Stiasny and Heinz, 2006).

*Flaviruses* enter host cells by receptor-mediated endocytosis a process whereby cells internalise an external particle or macromolecule using surface receptors that cross the cell membrane. These receptors cause the membrane lipid bi-layer to fold in on itself and bud into the cytoplasm creating an endosome, where, in the case of *Flavivirus* internalisation, the acidic pH causes first a dissociation of the E-protein dimer followed by its irreversible trimerisation. This structural reconfiguration allows the fusion peptide on domain II of the E-protein to fuse the endosome and viral membranes resulting in the release of the nucleocapsid into the host cytoplasm for translation of the ORF into the single polyprotein described above. The genome is replicated on intracellular membranes and immature non-infectious virions are created in the lumen of the endoplasmic reticulum. These virions mature into infectious particles in trans-Golgi

network by cleavage of the prM, these then exit the host by exocytosis (Lindenbach et al., 2007; Mukhopadhyay et al., 2005; Stiasny and Heinz, 2006).

Figure 3.1 – Image showing the structure of *Flaviviruses*. The E-protein dimers (red) sit on top of the membrane and are anchored in position by the membrane proteins (purple). The nucleocapsid is represented here by the yellowish structure. Image actually shows West Nile virus and is copyrighted to Russell Knightley Media.



### 3.2.3 JE Vaccines

The first Japanese Encephalitis vaccines were made available in the 1950s and up until 2008 there were seven vaccines available using various JEV strains; 3 mouse brain derived available in Japan and Korea and 4 mammalian cell derived (primary hamster kidney & Vero) available in China (Beasley et al., 2008; Halstead and Thomas, 2010). However, Valneva has since received approval from all major western regulatory bodies with the licenced commercial product IXIARO<sup>®</sup>/JESPECT<sup>®</sup> available in these territories.

There have been fears over adverse side-effects with the mouse brain derived vaccines (e.g. BIKEN & JE-VAX), specifically acute disseminated encephalomyelitis (ADEM, (Plesner et al., 1998)). As a result the Japanese government no longer recommends the use of mouse brain derived vaccines (Beasley et al., 2008; Halstead and Thomas, 2010). This has paved the way for more inactivated and live attenuated mammalian cell derived JE vaccines.

Attempts have been made to produce JEV subunit vaccines using purified recombinant E-protein, E-protein domain III antigens, subviral particles and plasmids encoding each of these types but few have been shown to be effective outside of mice models (Beasley et al., 2008).

## 3.3 Vaccine bioprocessing with application to JE vaccines

This section will focus primarily on exploring production and purification methods of Japanese Encephalitis whole virus vaccines. Other vaccines will be mentioned and described where applicable in relation to the techniques used.

### 3.3.1 Upstream & the Vero cell line

The Vero cell line was established from the kidney of an African green monkey in 1962 by Yasumura and Kawakita (Sugawara et al., 2002) and subsequently characterised (Hopps et al., 1963). Vero cells have also been used to develop a host of other

vaccines including rabies (Frazatti-Gallina et al., 2004), influenza (Kistner et al., 1998) and polio (van Wezel et al., 2009).

As stated, the first JE vaccines were purified from the brains of infected mice with production methods, which though fundamentally the same, they did improve and increase in scale over the years (Aizawa et al., 1980). A formalin inactivated JE vaccine has also been produced in Hamster kidney cells (Darwish and Hammon, 1966) and chick embryos (Warren et al., 1948).

Vero cells have been used with micro-carrier technology for development of an inactivated polio vaccine (Simizu et al., 2006). Prior to this, research had been done to improve the up-scaling problems seen with micro-carriers, such as using bead-to-bead transfer of Vero cells as opposed to traditional cell harvesting and splitting (Wang and Ouyang, 1999).

Another novel approach used an oscillating bioreactor to produce Japanese Encephalitis in Vero cells at 500 mL scale (Toriniwa and Komiya, 2007). Termed BelloCell, the system involved a packed bed of immobilised Vero cells which is alternately submerged in media then exposed for gaseous exchange within the cell using bellows integrated into the base of the bioreactor.

### **3.3.2 Downstream processing**

Most JE vaccine manufacturing processes essentially have two purification steps to remove host cell DNA (hcDNA) and host cell proteins. Common methods include hcDNA removal by precipitation with protamine sulphate and sucrose gradient centrifugation for removal of protein impurities and concentration of the virus product, both of which are described below.

#### **3.3.2.1 Removal of host cell DNA by protamine sulphate precipitation**

Protamine sulphate is a highly basic peptide (being 66% arginine) and is derived from the nucleus of fish milt (Suzuki and Ando, 1972). It is the highly cationic properties that

allow protamines to bind to DNA. The resulting nucleoprotein precipitate formed between protamine and DNA is exploited in bioprocessing for removal of nucleic acids in process material, and has been specifically documented for the purification of JEV for use as a vaccine is described (Aizawa et al., 1980; Gupta et al., 1991; Okuda et al., 1975; Pyo Hong et al., 2001). A substitute for protamine sulphate could be polyethylenimine, a highly charged polymer, which has also been shown to precipitate nucleic acids (Burgess and Jendrisak, 1975). Protamine sulphate has also been shown to significantly affect recovery of rabies virus in the production of a vaccine where the authors go so far as to recommend an additional sucrose gradient step (Kumar et al., 2002) to fully remove the protamine sulphate peptides.

### **3.3.2.2 Removal of host cell proteins by sucrose gradient centrifugation**

Sucrose gradient centrifugation, a type of isopycnic separation, separates on the basis of the sedimentation co-efficient of the particle within a sucrose medium undergoing centrifugation. The centrifugal forces acting on the material separates them along the centrifuge tube according to density with the densest particles settling furthest from the axis of rotation. The density range of the medium should cover the whole span of particle densities within a sample. The step is most often performed in an ultracentrifuge but a centrifuge can also be used to create the gradients, but over a longer period. Once the run has finished the material can be separated into different fractions, which each one tested for the desired product.

Sucrose gradient ultracentrifugation has been the dominant principle purification step for whole JEV for use a vaccine for decades (Gupta et al., 1991; Okuda et al., 1975; Pyo Hong et al., 2001; Srivastava et al., 2001; Toriniwa and Komiya, 2008). There are variations, such as using PEG as opposed to sucrose (Aizawa et al., 1980) or being followed by a cellulose-sulphate chromatography step (Sugawara et al., 2002).

When optimising rabies virus recovery, Kumar *et al.* (2002) used two continuous ultracentrifugation (isopycnic banding with sucrose) steps back to back. The gradient

was created with 60% sucrose being spun in an ultracentrifuge, with the feed introduced at 4-5 L/h . The selected fractions were then pooled and the process repeated. Having this second ultracentrifugation step was found to give better recovery rates than removing DNA using protamine sulphate and Tween-80. In fact, ultracentrifugation and continuous density centrifugation are also the most common methods for purifying rabies vaccines (Perez and Paolazzi, 1997).

### **3.3.2.3 Alternative purification methods**

Seeking and testing alternative purification methods for JEV lie within the scope of this project. Alternatives to current commercial manufacturing processes include automating density gradient steps and changing the type of isopycnic banding (e.g. to CsCl) and moving away from the current methods altogether towards chromatography or membrane based separation. There is a Hepatitis A vaccine which is purified using a complex mix of reagents but is essentially CsCl isopycnic banding with ultracentrifugation (Provost et al., 1986). This is merely an alternative form of most current methods and does not offer much benefit. The increased complexity of the step and its operation at a commercial manufacturing scale would result in this not being considered a viable alternative to current JEV targeting density gradient processes.

The nature of the JEV product as a large biological entity makes sucrose gradient centrifugation an ideal technique, due to separation based on density. The major drawbacks are not so much with the method itself but with the high labour and variable recovery rates (a result of operator input) associated with the method. Automation of the process is therefore the obvious step forward, though evaluating and testing large-scale equipment does not fall within the scope of the project, as a result only different methodologies will be mentioned here.

A significant disadvantage of sucrose gradient centrifugation and ultracentrifugation is their limited scope for scalability. Such processes require significant operator input leading to increased batch to batch variability, high labour costs and loss of potency

due to increased processing times (Andreadis et al., 1999; Lambert et al., 1980; Morenweiser, 2005; Saha et al., 1994; Todd et al., 1990). An alternative is the chromatographic purification of viruses which potentially offers easier scale-up and a reduction in processing times (Morenweiser, 2005). Evidence suggests that chromatographically purified vaccines are as effective as their sucrose gradient purified counterparts but associated with fewer adverse effects, though the mechanisms underlying these observations have yet to be properly elucidated. This was the case with one study (Lang et al., 1998) which compared two Vero cell derived rabies vaccines, one of which was purified using a single zonal centrifugation step, while the other was purified with a 3-step chromatography process. Although administration of the chromatographically purified vaccine apparently resulted in more localised adverse effects, systemic effects were significantly lower. The differences in adverse reactions noted in this study could be due to achieving a higher level of purity with several chromatography steps over a single zonal centrifugation step. The three chromatography steps would have separated process constituents based on 3 different properties, unlike the zonal centrifugation which would have been based solely on sedimentation coefficient. Furthermore another comparative study was described (Prem Kumar et al., 2005) between zonal centrifuge purification and a single chromatography step for purification of a Vero cell derived rabies vaccine. They found that a single ion exchange chromatography step yielded 50% more antigen than zonal centrifugation.

Chromatography is already used extensively in the production of biopharmaceuticals, but adapting such proven methods to the purification of viruses could require extended process development programs in order to determine optimal processing conditions. This is mainly due to the much larger size of viruses compared to most biopharmaceuticals, resulting in slower diffusion rates in solution and to adsorption being predominantly restricted to the surface of resin beads hence limiting binding

capacities (Lyddiatt and O'Sullivan, 1998; Morenweiser, 2005). Further limitations to the dynamic binding capacity can occur due to aggregation of the virus particles.

If viral absorbance is limited to only the surface of the resins then membrane absorbers for virus capture can also be considered. This has been studied for influenza (Opitz et al., 2007; Opitz et al., 2009) and *Vaccinia* (Wolff et al., 2010) viruses.

Monolith chromatography addresses this surface-only absorbance issue differently by having a single macroporous block of media as a continuous stationary phase as opposed to the individual porous resin beads of more traditional packed-bed chromatography. Monoliths for bioseparations are made using many different techniques on many different materials. Some examples of materials are polymethacrylate, compressed polyacrylamide gels, graphitised carbon, silica columns, cellulose and agarose. The production methods create highly interlinked channels in the media with diameters typically around 1500 nm. In comparison with more conventional media, this internal macroporous structure not only allows for higher flow rates, but also quicker mass transfer because surface absorption is dictated by convection not diffusion, as with porous resin beads. The initial published work on monolith purification of viruses gave promising results (Jungbauer and Hahn, 2004; Jungbauer and Hahn, 2008). More recently hydrophobic interaction monolith disks were successfully used to help isolate Hepatitis B surface antigens virus like particles from crude homogenised *Saccharomyces cerevisiae* feed (Burden et al., 2012).

Non-absorptive chromatographic purification of viruses has been achieved previously with Tick-Borne Encephalitis virus, also a *Flavivirus*, using gel filtration chromatography after concentration of the viral harvest (Crooks et al., 1990). However more recent literature concerned with the use of chromatography for virus separation focuses upon viral vector purification for gene therapy, where preserving viral activity, or infectivity, is the principal consideration. It is suggested that the mild processing conditions of ion exchange chromatography may offer the most favourable purification strategy to yield

intact virion recovery and selective elution of the product (Andreadis et al., 1999; Lyddiatt and O'Sullivan, 1998; Morenweiser, 2005). Similarly, with the production of a whole virus vaccine, surface antigen integrity and high purity are the key qualities of the final drug substance required in order to initiate the desired immune response with minimal adverse reactogenicity. These results indicate that serious consideration should be made as to the possibility of incorporating ion exchange chromatography into vaccine manufacturing processes.

Ion exchange chromatography has been documented for the purification of active respiratory syncytial virus (Downing et al., 1992) and for the production of an effective rabies vaccine (Frazatti-Gallina et al., 2004) where it acts as a principal purification step. The technique has also proved to be efficient when used in conjunction with poly(ethylene glycol) precipitation to produce a highly purified inactivated hepatitis A vaccine (Hagen et al., 1996).

### **3.3.3 Viral inactivation in vaccine production**

As stated, some vaccines are administered as live attenuated products, for example China's live attenuated JE strain SA 14-14-2 vaccine, but many are also inactivated. Formaldehyde inactivation will be covered in detail as this was the project's first area of investigation.

Viral inactivation in vaccine production is required not least to compromise the ability of the product itself to infect, replicate and cause harm to the patient, but also to inactivate any potential contaminating adventitious viruses lying dormant in the host (cell-line or otherwise) and those which may have been introduced during manufacture.

Furthermore, this inactivation procedure must be deemed sufficiently robust to inactivate a panel of model virus candidates in a viral clearance study (required for approval in biopharmaceutical products) as well as any potential as yet undiscovered viruses.

Inactivation methods can take many forms, yet the most common in vaccine manufacture appears to be chemical inactivation. Chemicals used for inactivation include: detergents (Jakubik et al., 2004), azirdines (Brown, 2001),  $\beta$ -propiolactone (Race et al., 1995), psoralens, sulphonates, sodium periodate (Sofer, 2003), and formaldehyde. Generally speaking, enveloped viruses, such as JEV, are easier to chemically inactivate than non-enveloped virus. This is because the phospholipid bilayer, unique to enveloped viruses and required for receptor mediated endocytosis entry to host cells (as stated in 3.2.2) makes much more sensitive to changes in environment than non-enveloped viruses.

### **3.3.3.1 Formaldehyde inactivation**

The precise conditions for viral inactivation using formaldehyde vary from virus to virus, with the common variables being formaldehyde concentration, temperature, time and pH. Formaldehyde has been used to inactivate toxins since the start of the 20<sup>th</sup> century (Loewenstein, 1909). Formaldehyde forms crosslinks with other proteins (Fraenkel-Conrat and Meham, 1949) which, when applied to viruses, results in their inactivation. Specifically, non-protonated amino groups form hydroxymethylamine with formaldehyde. This in turn then combines with the amino, amide, imidazole, phenolic or guanidyl group of another amino acid forming an inter- or intra-molecular methylene cross-link (Metz et al., 2004). This cross-linking effect prevents nucleic acids from leaving the nucleocapsid and infecting host cells.

The following examples highlight the variability of the technique with different targets for inactivation, or indeed, the scope for improvement in working with different conditions. Note that some studies quote formalin as opposed to formaldehyde; formalin is the form in which formaldehyde is commonly supplied at 40% v/v or 37% w/v formaldehyde often with methanol as a stabiliser.

One study demonstrated the capacity to inactivate the non-enveloped vesicular stomatitis virus (VSV) at 4°C over 30 minutes with 1% (10,000 ppm) formaldehyde or



over 18 h with 0.0625% (625 ppm). Yet both sets of conditions yielded preparations that induced immune responses in mice (Bachmann et al., 1993).

SARS-CoV, the corona virus which induces severe acute respiratory syndrome, was exposed to 0.009% (90 ppm) formaldehyde over 3 days at 4°C, 25°C and 37°C.

Inactivation failed at 4°C and some active virus was still detectable after day 3 at 25°C and 37°C (Darnell et al., 2004), highlighting that for this type of virus increases in time, temperature and formaldehyde concentration are required.

Measles virus (MV) inactivated with 1:100 formalin at 4°C over 24 hours causes an imbalance in the immune system due to the improper presentation of the MV nucleoprotein to murine class I restricted CLTs (Cardoso et al., 1995). This is evidence of recognised antigen binding sites or viral capsids being damaged to such an extent that they were not recognised by the murine immune system – a warning that excessive exposure to formaldehyde could render a vaccine product useless.

A 1984 study into formaldehyde inactivation of foot and mouth disease virus (FMDV) revealed rapid inactivation of around one log<sub>10</sub> reduction in plaque forming units per hour at 25°C with 0.04% (400ppm) formaldehyde at pH 8.5 for the first 2 to 3 hours. This then dropped to 0.2 log<sub>10</sub>/hour up until 30 hours when no more active virus was detected (Barteling and Woortmeyer, 1984). This 1984 study was conducted after safety concerns resulting from outbreaks due to incomplete inactivation using 0.02% formaldehyde (Barteling and Vreeswijk, 1991).

The first inactivated polio vaccine (IPV) was one of the earliest formaldehyde inactivated vaccines available and one which was to have profound consequences for all other vaccines. The first IPV vaccine was inactivated with 1:4000 formalin (approximately 0.001% (10 ppm) formaldehyde), yet two of the batches produced by Cutter in 1955 resulted in 260 cases of poliomyelitis with 10 fatalities. The subsequent investigation found that 'viral clumps' could hide infectious particles and that inactivation became non-linear towards the end of the inactivation period due to the

lower concentration of infectious particles. The process was immediately changed to include a filtration step to remove aggregates and the inactivation period was extended. The changes mattered little, however, as confidence was lost and, at the time, the oral polio vaccine proved safer and more effective (Bottiger et al., 1958; Furesz, 2006). However, the IPV has since proved crucial in the global fight against polio and is still widely used today.

An example of *Flavivirus* inactivation is with a dengue-2 virus vaccine which undergoes 0.05% (500 ppm) formalin inactivation at 22°C (Putnak et al., 1996).

While producing a JE vaccine in hamster kidney cells (HKCs), Darwish *et al.* (1966) compared inactivation without and without formalin (1:4000) at 30°C and 37°C, followed by a comparison between different formalin concentrations. Without the addition of formaldehyde the half-life of JEV was reported as being 14 hours at 30°C and 5 ½ hours at 37°C. Also inactivation of JEV occurred twice as fast at 37°C than 30°C at formalin concentrations of 1:1000, 1:2000, 1:4000 and 1:8000. For both temperatures it was discernible that higher concentrations of formaldehyde brought about quicker inactivation, it was also remarked that increasing the pH from 7.1 to 8.0 had no effect. The authors ultimately expressed fears for antigen integrity at higher concentrations of formalin and therefore decided to proceed with 1:4000.

Most other reports involving JEV inactivation by formaldehyde for a vaccine product fail to mention product recovery rates but are each fairly similar to one another; a summary can be seen in Table 3.2. The conditions vary from a few days at 22°C to a few months at 4°C with the formaldehyde (as formalin) concentration varying considerably with little explanation for the conditions in their respective papers with the exception of the addition of glycine (Toriniwa and Komiya, 2008) which was the best performing of 4 stabilisers tested, the others being sorbitol, L-glutamine and Lactose.

<b>Authors</b>	<b>Location in process</b>	<b>Conditions</b>	<b>Additives</b>
(Okuda et al., 1975)	After purification.	1:2500 formalin, 30 days in a cold room	0.01% w/v Thimerosal
(Gupta et al., 1991)	After protamine sulphate treatment of concentrated harvest, prior to ultracentrifugation.	0.01% formalin, 35 days at 4°C.	-
(Pyo Hong et al., 2001)	After purification (various methods).	0.05% formalin, 7 days at 22°C.	-
(Srivastava et al., 2001)	After sucrose gradient centrifugation purification.	0.05% formalin, 10 days at 22°C.	-
(Sugawara et al., 2002)	After harvest concentration prior to ultracentrifugation.	0.08% formalin, a few months in a cold room.	-
(Toriniwa and Komiya, 2008)	After ethanol precipitation of concentrated harvest and prior to ultracentrifugation.	0.05% formalin, 3 months at 4°C	0.5% glycine*

Table 3.2 – Summary of selected formaldehyde inactivation procedures performed on Japanese Encephalitis virus for use as a vaccine. Conditions are quoted as they appear in the publications, N.B formalin = 37 – 41% w/v formaldehyde in water. \*Best performing stabiliser of the four tested.

The studies described above illustrate the variability of formaldehyde inactivation and the importance that optimal conditions are met to achieve complete inactivation of the live virus. In the case of formaldehyde treatment of purified JEV this is achieved in 72 hours, as can be seen by the inactivation kinetics plot in Figure 3.2, but the treatment was allowed to continued up to 240 hours. As previously stated, this is to ensure not only complete inactivation of the viral product but any other adventitious agents which may have been undetected in animal derived components or introduced with other raw materials during production. Based on the different conditions quoted in Table 3.2 it is

assumed that the rate of inactivation decreases with temperature, thus the kinetics slow down at lower temperatures and therefore would require longer reaction times to achieve the same result.

The increased cross-linking effect on proteins by formaldehyde at higher concentrations and for extended periods could be seen as the cause of variable immunological responses in terms of antigen recognition. A certain degree of product loss could therefore be attributed to this cross-linking effect during formaldehyde inactivation – an effect that can be measured using ELISA or Western Blot assays, as immunoassays dependant on antigen recognition – reducing such losses would be a key milestone for any such process development.

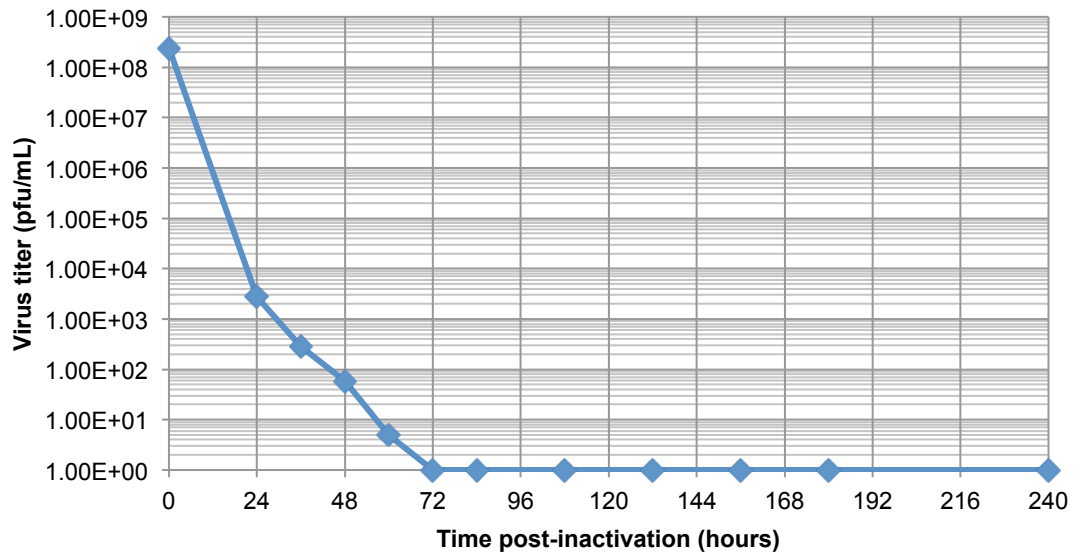


Figure 3.2 – Inactivation kinetics of purified Japanese Encephalitis virus treated with 0.05% formalin for 10 days at 22°C, for final use as a vaccine. This figure was produced using data from the literature (Srivastava et al., 2001); plaque forming units (pfu) were counted by direct assay onto cultured Vero cells.

### **3.4 *Microscale process development***

Process development, whether it is the initial development on the route to commercial licensure and manufacture or optimisation of an established process, is critical to achieving a profitable product, yet pressure exists to obtain results using minimal resources. Microscale process development allows for the rapid acquisition of large amounts of data across many different conditions using only microliter amounts of starting material. Such characterisation and development is applicable to both upstream and downstream processing. The key challenges of these microscale methods is the successful transfer to larger scale and understanding the mechanisms and limitations with which this can be done – i.e. to what extent is such work representative of commercial scale (Micheletti and Lye, 2006). Microscale development also ties in nicely with Quality by Design (QbD), which is increasingly important in the early stages of bioprocess development including vaccine production (Josefsberg and Buckland, 2012), as this development platform intrinsically allows for the creation of design spaces within which a process can be characterised.

Microscale development can range from whole processes to individual unit operations but each application often involves the use of multiple high-throughput technologies representing large scale followed by actual testing at large scale. In order to select a suitable biocatalyst, one study automated a whole microscale process involving fermentation, enzyme induction and bioconversion was performed and optimal conditions were selected for successful replication at the 2 L scale (Ferreira-Torres et al., 2005). Cell disruption to release an intracellular product from yeast was characterised in another study using adaptive focused acoustics and milligrams of test material to mimic homogenisation at laboratory scale (Wenger et al., 2008). This latter example involved some level of statistical analysis, yet the nature of microscale process development has allowed for multiple rounds of design of experiments (DoE), e.g. the screening for significant factors and subsequent optimisation in lentivirus

production in microwell suspensions (Guy et al., 2013) and in the production of firefly luciferase, also in microwells (Islam et al., 2007).

However, research exploring high-throughput microscale downstream process development for virus products is somewhat lacking though not because the downstream units, such as chromatography, have not been investigated. The broad range of available resins as well as their associated binding and elution conditions combined with the cost and time of producing test material from cell-culture requires that novel development strategies and innovative experimental techniques be developed for identifying suitable chromatographic purification strategies for biopharmaceutical manufacture. The use of high-throughput methodologies and technologies for chromatography media screening and optimisation is well-documented (Chhatre and Titchener-Hooker, 2009; Coffman et al., 2008; Hahn, 2012; Kelley et al., 2008). Such development activities are often centred around the use of a Design of Experiments approach, a multiwell platform e.g. 96-well plate experimental formats and a robotic liquid handling mechanism (Chhatre and Titchener-Hooker, 2009; Coffman et al., 2008; Kelley et al., 2008). Such is the demand for high-throughput process development of biopharmaceutical manufacturing processes that, for example, filter plates pre-packed with resins are now readily available (Bergander et al., 2008). Alternatively, chromatography resin packed into pipette tips has been used to predict laboratory scale yield and purity and outline a process for purification (Wenger et al., 2007). Two of the most recent studies using the microplate format demonstrate its use in developing purification strategies for a glycosylated protein using cation exchange and hydrophobic interaction media (Sanaie et al., 2012) and screen resins for viral clearance potential in antibody production (Connell-Crowley et al., 2013).

### **3.5 Project aims and objectives**

The literature review illustrates the variation of vaccine, and indeed JEV, production and processing but hence also the scope for process development. From this review, a

typical production process for a cell-culture derived Japanese Encephalitis whole virus purified inactivated vaccine (JE-PIV) is proposed and can be seen in Figure 3.3. The steps highlighted in red were those identified for development and investigation as part of this project: sucrose gradient centrifugation and formaldehyde inactivation. Sucrose gradient centrifugation was often cited as the primary purification step in the process described above, yet its limited scalability, labour intensiveness and inherent variability in some formats make it a target for replacement. Overall in such a production process, a formaldehyde inactivation step ultimately has one specific criterion to achieve, to render any and all pathogens in the final product replication incompetent and harmless. It could be argued from the examples above that product yields and recovery rates over the inactivation steps come a distant second to complete inactivation of the cited products and that as a result, thorough characterisation of the step also suffers. Hence the focus of this project was on these two steps with the full scope, challenges and objectives outlined as follows.

### **3.5.1 Formaldehyde inactivation of JEV**

For better process understanding, it was thought that formaldehyde inactivation of JEV required a more thorough characterisation, not only of the step itself but also its location in a production process. From this increased understanding it was hoped to be able to identify the key factors of formaldehyde inactivation of JEV, suggest potential step improvements or modifications and theorise on the effect these may have further downstream.

The challenges for this work included many variable factors requiring investigation and limited availability of fully purified JEV. As will be seen in Chapter 5, 'Formaldehyde inactivation of Japanese Encephalitis virus', these were met by using fractional factorial designs to identify significant factors at different stages of a production process maximising the amount of information acquired from limited amounts of material. Once such factors were identified, the findings were verified outside of a DoE setting and applied to settings further downstream.



### 3.5.2 Purification of JEV

After highlighting the limitations of sucrose gradient centrifugation it was decided to investigate an alternative step as the predominant purification step of a JEV production process. Scalability, variability and labour intensiveness were the principle limitations highlighted thus a technique that could address each of these was selected for investigation: bind and elute resin-based chromatography.

Although in some contrast to the formaldehyde inactivation work, in that this is more of a fundamental step change instead of improvement of an existing one, there is overlap in the challenges faced and the methods used. Despite deciding on anion exchange chromatography there were still many factors to explore such as which specific resin and binding conditions. This task of investigating multiple factors was met with the use of existing high-throughput screening (HTS) methodologies and by adapting a key product specific assay for use within such development methods. Chapter 6, 'Microscale investigation of chromatography resins for JEV purification', details this HTS approach at this scale and identifies an anion exchange resin to be taken forward for studies at larger scale in a system more closely resembling process scale. In turn, Chapter **Error! Reference source not found.**, entitled 'Chromatography scale-up of Japanese Encephalitis virus capture and elute' highlights the difficult transition from microscale HTS techniques to a pre-packed column using the same conditions. However, it is demonstrated that knowledge gained from process characterisation in Chapter 5 is used to somewhat mitigate unforeseen shortcomings of such scale-up observed in Chapter 7 when a new purification strategy was implemented.

### 3.5.3 Overarching challenges and objectives

A consistent challenge that runs through this project is that JEV is a relatively labile product, susceptible to degradation even when stored for relatively short periods of time. Another challenge was the limited availability of test material, reference material, reference standards and antibodies raised against purified JEV as will be evident in the

coming chapters. In a sense, such limited availability of materials vindicates the use of microscale and HTS methodology as well as requiring innovative adaptation of established immunoassays. These aspects will be investigated and addressed throughout the rest of this thesis but it follows that an overall objective would be to evaluate the development and investigation methods used in this project. Are these methods suitable for vaccine process development and have they contributed to a greater understanding of Japanese Encephalitis vaccine production? Overall the objectives for this project can be summarised as follows:

- Characterisation of formaldehyde inactivation of JEV to identify key factors and suggest process improvements.
- Evaluate anion exchange capture chromatography for the purification of JEV
  - Use high-throughput microscale techniques to screen for suitable resins and conditions.
  - Transfer from batch binding and elution to a larger scale more closely resembling commercial processing conditions.
- Increase overall process and product knowledge.
- Evaluate suitability of the methods used for this type of product and process.

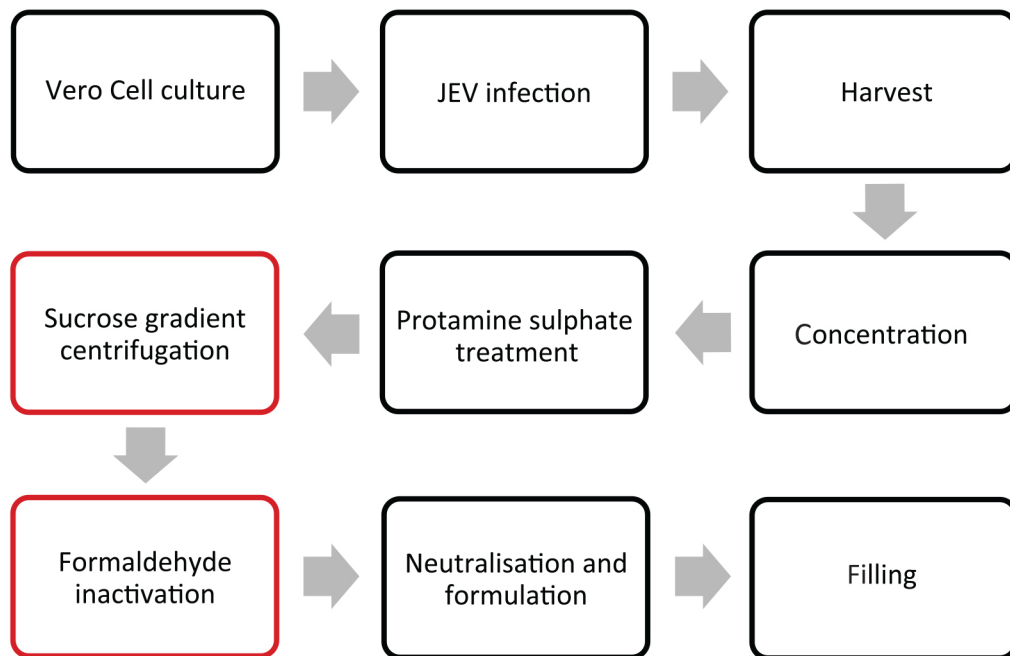


Figure 3.3- Flow schematic of a typical Japanese Encephalitis purified inactivated vaccine (JE-PIV) manufacturing process adapted from the literature (Okuda et al., 1975; Pyo Hong et al., 2001; Srivastava et al., 2001) Steps highlighted in red indicate those identified for investigation as part of this project. Sucrose gradient centrifugation is labour intensive, variable and not amenable to scale-up and anion chromatography is evaluated as a potential alternative. Characterisation of the formaldehyde inactivation step leads to greater process understanding and suggestions for improvement and potential re-location.

# 4 Materials and Methods

---

## **4.1 Working viral seed and cell banks**

A working cell bank (WCB) of Vero cells and a working viral seed bank (WVSB) of Japanese Encephalitis virus SA<sub>14</sub>-14-2 (attenuated vaccine strain) were provided by Valneva Scotland Ltd. and stored in liquid nitrogen and at -80°C, respectively, until required for use.

## **4.2 JEV production and test material**

Certain process data relating to JEV production at lab-scale in the ACBE can be found in the Appendix as highlighted below. Process analytics from the concentrating and protamine sulphate treatment of an example batch can be found in Appendix 10.3.

### **4.2.1 Cell culture**

Vero cells at passage 143 (Valneva Scotland Ltd., Livingston, U.K.) were thawed and proliferated through a minimum of 3 passages using Eagle's minimum essential medium (E-MEM, Life Technologies Ltd., Paisley U.K.) supplemented with 10% v/v foetal bovine serum (FBS, Fischer Scientific, Loughborough, U.K.), 2 mM L-glutamine (Life Technologies Ltd., Paisley U.K.) and 2.5 µg/mL Fungizone (Lonza, Slough, U.K.) at 37°C. Cell monolayers were washed with 1 x phosphate buffered saline (PBS, Fischer Scientific, Loughborough, U.K.) and removed with 0.25% trypsin-EDTA (Life Technologies Ltd., Paisley U.K.) incubation at 37°C for 5 minutes. Accumulated cell passage data can be seen in Appendix 10.1.

### **4.2.2 Viral infection and concentration of harvest pool**

After the final cell expansion, the cells were inoculated with an attenuated Japanese Encephalitis Virus strain SA<sub>14</sub>-14-2 (Valneva Scotland Ltd., Livingston, U.K.) using a

multiplicity of infection (MOI) of 0.01. The infected cells were further incubated for 9 days with harvests on days 3, 5, 7 and 9 post infection. Typical viral harvest titres can be seen in Appendix 10.2. Harvested material was filtered through 0.22 µm PVDF membranes (Millipore Ltd., Watford, U.K.) to remove cell debris and stored at 2°C - 8°C. The harvests were subsequently pooled, creating the harvest pool (HP), and, if not used in experiments at this stage, this HP concentrated approximately 18 times using a Pellicon XI 50 Biomax Polyethersulfone Polypropylene membrane (Millipore, Watford, U.K.) with a 100 kDa cut-off. The concentrated material diluted with an equal volume of PBS (Fischer Scientific, Loughborough, U.K.) and mixed. This was the concentrated harvest pool (cHP).

#### **4.2.3 Protamine Sulphate treatment**

Protamine sulphate (Sigma, Gillingham, U.K.) was added to the cHP to a nominal concentration of 2 mg/mL and the mixture incubated for 3 hours ± 1 hour at 2°C - 8°C to precipitate out host cell DNA. This material was then centrifuged at 4,000 g for 10 minutes at 4°C (Eppendorf Centrifuge 5810R) and the resulting supernatant was filtered through a 0.22 µm PVDF membrane (Millipore, Watford, U.K.) to yield protamine sulphate treated material (PST), the test material for chromatography studies.

#### **4.2.4 Storage of test material**

Test material for different experiments, either HP, cHP or PST (as defined above), was either stored for up to one week at 2 - 8°C or at -80°C for longer periods.

#### **4.2.5 Purified JEV**

Purified Japanese Encephalitis virus, used in formaldehyde inactivation studies, was provided by Valneva Scotland Ltd. (Livingston, U.K.). This material had a protein concentration of 52.11 µg/mL based on their qualified Bradford total protein assay, this

was within specification of their manufacturing process. Upon arrival at UCL it was stored at -80°C.

### **4.3 Inactivation experiments**

The material used for inactivation studies was representative of different stages in a typical production process as described in Figure 3.3: harvest pool (HP), concentrated harvest pool (cHP), protamine sulphate treated material (PST) and purified JEV. Where required, pH was altered with 1 M NaOH and 1 M HCl (both Fischer Scientific, Loughborough, U.K.). Stabilisers and additives were added to make up the final concentrations as detailed from stock solutions as follows: 20% w/v glycine, 1% v/v formaldehyde, 50% sorbitol, 50% glycerol (all Fischer Scientific, Loughborough, U.K.), 50% polyethylene glycol M<sub>n</sub> 400 (PEG), and 10% lysine (both Sigma, Gillingham, U.K.). Samples were mixed on a vortex mixer upon addition of each one and formaldehyde was always added last. Samples were incubated in incubators at temperatures above 22°C, in a fridge at 2-8°C when 4°C was required and in a water bath when 22°C was required. At the end of each inactivation, formaldehyde was neutralised with excess of solution of sodium metabisulphate (NaMe, Sigma, Gillingham, U.K.) of equivalent concentration, e.g. if 100 µL of 1% formaldehyde was required to make up to 0.02% (200 ppm or 6.65 mM) formaldehyde, 200 µL of 200 mM NaMe was used to neutralise representing twice the required amount for like for like quenching.

### **4.4 Shear experiment**

20 mL of pooled JEV harvest material was injected into an ultra-scale down shear device (UCL Biochemical Engineering, London, U.K.) and exposed to shear through a rotating disc in a sealed chamber spun at either 1000 or 6000 rpm for 30 seconds. The first such device in use had a Perspex casing (Boychyn et al., 2001; Levy et al., 1999), this experiment used a stainless steel device described later (Tait et al., 2009).

## **4.5 Chromatography resin selection & optimisation**

### **4.5.1 PreDictor Plates (G.E. Healthcare)**

Anion exchange resin screening and single media Predictor Plates (G.E. Healthcare, Amersham, U.K.) were used in this project. The 96 well resin screening plates contained 24 wells each of Cpto Q (2  $\mu\text{L}/\text{well}$ ), Cpto DEAE (2  $\mu\text{L}/\text{well}$ ), Q Sepharose Fast Flow (6  $\mu\text{L}/\text{well}$ ) and Cpto Adhere (6  $\mu\text{L}/\text{well}$ ). The single resin plates, used for wash and elution studies contained 20  $\mu\text{L}$  of the test resin in each well. The plates were prepared as per the manufacturer's instructions. Briefly, each plate was equilibrated using 3 washes of load buffer (0 – 60 mM NaCl, 50 mM tris at pHs 7.5 to 8.6, exact composition dependant on the experimental run). Load buffer and feeds were prepared in separate 96 deep well microtitre plates. The preconditioned feed for each well was prepared to the required salt concentration and pH by diluting PST by a third with the appropriate buffer and salts. Separate material was prepared and pH tested to ensure correct loading conditions.

Screening plates were loaded with 200  $\mu\text{L}$  of preconditioned feed with a protein concentration of 260  $\mu\text{g}/\text{mL} \pm 10\%$  per well, the plate was incubated on an orbital shaking platform (Model MS3, IKA, Staufen, Germany) set to 1100 rpm, with a shaking diameter of 4.5 mm at room temperature for 2 hours. This ensured complete saturation of the resin with the feed. The plate was then centrifuged at 500g for 1 minute, allowing the feed to pass through the screening plate and flow through to be collected in a separate 96 well plate. A wash step was subsequently conducted using the centrifugation conditions stated above using 200  $\mu\text{L}$  loading buffer and the wash fluid collected on to a separate 96 well plate.

The single resin plates were prepared as above, except that 290  $\mu\text{L}$  of preconditioned feed (Protein content = 186  $\mu\text{g}/\text{mL}$  for Q Sepharose FF and 259  $\mu\text{g}/\text{mL}$  for Cpto Adhere) was loaded into each well at either pH 8.0, 8.3 or 8.6, and incubated at 1100 rpm on a shaking platform for 2 hours followed by centrifugation at 500 g for 1 minute.

A separate 96 well plate was placed underneath the resin plate to collect the centrifuged flow-through. 3 washes using 200  $\mu$ L loading buffer per well were then performed prior to elution using 200  $\mu$ L of the same loading buffer but increasing NaCl concentration from 100 to 800 mM at 100 mM increments. During elution the resin was incubated for 1 minute on a 1100 rpm shaking platform followed by centrifugation at 500 g for another minute onto a separate 96 well collection plate.

#### **4.5.2 ÄKTA method**

Chromatographic JEV purification was performed on an AKTA purifier (G.E. Healthcare, Amersham, U.K.) with a 1 mL HiTrap Q Sephrose Fast Flow column (G.E. Healthcare, Amersham, U.K.). During column loading, washing and elution the flow rate was kept constant at 1 mL/min. Starting material was either buffer exchanged or diluted 1/3 with loading buffer (50 mM tris, pH 8.3 or 8.6, Sigma, Gillingham, U.K, see below). All buffers and feeds were filtered prior to use: feeds using syringe filters with 0.2  $\mu$ m PES membranes (Sartorius Stedim UK Ltd., Epsom, U.K.) and buffers using 0.22  $\mu$ m PVDF membranes (Millipore, Watford, U.K.). The column was equilibrated with at least 20 column volumes (CVs) of loading buffer prior to feed challenge.

##### **4.5.2.1 Loading and washing**

The feed was loaded onto the column at 1 mL/min with an injection loop. The column was then washed with 10 column volumes (CVs) of loading buffer. Where stated, a second post-load wash was performed using 200 mM NaCl 50 mM tris at pH 8.3 or 8.6 over 20 CVs and separated into 2 mL fractions.

##### **4.5.2.2 Elution and final wash**

Elution was performed with 400 mM NaCl 50 mM tris pH 8.3 or 8.6 over 20 CVs into 1 mL fractions. A final wash with 20 CVs 1 M NaCl 50 mM tris-base pH 8.3 or 8.6 was also performed to regenerate the resin.



### **4.5.3 Buffer exchange for AKTA chromatography**

Where stated, feeds for AKTA chromatography were buffer exchanged into loading buffer using 20 mL 50 kDa MWCO Vivaspin centrifugal units (Sartorius Stedim UK Ltd., Epsom, U.K.). 10 mL of test material was loaded into the unit with 10 mL of loading buffer then spun at 5,000g (Beckman Coulter Avanti J-E centrifuge, JS-5.3 rotor) for 10 minutes. The amount of fluid that had crossed the membrane was measured and replaced with loading buffer. This was repeated up to 6 times, depending on the volume reduction, until less than 10% of the original fluid remained (equivalent to a 10 fold buffer exchange).

## **4.6 Analytical techniques**

### **4.6.1 Plaque assay (viral infectivity plaque titre determination)**

Vero cells were thawed and passaged as described in section 4.2.1. Each well on a 6 well tissue culture plate was seeded with 3 mL of Vero cell suspension diluted to approximately  $8.4 \times 10^4$  viable cells per mL. Cells were incubated for at 37°C for 3-4 days until 95% confluent. These plates were then used for plaque assays. Virus samples were serially diluted using a 1 in 10 dilution, a maximum of 8 times (thus, effective dilutions of  $10^{-1}$  to  $10^{-8}$ ), using a volume of 200  $\mu$ L sample into 1.8 mL of plaque assay dilution media. The dilution media was composed of Eagle's Minimum Essential Medium (Life Technologies Ltd., Paisley U.K.) supplemented with 2% v/v foetal bovine serum (Fischer Scientific, Loughborough, U.K.), 2 mM L-glutamine and 2.5  $\mu$ g/mL Fungizone (Life Technologies Ltd., Paisley U.K.). The 0.2mL of the serially diluted samples were loaded onto the Vero confluent 6 well plates, alongside a negative control of dilution media. Samples were run in duplicate, with a positive control plate of WWSB ( $\approx 1 \times 10^6$  pfu/mL) and a negative control. After loading the samples at the respective dilutions (see below) onto the plates, they were incubated at 37°C for 70 minutes  $\pm$  10 minutes. After which, 3 mL of a plaque solution, Eagle's Minimum Essential Medium supplemented with, 10% FBS, 2 mM L-glutamine, 2.5

$\mu\text{g/mL}$  Fungizone and 1% w/v Sea Plaque® agarose (Lonza, Slough, U.K.) was layered onto the top of each of the wells. This was allowed to set prior to incubation for 72 hours at 37°C. After this period, each well was stained with 3 mL plaque staining solution (1% w/v Sea Plaque® agarose containing 0.02% neutral red solution (Sigma, Gillingham, U.K)) and allowed to set and incubated for a further 18 to 24 hours at which point plaques could be visualised and counted.

The sample dilutions which were loaded into the wells were as follows: standard harvest samples and harvest pool:  $10^{-3}$  to  $10^{-7}$ ; harvest inactivation DoE experiment samples:  $10^{-1}$  to  $10^{-5}$ ; other inactivation samples in section 5.1.3: 0.5 mL of neat sample; WVSB positive control:  $10^{-4}$  to  $10^{-6}$ .

#### **4.6.2 Thermo Scientific Pierce BCA Protein Assay**

BCA protein assays were performed in 96 well micro-titre plates according to manufacturer's instructions. Briefly, samples were mixed in a 1:8 ratio with the working reagent (50 parts bicinchoninic acid solution [exact composition not given] to one part 4% copper sulphate solution) and incubated at 37°C for 30 minutes. Plates were read at 562 nm in a plate reader (Safire 2, Tecan; Männedorf, Switzerland) and sample absorbances compared against a standard curve prepared using diluted bovine serum albumin (BSA) protein reference standards supplied with the kits (0 – 2 mg/mL,  $R^2 \geq 0.995$ ). Where possible BSA reference standard samples were diluted using the same buffer as the test material; all buffers were also tested as blank readings and these absorbance values were subtracted from test material readings as required. An example of a BSA standard curve can be found in Appendix 10.4.

#### **4.6.3 Life Technologies Picogreen assay**

Quant-iT™ PicoGreen® assay kits (Life Technologies, Paisley, U.K.) were used to quantify dsDNA as per the manufacturer's instructions. Briefly, samples and reference standard (bacteriophage- $\lambda$  DNA, supplied) were diluted with a working solution of 1 x tris-EDTA buffer (supplied) as required and assayed on a 96 well microtitre plate with a

1 to 1 ratio of the PicoGreen working reagent. Plates were incubated for 5 minutes at ambient temperature then excited at 483 nm and emissions were read at 525 nm in a 96 well plate reader (Safire 2, Tecan; Männedorf, Switzerland). The sample absorbances were compared against the standard curve prepared on the same plate (25 – 2000 ng/mL,  $R^2 \geq 0.995$ ). An example of the bacteriophage- $\lambda$  DNA standard curve can be found in Appendix 10.5.

#### 4.6.4 **SDS-PAGE and SilverQuest™ staining**

Sodium dodecyl sulphate polyacrylamide gel electrophoresis (SDS-PAGE) was used to separate proteins, in chromatography samples (loading, wash and elution), by size.

The JEV envelope protein should appear as a band around 52 kDa sometimes alongside the capsid and membrane proteins at 14 and 7 kDa, respectively.

Samples were loaded onto pre-cast 12 well 1.0 mm 4-12% Bis-Tris gels (Life Technologies Ltd., Paisley U.K.) with LDS (x4) sample buffer (Life Technologies Ltd., Paisley U.K.) at a 4:1 ratio, total volume loaded always <20  $\mu$ L. The gels were run in 1 x MES buffer in a Life Technologies XCell SureLock™ Novex Mini-Cell electrophoresis system (Life Technologies Ltd., Paisley U.K.) at constant voltage of 200 V for 40 minutes. Gels were removed from their casing, washed with reverse osmosis water, (pure – RO water), fixed overnight with 10% v/v acetic acid, 40% v/v ethanol and stained as per the SilverQuest staining protocol (Life Technologies Ltd., Paisley U.K.). Stained gels were scanned using a GE Image Scanner III (G.E. Healthcare, Amersham, U.K.).

#### 4.6.5 **Immunoassays**

Western blotting and enzyme-linked immunosorbent assays (ELISAs) were used to identify JEV protein bands in SDS-PAGE gels and quantify JEV antigen in samples, respectively. The anti-JEV antibodies were supplied by Valneva Scotland Ltd.

(Livingston U.K.), and were purified from sera originating from sheep and rabbits inoculated with purified formaldehyde inactivated JEV. The same batch of sheep anti-

JEV was used as the primary antibody in Western blotting and as the coating antibody in the ELISAs. Two different batches of Rabbit anti-JEV were used as the primary antibody in the ELISAs, to be used at different concentrations depending on the batch. There were also two different batches of JEV reference standard (purified formaldehyde inactivated JEV) provided by Valneva Scotland Ltd., at two different concentrations. The concentrations at which these antibodies and standards were used were based on guidance from Valneva Scotland Ltd. The secondary antibody conjugate, used in both the western blots and the ELISAs, was available commercially and also used at a concentration based on the suppliers guidelines.

#### **4.6.5.1 Western blotting**

Samples were run on SDS-PAGE gels as described above except that prior to staining they were transferred onto Novex 0.2 µm PVDF pre-cut blotting membranes (Life Technologies Ltd., Paisley U.K.) using an XCell II Blot Module (Life Technologies Ltd., Paisley U.K.) for use with the electrophoresis system described above. Transfer was performed at constant voltage of 30 V over 1 hour. Western blots were developed at room temperature on a rotating platform by first blocking for 1 hour with 1% w/v BSA (Sigma, Gillingham, U.K.) in phosphate buffered saline (0.01 M phosphate and 0.154 M sodium chloride pH 7.4, hereafter referred to as 1 x PBS) for 1 hour. The membrane was then washed 3 times with 30 mL 1 x PBS with 0.05% tween 20 (supplied by Sigma, Gillingham, U.K., the composition is hereafter referred to as PBS-T) and incubated in 30 mL of primary antibody solution (1:30,000 sheep anti-JEV (Valneva Scotland Ltd., Livingston U.K.)) for 1 hour. This primary antibody was then discarded and the membrane washed 3 times with PBST and incubated with 30 mL of the secondary antibody conjugate solution (1:10,000 donkey anti-sheep horseradish peroxidase (Stratech Scientific, Newmarket U.K.)) for 1 hour. Both the primary and secondary antibodies were diluted to the required concentrations from stocks with PBS-T. After the second incubation the liquid was discarded and membrane washed 3 times with PBST. The membrane was then incubated with 20 mL of Opti 4CN substrate

solution prepared as stated by the supplier (Bio-Rad Laboratories Ltd. Hemel Hempstead, U.K.) and left until desired band intensity has been reached then washing 3 times with purified water.

#### **4.6.5.2 JEV ELISA**

96 well microtitre plates were coated overnight ( $18 \pm 1$  hour) with 100  $\mu$ L/well 1:1,000 sheep anti-JEV (Valneva Scotland Ltd., Livingston U.K.) in carbonate buffer (0.05M  $\text{NaHCO}_3$ , pH 9.6). After washing 3 times with 300  $\mu$ L/well PBS-T remaining binding sites on the plate were blocked with 200  $\mu$ L/well 5% w/v BSA in PBS-T at 37°C for 1 hour followed by another 3 washes with 300  $\mu$ L/well PBS-T. For antigen content determination the samples and standard (purified JEV supplied by Valneva Scotland Ltd., Livingston U.K.) were loaded in triplicate alongside negative controls in a 1:3 dilution series down the plate. JEV reference standard was added at 90  $\mu$ L/well of 1:10 or 1:5, depending on batch, samples were added at 90  $\mu$ L/well with dilution depending on the sample. Once loaded plates were incubated for 1 hour at 37°C. The primary antibody, rabbit anti-JEV (Valneva Scotland Ltd., Livingston U.K.), was added, 100  $\mu$ L/well at 1:1,000 or 1:5,000 depending on the batch, and similarly incubated for 1 hour at 37°C. The plate was then washed 3 times with PBS-T and incubated with 100  $\mu$ L/well of 1:10,000 of the secondary antibody conjugate, donkey anti-rabbit-HRP (Stratech Scientific, Newmarket U.K.), at 37°C for 1 hour. 3 washes with PBS-T were applied again after incubation with the secondary antibody. The plates were incubated with the TMB substrate solution, BD OptEIA (BD Biosciences, Oxford, U.K.) for 20 minutes at 37°C after which the reaction was stopped with 2 M sulphuric acid (Fischer Scientific, Loughborough, U.K.). The plates were read at 450 nm in a plate reader (Safire 2, Tecan; Männedorf, Switzerland) plate reader and samples compared against the standard curve generated from the same plate ( $R^2 = 0.99992$ ). Dilutions and serial dilutions of samples and the reference standard was performed with 1 % BSA in PBS-T, this diluent was also the negative control.

For relative absorbance determination as used in Chapter 6 in the form of the modified ELISA, samples were diluted as required based on known concentration of the feed, with no standard loaded alongside the samples, and then treated as above.

#### **4.6.6 Zeta potential and dynamic light scattering**

A Zetasizer Nano ZS (ZEN3600, Malvern; Malvern U.K.) was used to determine zeta potential of samples and size based on dynamic light scattering (DLS). For zeta potential, samples were injected into folded capillary cells (Malvern; Malvern U.K.) using a syringe as per the manufacturer's guidelines. For size measurements, 400  $\mu$ L of sample was measured in low volume disposable cuvettes. The same standard operating procedure (SOP) was created using the instrument's software and used for all size measurements. The SOP characteristics were as follows: a size measurement of a protein sample in phosphate buffer with a 5 minute equilibration at 25°C; 5 measurements were taken at 1 minute intervals for each sample; the length of each measurement was determined automatically (default machine setting). Phosphate buffer was selected as the dispersant in the software as it most closely resembles the process material tested.

#### **4.6.7 Nanoparticle tracking analysis**

Nanoparticle tracking (NTA) analysis was performed using a Nanosight LM10 with version 2.3 of the associated software. A 1 mL syringe was used to inject 0.4 mL of the sample into the 0.29 mL chamber; the syringe was left in for stability during video capture. 3 60-second videos were recorded per sample with the camera level (an arbitrary value of 1 to 10 assigned to configurations of the camera gain and aperture length) optimised for each sample but usually between 2 and 6. A separate temperature probe was used to measure the temperature inside the chamber which was recorded at the end of each video. For the analysis of the videos, minimum particle size was set to 30 nm and the remaining options set to default.

Two data analysis methods were employed, a percentage in class measurement of particles in the 35 to 60 nm range and a particle ratio with a cut off of 80 nm. For the percentage in class calculation, the number of particles with the 35 – 60 nm range was determined as a percentage of total particles in the sample. With the particle ratio, the number of particles below 80 nm was divided by the number of particles above 80 nm. Both analyses used an average measurement from the analysis of all 3 videos from each sample.

#### **4.6.8 Amino acid sequencing**

Amino acid sequencing was outsourced to Alta Bioscience Ltd. (Birmingham, U.K.). Samples were acquired using the SDS-PAGE method described above except for dyeing with Coomassie blue as opposed to Silver Stain. Gels were removed from their casing and washed with purified water for 20 minutes, then submerged in Coomassie Blue (Bio-Rad Laboratories Ltd. Hemel Hempstead, U.K.) for an hour and finally washed in purified water again for an hour, all on a rotating platform. Desired gel bands were excised with a scalpel on light box and sent to Alta Bioscience for N-terminal sequencing. Once the results were received from the company, each potential combination of the 5 or 10 amino acid sequences were entered into the BLAST programme on the UNIPROT website ([www.uniprot.org](http://www.uniprot.org)).

#### **4.6.9 Liquid Chromatography-Mass Spectrometry protein identification**

Samples were prepared for Liquid Chromatography-Mass Spectrometry Ion trap Time of Flight (LC-MS ITTOF) analysis by running an SDS-PAGE gel with Coomassie staining, as above, and excising the required bands. The gel pieces were de-stained and trypsinised using an in-gel de-stain and digestion kit (Sigma, Gillingham, U.K.). Briefly, the excised gel pieces were covered with 200 µl of destaining solution and incubated at 37 °C for 30 minutes. The solution was removed and discarded, then this step was repeated prior to them being dried in a Speed Vac SC100 (Eppendorf,

Stevenage, U.K.) for 15 to 30 minutes. Then 20  $\mu\text{l}$  of the prepared trypsin solution (0.4  $\mu\text{g}$  of trypsin) and 50  $\mu\text{l}$  of the trypsin reaction buffer were added to each piece. The samples were incubated overnight at 37 °C then the liquid removed from each of the gel samples and transferred to a fresh container to be handed over to the UCL Wolfson Institute (London, U.K.) for analysis. The results were inconclusive and can be seen in Appendix 10.14.

#### ***4.7 Design of Experiments***

2-level fractional factorial designs were generated and analysed using Design Expert 8 (build 8.0.1, Statease Inc., Minneapolis, MN, U.S.A.) all with a minimum resolution of IV and each containing 4 centre points. The software was able to determine significant factors as described in Chapter 5.1.



# 5 Formaldehyde inactivation of Japanese Encephalitis virus

---

The inactivation step for some JE vaccine manufacturing processes is performed on purified JEV, often diluted density gradient pools. The rationale for formaldehyde inactivation during the manufacturing process is two-fold, not only to ensure that no Japanese Encephalitis Virus in the final drug substance is able to replicate but also that adventitious agents (viruses, bacteria or other pathogens...) which may have been accidentally introduced during manufacture are unable to propagate. Potential sources of such contamination could include animal derived products used during production (e.g. foetal bovine serum) that could contain adventitious agents and dormant or as yet uncharacterised pathogens that could lie within the cell and virus banks. Ultimately the robustness of this step will be judged on its ability to inactivate any such biological contaminants whilst minimising product losses. Although the final inactivation step in licensed vaccines is benchmarked on a panel of viruses, the work here focused on the impact formaldehyde inactivation had on JEV product recovery. The formaldehyde inactivation step was identified as a target for improvement due to product losses observed over extended inactivation periods and it was seen as an opportunity to reduce the overall processing time for such inactivation steps. The objective was to keep formaldehyde as the method of inactivation but investigate different conditions in an attempt to improve antigen recovery over the course of the step, increase process knowledge and consider the use of additives. In this instance of formaldehyde inactivation, additives, or stabilisers, were compounds generally regarded as safe (GRAS) which could be included in the inactivation step to increase product recovery

without compromising the step's potential to inactivate the virus and aforementioned pathogens.

As previously discussed, the theory underlying formaldehyde inactivation is based on the molecule's ability to cross-link proteins; this action on the envelope or capsid of a virus nullifies the virus' ability to disassociate and introduce nucleic acids into the host cell. More specifically, this is done by disrupting the potential for receptor-mediated endocytosis and nucleic acids being unable to leave the nucleocapsid due to the cross-linking of its structural proteins. It is also possible that the formaldehyde also crosslinks the nucleic acids to the capsid proteins. Whilst this cross-linking is beneficial when acting more internally on virus particles, their surface antigens on the virus envelope will also be affected, possibly more so due to their increased exposure to the medium. These structural changes could negatively impact on sites expected to be recognised by the immune system of the vaccine recipient and effectively result in product losses.

It is possible that the inclusion of additives within this step might be able to mitigate these losses without compromising inactivation. Glycine and sorbitol have previously been used in JEV vaccine production as stabilisers during inactivation and storage (Toriniwa and Komiya, 2008) and therefore were initially tested alongside other common stabilisers; polyethylene glycol (PEG), lysine and glycerol. It has been speculated that the addition of these stabilisers help to reduce loss due to aggregation, though little is known about the specific mechanism of action.

When situated towards the end of the manufacturing process, as the penultimate step prior to formulation, the purified product has high value making losses important to avoid. With inactivation and the inherent product losses owing to it inevitable, there is already a case for carrying out inactivation at an earlier stage in the process.

Characterisation of formaldehyde inactivation of JEV at the start and the end of the vaccine production process was undertaken using design of experiments-based investigations to determine significant factors. The principle assessment techniques

were antigen recovery and JEV inactivation using ELISAs and plaque assays, respectively; though particle sizing was also investigated in an attempt to identify possible sources of aggregation.

## **5.1 Inactivation Results**

The characterisation of formaldehyde inactivation of Japanese Encephalitis Virus was carried out initially with fractional 2-level factorial investigations, giving the opportunity to screen numerous factors simultaneously, followed by confirmation of findings. Fractional 2-level factorial designs are used to identify significant factors and interactions between factors within a particular design space without having to investigate all possible combinations of those factors. As the name implies, this is done by experimenting with the factors at 2 levels, high (+1) and low (-1), where the selected subset of experimental conditions chosen is a fraction of the total number of experiments required for a full-factorial design. A full 2-level factorial would have  $2^x$  sets of experimental conditions (where  $x$  = the number of factors) but a fractional factorial, in this case, would be suitable to identify main effects as well as any likely interactions between effects but with a significantly reduced number of experimental conditions. For example the first investigation below looked at 8 different factors over 2 levels, a full factorial would involve 256 different sets of conditions but the fractional factorial involved just 32 but identified the main effects and interactions out of those measured. This reduction is generally successful due to the scarcity-of-effects principle, which states that most systems are dominated by a few factors and low-order interactions (interactions between 2 factors) while high-order interactions (those involving 3 or more factors) are extremely rare and can be ignored (Montgomery, 2009). The ability of this type of experimental design to be able to distinguish between single effects, low-order and high-order interactions is dependent on its resolution, with higher resolutions requiring more runs.

The initial experimental designs for these sets of experiments were constructed and analysed using Design Expert 8 software (build 8.0.1). The designs had a resolution of IV and each included 4 centre points. Resolution IV allows for identification of main effects without them being aliased with 2 factor (or higher) interactions but two factor interactions can be aliased against each other as well as higher-order interactions (Montgomery, 2009). In other words, in order for these fractional factorial designs to have a reduced number of runs, any observed interaction effects involving more than one factor were aliased to other such interactions as fewer combinations can be accounted for at lower resolutions. Therefore combining the factors at different levels in such a way to accommodate this desired resolution created the individual sets of conditions, or runs. It should be noted that for the design to work all runs should be completed to have adequate data to identify significant factors for each response.

The details for each design, including lists of aliases can be found in the Appendices as detailed. Centre points are included in designs without replicates to estimate the experimental and analytical error without significantly increasing the number of runs.

The effect of a factor is numerically determined by the change in average response when a factor goes from its low level (-1) to its high level (+1), which can be either positive or negative. Significant effects, or factors and combinations thereof, were elucidated for each response below using half-normal probability plots. Whereby absolute values of the effects are plotted against their cumulative normal probabilities, a straight line is always included representing the estimated normal distribution.

Factors that line-up to the bottom left of the plot are effectively noise, used in the estimation of error, whereas factors in the top right, distinctly apart from the line, are significant terms which can be included in a model should one be chosen. The half-normal probability plots allowed for easy and rapid determination of significant factors and interactions for each response. In terms of aliasing, where two or more factors were involved in an interaction, the software allowed the user to select which combinations of factors they deemed most probable.

The selection of each factor's high and low levels for each experiment was based on a combination of practicality, previously published studies, common sense and desire for reliable effects estimations. The latter of these reasons is the possibly the only one of the four which requires an explanation – simply speaking when dealing with single replicate designs one cannot be wholly sure that the observed effect is reflective of the true effect or an artefact of error. To a certain extent the inclusion of centre points, help resolve this problem, but increasing the distance between the high and low adds further robustness to the estimation of effects. This can be seen below with the investigation of the stabilisers whereby a ten-fold difference between the low and the high levels was used.

### **5.1.1 Formaldehyde treatment of purified JEV**

The first examination of formaldehyde inactivation was performed using purified JEV, providing results under limited influence from other components of the process material; thus, experimentation at this stage of the process was more directly representative of formaldehyde inactivation of JEV than at any other stage of the manufacturing process.

8 factors were each observed at 3 levels (-1, 0 and +1) as detailed in Table 5.1 alongside the coded term that represents the factor in this particular design.

Formaldehyde concentration was expected to have to the most negative impact on antigen recovery but it was also assumed that at higher formaldehyde concentrations the JEV would be inactivated more rapidly. Personal communications from Valneva suggested that JEV inactivation and stability are pH sensitive thus, this was included in the investigation with the range confined to pH 7-9. Temperature was also explored between a range of 22°C and 37°C as the high and low, respectively, with the rationale being related to inactivation kinetics in that despite a potential increases in product losses, more rapid inactivation of viruses would occur at higher temperatures. The 5 potential stabilisers investigated at this stage are all standard GRAS additives used in

the pharmaceutical industry with glycine and sorbitol having previously been explored for inactivation studies. (Toriniwa and Komiya, 2008).

Factor	DoE coded term	Level		
		-1	0	+1
Formaldehyde concentration (v/v %)	A	0.02	0.03	0.04
pH	B	7	8	9
Temperature (°C)	C	22	28.5	35
Glycine (w/v %)	D	0.05	0.275	0.5
Lysine (w/v %)	E	0.05	0.275	0.5
Sorbitol (w/v %)	F	0.1	0.55	1
Glycerol (v/v %)	G	0.1	0.55	1
PEG (v/v %)	H	0.1	0.55	1

Table 5.1 – factors for 2-level fractional factorial experiment with purified JEV, together with their respective coded terms and value at each level.

Using the Design Expert software a fractional factorial design was produced encompassing 36 experimental runs of which 4 were centre points (level 0) with identical conditions and 32 were completely individual sets of conditions each with different combinations of -1 and +1 levels. The conditions were implemented as described for 96 hours before quenching the formaldehyde inactivation with an excess of sodium metabisulphite. The experiment was allowed to run for 96 hours as this is a point at which all JEV was assumed to be inactivated, based on data from the literature as shown in Figure 3.2. The full details of the experimental design can be found in Appendices 10.6 (design summary), 10.8 (design evaluation) and 10.9 (conditions and results).

Figure 5.1 shows a half-normal probability plot obtained after inputting the ELISA data from each of the 36 experimental runs back into the Design Expert. Unsurprisingly,

formaldehyde concentration was shown to have the largest overall negative effect on antigen recovery as the cross linking effect would be indiscriminate and also alter the surface antigens. Temperature was deemed to have no significant effect on antigen recovery within the range observed. Glycine was by far the best performing stabiliser, with glycerol and sorbitol also shown to have minor beneficial effects. Glycine was also involved in an interaction with glycerol, where increases in both factors help reduce antigen losses. However, as stated, the resolution of this design still allows for some aliasing to occur between interactions and so careful interpretation of each potential interaction is required. In the case of glycine and glycerol (DG), the aliased interactions are temperature and sorbitol (CF) and formaldehyde concentration and pH (AB). The AB interaction would suggest that the antigen losses observed when increasing formaldehyde concentration could be somewhat mitigated by also increasing the pH. CF is unlikely as temperature is not identified as significant and sorbitol only has a minor effect. Therefore DG is much more plausible, than both instances, as glycine and glycerol are stabilisers, which were also shown to have positive effects individually; therefore combining the two should also be beneficial. Another less significant but negative interaction was highlighted with formaldehyde concentration and glycine (AD), a feasible consideration due to having already identified glycine as a stabiliser and the strong negative effect of increasing formaldehyde. This interaction serves to reinforce the individual identification of formaldehyde and glycine and demonstrates that glycine reduces the magnitude of the formaldehyde's negative effect. However, this argument could work both ways in that the benefits of glycine could be reversed in the presence of too much formaldehyde. This formaldehyde concentration and glycine (AD) interaction was aliased with pH and glycerol (BG) as well as lysine, sorbitol and PEG (EFH) both of which are extremely unlikely as none of those factors, except for glycerol as a positive effect, are identified as significant on their own.

Design-Expert® Software  
antigen

▲ Error estimates

Shapiro-Wilk test  
W-value = 0.971  
p-value = 0.687

A: Formaldehyde concentration  
B: pH  
C: Temperature  
D: Glycine  
E: Lysine  
F: Sorbitol  
G: Glycerol  
H: PEG

■ Positive Effects  
■ Negative Effects

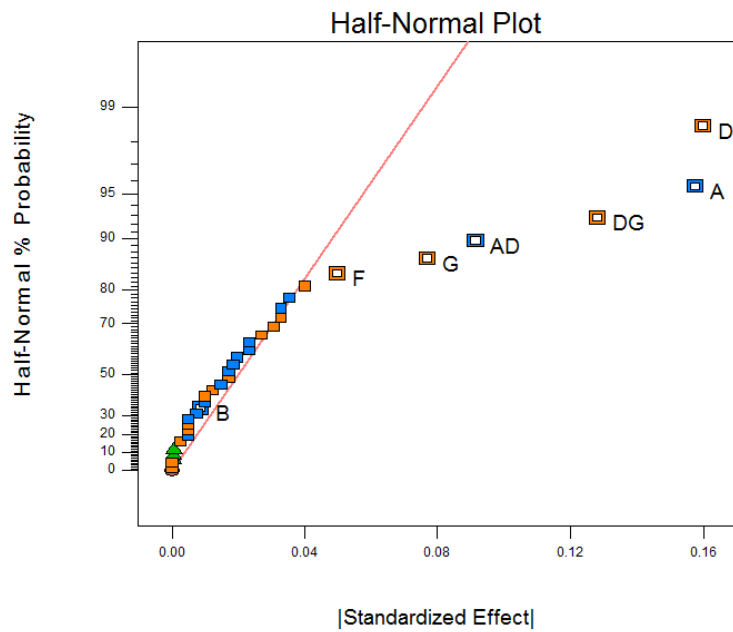


Figure 5.1 – Antigen concentration response Half-Normal probability plot from formaldehyde inactivation experiment with purified JEV. The factors highlighted, with their coded terms evident, are those deemed to be statistically significant as they deviate from the normal distribution as defined by the software. The factors are split into two colours according to the overall effect of switching to their higher level, orange for positive (more antigen) and blue for negative (less antigen). Note that due to the design the following interactions are aliased: DG is aliased to CF and AB; and AD is aliased to BG and EFH. DG and AD were highlighted because they are the most likely to be responsible for significant effects as one or both of the terms had already been singled out as such.



## 5.1.2 Formaldehyde treatment of harvest material

The first experiment focused on optimising the step as it is found in some production processes with relatively minor adjustments on purified virus prior to formulation. Viral inactivation is also sometimes conducted after a concentration step in order to reduce the volumes of formaldehyde required. However, it could be suggested that formaldehyde treated virus particles are more robust due to the cross-linking effect of the formaldehyde and potentially then able to resist process damage experienced further downstream. Therefore, it may be advantageous to inactivate the virus particles further upstream prior to sucrose gradient centrifugation in order to increase overall recovery. However, the material is very different at this stage as the virus will be less concentrated (around 10 fold) and there will be no residual sucrose or concentrated co-contaminants that may have carried over from gradient centrifugation step.

Another 2-level fractional factorial experiment was designed for pooled JEV harvest material. Figure 3.3 shows that the process material at this stage has undergone no purification other than clarification by filtration through a 0.22 µm membrane to remove cell debris. Table 5.2 shows the details of each factor and their respective levels.

Fewer factors, 6, were included in this instance, with lysine glycerol and PEG removed and formaldehyde incubation time included. Lysine and PEG were shown to have no effect on purified material in the previous experiment and thus were excluded. Glycerol was also removed despite showing a slight benefit in the previous experiment as it was decided to reduce the number of factors overall but to investigate more responses (see below). Although, sorbitol was left in because of evidence in the literature which states that including sorbitol and glycine can increase antigen recovery during formaldehyde inactivation of JEV (Toriniwa and Komiya, 2008); pH also remained due to the potential interaction effect described above in 5.1.1. Time was included as a factor in an attempt to gauge whether any factors became more significant the longer inactivation proceeded. Temperature and formaldehyde concentration were included again but with

a larger range between levels for broader investigation, this is especially relevant for temperature as some viral inactivation procedures are performed at 4°C.

The resulting design contained 16 different sets of conditions and 4 centre points with the same resolution as previous allowing for individual factors to be singled out a significant and only potential interactions aliased to each other. A design summary from the experiment can be found in Appendix 10.10 and a design evaluation, together with a list of aliased terms, can be found in Appendix 10.11.

Factor	DoE coded term	Level		
		-1	0	+1
Time	A	24	60	96
pH	B	7	8	9
Temperature (°C)	C	4	20.5	37
Formaldehyde concentration (v/v %)	D	0.01	0.03	0.05
Glycine (w/v %)	E	0.1	0.55	1
Sorbitol (w/v %)	F	0.1	0.55	1

Table 5.2 – factors for 2-level fractional factorial experiment with JEV harvest material, together with their respective coded terms and value at each level.

As stated, more responses were included with this experiment. In addition to antigen recovery the following responses were also measured: infectivity (measured by plaque assay and defined as plaque forming units per millilitre (pfu/mL)), size (measured by dynamic light scattering (DLS) and nanoparticle tracking analysis (NTA)) and the electrophoretic properties of the samples (measured by Malvern Nano ZS zetasizer).

Measuring infectivity as a response was contingent on including time as factor to potentially gain an understanding of inactivation kinetics under different conditions. The

high level was set at 96 hours, the level after which there is unlikely to be any remaining infective JEV particles, as can be seen in Figure 3.2.

The electrophoretic properties (zeta potential, mobility and conductivity) of the samples were measured in an effort to observe if any of factors altered the stability of the medium in this way. As it transpired no significant differences were witnessed for these responses within this design space and therefore they are not discussed in detail below. Two particle sizing methods were also used, DLS for average particle size in the samples and NTA for particle size distribution between 10 and 1000 nm. The DLS results are discussed below. However, no significant results were obtained from the NTA analyses. One result was a percentage in class analysis of the number of particles within a 35 – 60 nm size range. This produced no significant changes across the observed conditions. The other result was an attempt to distinguish the samples based on a particle ratio, divided at an 80 nm cut off. Again, no significant effects for this response were identified, which was somewhat at odds with the DLS observations as will be discussed below.

A complete list of the experimental conditions and the results obtained for each can be found in Appendix 10.12.

#### **5.1.2.1 Infectivity**

From the 20 sets of conditions, just 5 were found to contain infective JEV particles by yielding positive results in the plaque assays. This response is too small a sample set for the statistical software to generate a half-normal probability plot, as 15 samples gave a zero result. Therefore, Figure 5.2 shows these results as a bar chart of the results with the details of each set of conditions. The only correlation that can be drawn is that all of the samples containing active JEV underwent a 4°C incubation and only one, with the lowest infectivity, included formaldehyde at the high concentration. However this run also included glycine (at +1), which as we have observed from Figure 5.1 reduces the net negative effect of formaldehyde and might go some way to

providing an explanation as to why this sample still contained some infective JEV.

Perhaps the inactivation potential of the increased level of formaldehyde was mitigated somewhat in the presence of higher levels of glycine.

The 3 remaining runs at low temperature, of the 8 in total, which did not exhibit any viral infectivity all had increased formaldehyde concentration. From this it can be assumed that the two most significant factors in terms of infectivity are temperature and formaldehyde concentration, respectively; from what is known of the mode of action of formaldehyde inactivation it is unlikely that any of the other factors were significant.

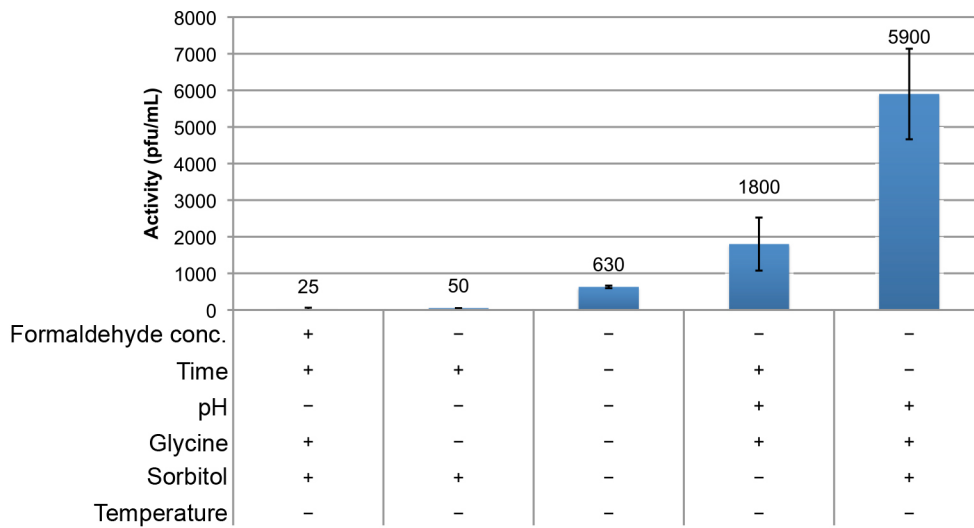


Figure 5.2 – Details of samples still found to contain active JEV particles. The + and –symbols correspond to the high (+1) and low (-1) values for each factor, as detailed in Table 5.2. Error bars are based on standard deviation across 2 plaque assay plates.

### 5.1.2.2 Antigen recovery

As with the previous experiment the antigen content of the samples was measured by ELISA. The half-normal plot of the results from DX8 can be seen in Figure 5.3. Immediately apparent is that fewer significant factors affecting antigen recovery were identified with this experiment on harvest material than with purified JEV, with 3 factors having a negative effect and one interaction having a slightly positive effect. The most significant factor for this response was deemed to be temperature followed by formaldehyde concentration and time, respectively, all of which negatively impacted on the antigen content of the samples when their levels were increased. These results follow expected logic that measurable antigen was reduced by increased exposure (time), increased concentration of the cross-linking agent (formaldehyde) and increased energy in the system (temperature). Consistent with the previous experiment, formaldehyde was also a significant factor though not temperature, most likely due to the much smaller difference between levels used previously. The only, albeit small, positive effect observed was an apparent interaction between glycine and sorbitol. Both factors were also singled out individually as reducing antigen losses during formaldehyde inactivation of purified material, but this interaction effect is more in line with the literature (Toriniwa and Komiya, 2008). As with all possible interactions in these designs, this positive effect glycine and sorbitol interaction (EF) is aliased to time and formaldehyde (AD). As these have both been shown to significantly impact negatively on antigen recovery as individual factors, it is extremely unlikely that such an interaction would have a beneficial effect.

Design-Expert® Software  
Antigen

▲ Error estimates

Shapiro-Wilk test

W-value = 0.929

p-value = 0.470

A: Time

B: pH

C: Temperature

D: Formaldehyde conc

E: Sorbitol

F: Glycine

■ Positive Effects

■ Negative Effects

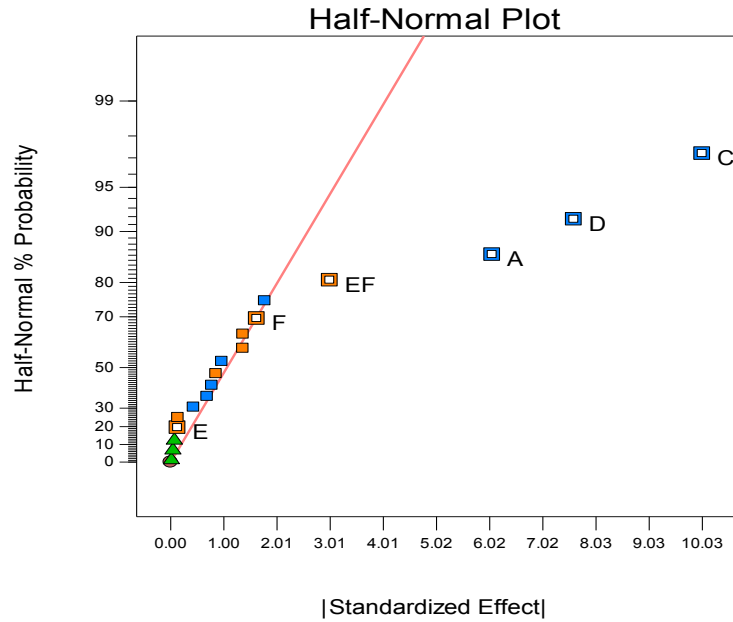


Figure 5.3 – Antigen concentration response Half-Normal probability plot from formaldehyde inactivation experiment with JEV harvest material. As in Figure 5.1, the factors highlighted, with their coded terms evident, are those deemed to be statistically significant as they deviate from the normal distribution as defined by the software. The factors are split into two colours according to the overall effect of switching to their higher level, orange for positive (more antigen) and blue for negative (less antigen). Note that due to the design the positive EF interaction is aliased to AD.

### 5.1.2.3 Average particle size

In order to gain greater understanding of the cross-linking effect of formaldehyde and whether it could affect particle aggregation levels at this early stage of the process, dynamic light scattering (DLS) was used to determine the size distribution of particles in the samples. The samples were by no means homogenous, despite this pooled harvest material having been filtered through a pore size of 0.22  $\mu\text{m}$ , they contained a wide particle size distribution up until this diameter. This is illustrated by the fact that the polydispersity index (PDI) for these samples averaged 0.485. The PDI is a dimensionless number calculated from a 2 parameter fit to the correlation data, effectively all the readings from a particular sample. It is scaled such that values smaller than 0.05 are rarely seen other than with highly monodisperse standards and values above 0.7 indicate that the sample has a very broad size distribution and is probably not suitable for DLS analysis (Zetasizer Nano Series User Manual, 2004). Thus the DLS results inputted into the software represented the average particle size of all the size populations in a sample as opposed to having a homogenous sample of particle of the size measured.

Figure 5.4 shows the half-normal plot of the data fed into DX8. In this instance temperature and time are the two standout factors which, when increased, contribute to increasing the average particle size in the samples. Furthermore they are the most likely factors for the interaction effect also observed, as the aliased interaction is pH and sorbitol (BE). This response follows similar logic to that described for the antigen recovery, if one assumes that the particles in solution increase in size due to aggregation, simple Brownian motion dictates that increased time and energy in the system will promote this process.

As with the antigen recovery, the only factor that appeared to mitigate an increase in particle size, was the interaction effect of glycine and sorbitol, again with only a slight effect compared to the main effects. Having the same significant factors for two different responses not only to a certain extent validate the results but also suggests a



link between the two. From the data, it could be suggested that alongside the product losses due to formaldehyde cross-linking antigen sites, major losses could also be due to aggregation phenomena brought about by increases in temperature over extended periods of time. Temperature was been singled out as a significant factor in all of the above analyses except for the experiment on purified JEV where the difference between the measured levels was potentially too small to register an effect.

Design-Expert® Software  
Size DLS

▲ Error estimates

Shapiro-Wilk test

W-value = 0.918

p-value = 0.454

A: Time

B: pH

C: Temperature

D: Formaldehyde conc

E: Sorbitol

F: Glycine

■ Positive Effects

■ Negative Effects

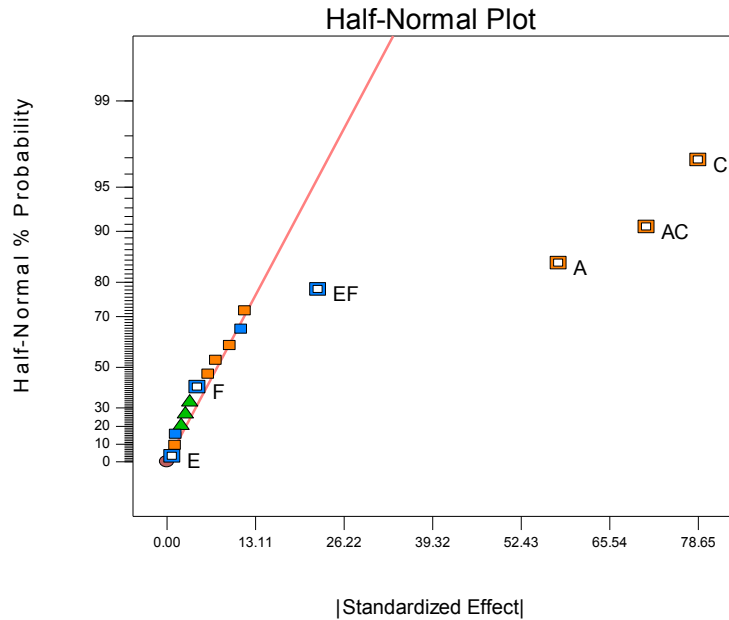


Figure 5.4 – Dynamic light scattering response Half-Normal probability plot from formaldehyde inactivation experiment with JEV harvest material. As with the two previous figures, the factors highlighted, with their coded terms evident, are those deemed to be statistically significant as they deviate from the normal distribution as defined by the software. The factors are split into two colours according to the overall effect of switching to their higher level, orange for positive (average particle size increases) and blue for negative (average particle size decreases). Note that due to the design the positive AC interaction is aliased to BE and EF is aliased to AD.

### 5.1.3 Interpretation of DoE results

The 2-level factorial experiments described above helped characterise formaldehyde inactivation at the start and end of a production and purification process for JEV. Overall the analysis is consistent with literature in that during the inactivation process, time, temperature and formaldehyde were all significant factors; increasing these dominant factors will always serve to reduce antigen recovery. Perhaps more unexpected is the effect of glycine, the potential role of which would be to mitigate these losses. Although singled out in the literature (Toriniwa and Komiya, 2008) as a stabiliser during formaldehyde inactivation and as a storage stabiliser alongside sorbitol, glycine in this study showed only a comparatively small effect as an interaction with sorbitol on harvest material but a very significant effect on retaining the antigenic sites with purified JEV. The mechanism has also somewhat been alluded to as the presence of glycine serves to reduce the average particle size and therefore may be reducing aggregation. Therefore an attempt was made to ascertain the usefulness of glycine during inactivation at various stages of the purification process. Additionally, should the inactivation step be brought further upstream there could also be some benefit in processing more robust viral particles brought about by the cross-linking effect of formaldehyde treatment. An ultra-scale down shear device, which has been shown to mimic the shear experienced in the feed zones of industrial scale centrifuges (Boychyn et al., 2004; Hutchinson and Bingham, 2006; Tait et al., 2009), was used to determine the effect of shear on formaldehyde treated harvest material and non-treated material.

#### 5.1.3.1 Glycine

Glycine was shown to be the most significant factor in the experiment with purified JEV but only has a slight benefit in conjunction with sorbitol when formaldehyde treating harvest material. A possible reason for this could be that harvest material, by definition, contains so many more impurities alongside a much lower concentration (~10 fold) of virus particles, creating a situation where the formaldehyde and glycine then have more

components to interact with but much less JEV – therefore any possible beneficial effects could pass unnoticed.

It was decided to initially test the interaction effect between formaldehyde and glycine. In the first instance pooled harvest material (HP) was exposed to 0.02% (200 ppm) formaldehyde over 96 hours at 20°C in the presence and absence of glycine at two concentrations of 0.5% and 2%. This was to see if the excess glycine (2%) would overcome the issue of high levels of impurities. In order to ensure inactivation of JEV, the infectivity was tested: all those treated with formaldehyde were shown to contain no plaque forming units at the end of the experiment. The non-treated HP, however, contained 9630 pfu/mL down from  $2.3 \times 10^5$  pfu/mL at the start of the experiment. This represent a reduction in infectivity of over 95% from 4 days at 20°C with no additives and highlights the instability of JEV at ambient temperature.

Figure 5.5 shows the antigen content of each of the samples after the incubation period, sample HP was a control sample with no additives. The chart demonstrates that neither the 0.5% nor the 2% additions of glycine had any significant effect on reducing the losses due to exposure to formaldehyde – the slight benefit observed with 0.5% glycine is within error range of the sample containing just 0.02% formaldehyde. As stated, perhaps at this stage, due to the small concentrations of measurable antigen, any benefits due to glycine may not yet be distinguishable. In order to further investigate the issue the concentration of virus particles must be increased, however, the test material ceases to be process equivalent harvest material. Therefore the testing should move on to after the next step in this purification process, concentrating the harvest material where we obtained concentrated harvest pool (cHP).

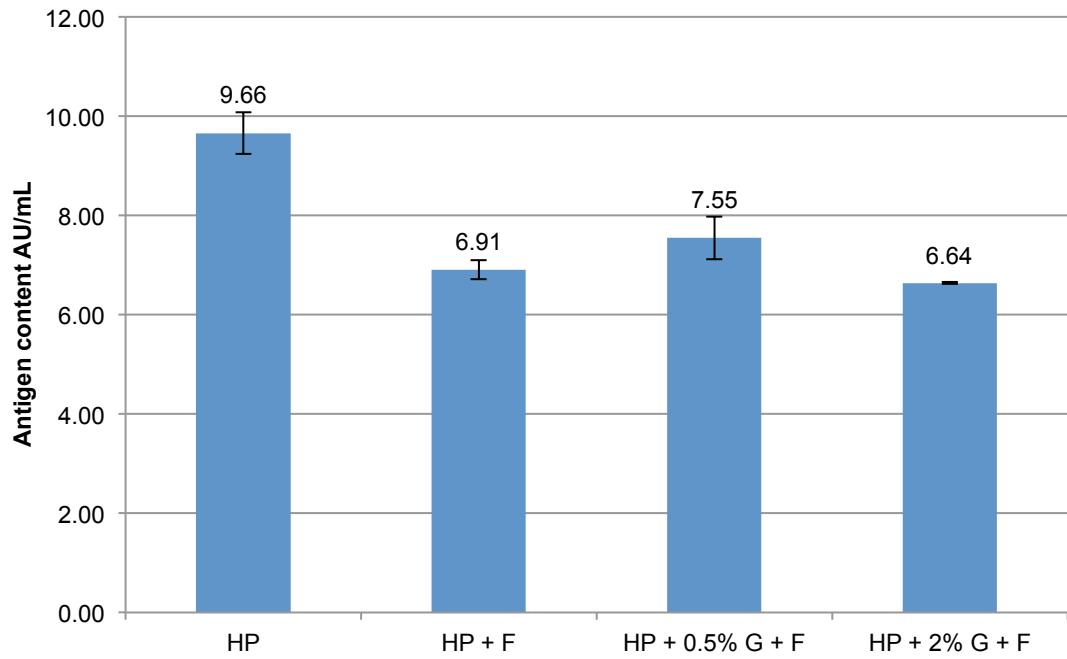


Figure 5.5 – ELISA antigen data of JEV harvest material, with and without 0.02% formaldehyde and glycine at different concentrations over 96 hours at 20°C. Key: HP = harvest pool, F = 0.02% formaldehyde, G = glycine.

In addition to investigating the effect of glycine during formaldehyde inactivation of cHP, there is one other purification step, apart from sucrose gradient centrifugation, after which there is a hold point that could be used for inactivation. This is the protamine sulphate precipitation step used to remove host cell DNA. As previously described, this is where cHP is incubated with protamine sulphate. DNA precipitates with the protamine sulphate and the material is then centrifuged with the supernatant kept for further processing, this is protamine sulphated treated material (PST). The next step in the process is sucrose gradient centrifugation (SGC), which was not available for purifying this virus at UCL at the time. However, in order to mimic the effect of post SGC material, 5%v/v sucrose was added to the PST. The 5% sucrose value is based on values from the literature which state that JEV would band just below 40% sucrose (Sugawara et al., 2002) and the resulting pooled fractions would be diluted approximately 8 times (Srivastava et al., 2001). This separation of variables allowed for the independent testing of the effect of concentrated virus and glycine-sucrose interaction effects on antigen recovery.

Concentrated harvest pool (cHP), protamine sulphate treated material (PST) and PST with 5% sucrose were all exposed to 0.02% formaldehyde over 96 hours at 20°C with and without 0.5% glycine. 3 controls with no formaldehyde or stabilisers added were also examined as part of this experiment: starting cHP, starting PST and cHP incubated alongside the formaldehyde treated samples. The infectivity of all samples and the two cHP controls was tested, the infectivity of the PST was not tested. All formaldehyde treated samples were shown to contain no active virus particles. The cHP control sample infectivity dropped from  $6.6 \times 10^5$  pfu/mL to  $1 \times 10^5$  pfu/mL over the course of the 4 day incubation at 20°C, an 85% drop in active virus particles.

Figure 5.6 shows the antigen data for each of the samples alongside the 3 controls, starting cHP and PST (st exp) as well as cHP incubated alongside the other samples with no additives. The 3 controls illustrate potential product losses observed during general processing and storage at 20°C. The treatment of concentrated harvest pool

with protamine sulphate incurred antigen losses of approximately 35% in this instance, as can be seen in by the drop in antigen content between '*cHP st exp*' to '*PST st exp*'. The incubation of cHP over 96 hours at 20°C equated to losses of approximately 30%, as shown by the drop between '*cHP st exp*' and '*1-cHP*'.

With the samples which underwent the formaldehyde treatment, there is clear evidence of the effect that glycine had in preserving the antigen sites at the cHP and PST stages of the process with 20% and 30% less antigen lost, respectively. Perhaps more surprising are the significant losses observed when PST material is exposed to formaldehyde, around 95% of the antigen lost without glycine and approximately 63% with glycine – thus reasoning a prohibition on formaldehyde treatment at this stage. The addition of 5% sucrose does not seem to have an effect with or without glycine, ruling out the possibility of it having a stabilising effect.

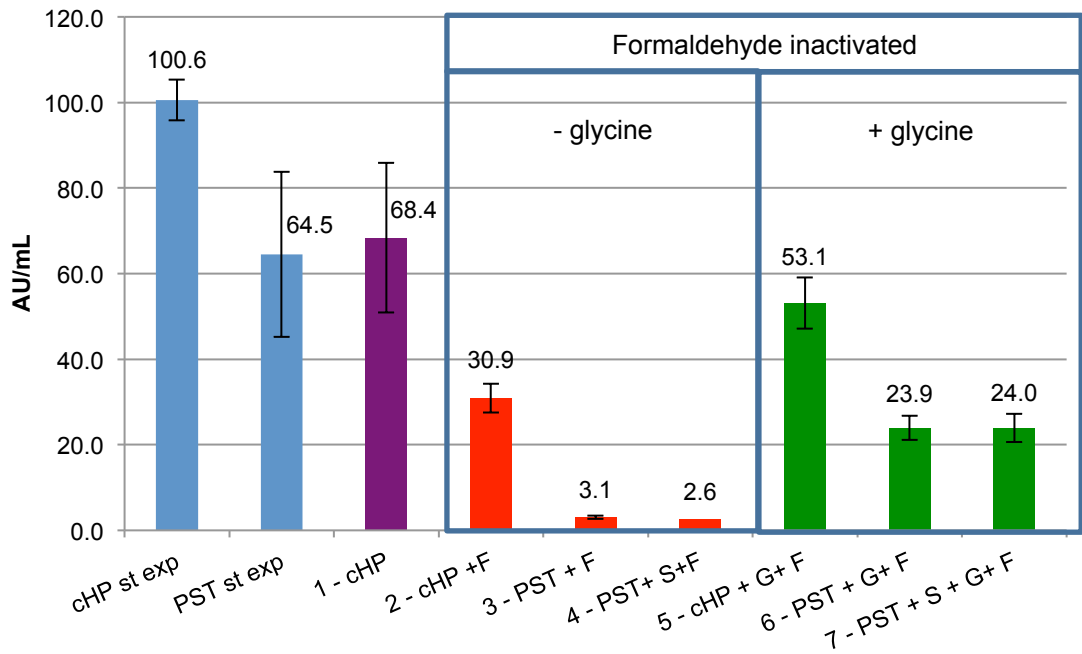


Figure 5.6 – ELISA data showing the effect of glycine during formaldehyde treatment at different stages of the JEV purification process. Key: st exp = start of the experiment, cHP = concentrated harvest pool, PST = protamine sulphate treated material, F = 0.02% formaldehyde, G = 0.5% glycine, S = 5% sucrose. Samples 1 to 7 underwent the incubation at 20°C for 96 hours, sample 1 was a control with no formaldehyde or stabilisers added.



### **5.1.3.2 Effect of shear**

Harvest material was again treated with 0.02% formaldehyde and incubated for 96 hours at 20°C, this treated material, along with non-treated harvest material, was exposed to low (1000 rpm) and high (6000 rpm) shear levels for 30 seconds in an ultra-scale down shear device. The rpm relates to the rotation speed of the disc inside the device which mimics the effect of shear found during processing, 6000 rpm is approximately equivalent to the stresses found in the feed zone of hermetic disc stack centrifuge (Hutchinson and Bingham, 2006). Figure 5.7 shows the ELISA results and the relative antigen recovery compared with the non-sheared samples. It would appear that there is no significant effect of formaldehyde treated material being able to better withstand stand the forces than the non-treated material, with the recovery rates within the error range. These results do however show that in general, harvest material is not significantly impacted by these high shear forces, with losses of just around 10% observed, in both instances.

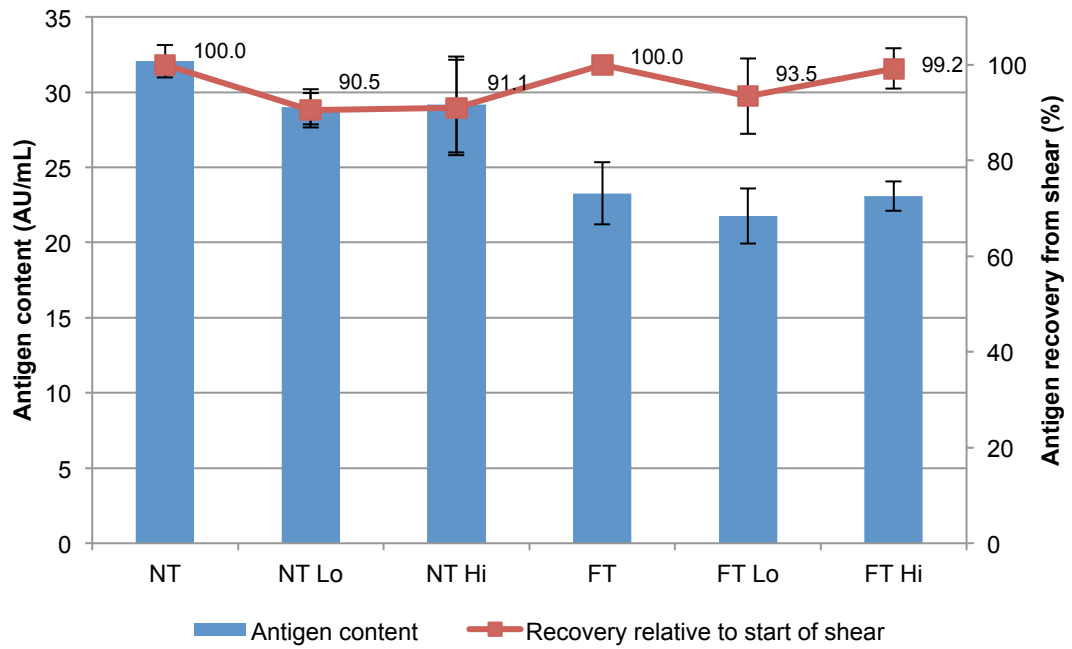


Figure 5.7 – Antigen recovery data from non- and formaldehyde treated harvest material exposed to high and low shear in an ultra scale down shear device. Key: NT = non-treated, FT = Formaldehyde treated, Lo = 1000 rpm, Hi = 6000 rpm

## **5.2 Formaldehyde treatment discussion**

Across the results from this formaldehyde inactivation investigation, the consistently significant factors for antigen recovery, infectivity and particle size are formaldehyde concentration, glycine and, arguably, temperature. Although temperature variation did not significantly effect the inactivation of purified JEV, this was investigated across a smaller range – 22°C to 35°C appeared to have no effect but 4°C to 37°C definitely did. Temperature is certainly the key factor for the responses of infectivity, antigen recovery and particle size with treatment of harvest material. Furthermore, temperature has previously been shown to be a key factor in adenovirus aggregation (Galdiero, 1979). Therefore, discounting formaldehyde concentration for the moment, the significant factors for both antigen recovery and particle size distribution are similar. Even in rank, it is possible to determine that antigen recovery and aggregation are strongly related within this system. Viral antigen losses due to aggregation that are driven by increases in temperature should be seen as a major concern for JEV processing and indeed any virus production process. Moreover, with the sorbitol and glycine interaction singled out as slightly benefiting antigen recovery as well as slightly showing to affect a reduction in observed particle size perhaps this positive outcome is owing to their ability to jointly mitigate aggregation. The caveat to this theory, however, is the lack of correlation with the electrical properties of the samples, which in turn showed no significance within the design and indeed very little evidence of variation across all the conditions (Appendix 10.12). The average zeta potential across the 20 samples was  $-14.67 \pm 1.93$  mV which is considered relatively low, meaning that the system is unstable and particles within prone to agglomeration. The electrical properties of solutions have long been linked to stability (Besra and Liu, 2007), with particles in solution carrying a large charge less likely to aggregate due to electrostatic repulsion, this lack of deviation from low zeta potential values throughout the samples would suggest a different mechanism of aggregation mitigation than electrical stability of the particles in solution brought about by these two stabilisers.

The harvest material offered a more complex medium for experimentation that could explain the relative lack of impact of the stabilisers when compared with purified JEV experimentation. This harvest material contained spent metabolites from cell culture along with other waste products that could present a process challenge. Each stabiliser would have had more components to act on and, as stated, any effects may not have been visible within the design. One option could be to increase the concentrations of the stabilisers, as was attempted with glycine, certainly with sorbitol and glycine this could be interesting. Time and temperature were identified as significant effects with harvest material though these will obviously not be affected by increases in test material components

The cross-linking effect of formaldehyde between amino acids in peptide and protein chains as well as the inclusion of glycine has been shown before (Metz et al., 2004; Metz et al., 2005; Metz et al., 2006), with glycine interacting with formaldehyde to form a Schiff base which then binds to primary amino groups on certain amino acids. During formaldehyde inactivation of viruses, it is possible this process would have occurred outside of the virus envelope, around the antigen sites, with the glycine and the glycine-formaldehyde complex too large to enter between the envelope proteins and certainly gain access to the nucleocapsid underneath – unlike the much smaller formaldehyde molecules. Thus, this could be the reason why glycine is shown to improve antigen recovery, formaldehyde reactions near the virus surface are more likely to also involve glycine and being the smallest amino acid the conformational changes on the antigen sites should be minimal. Yet amino acid cross-linking due to formaldehyde occurring within the virus particle would still render it inactive but also with minimal topological changes.

Data acquired by DLS proved to be of significance with one of the above designs, in contrast to the NTA data that yielded no significant results. At first, it would appear that the two sizing techniques were at odds yet the two techniques were effectively analysing different aspects of the same particle distributions. The NTA attempted to

distinguish the different size populations within the samples whereas DLS observed the average changes in the population as a whole, as DLS is unable to resolve particles within a sample where there is not at least a 3-fold difference in diameter (Filipe et al., 2010). Yet, the shifts detected by the DLS as an average size of the whole population was not picked up using the analysis methods of the NTA readings of the different size populations within the samples. NTA is a relatively new technique compared to DLS, it is possible that the analysis methods of the NTA data are flawed or even that the settings used to acquire the data are not optimised for these samples and this target – JEV is bordering on the lower limit of this technique’s capabilities.

The high shear rate (6000 rpm) investigated is equivalent to an energy dissipation rate of approximately 30300 W/Kg (Levy et al., 1999) and is similar to the higher end forces experienced in agitated reactors (Davies, 1987) or the feed zone of a hermetic disc stack centrifuge (Hutchinson and Bingham, 2006). Such forces are not currently experienced in the vaccine manufacturing process but should increases in scale be sought it is useful to know that the product is relatively safe in this environment. It may also be that formaldehyde treatment of JEV does begin to demonstrate some shear resistance at higher rates, though undetected in this instance.

### ***5.3 Inactivation summary***

Temperature and formaldehyde concentration are the principle considerations with formaldehyde inactivation of JEV. With these in place the duration of the virus’ exposure to formaldehyde will depend on the requirements of the step, whether to inactivate just the product or a panel of model viruses. The most important finding is the use of glycine to increase product recovery. This has been observed during formaldehyde treatment at nearly every potential step of the process (Figure 5.6). It has also been demonstrated that more product loss is observed when formaldehyde treating PST than treating CHP. Thus perhaps formaldehyde inactivation of concentrated harvest pool would be a more ideal location for the step. Certainly moving

the step further upstream has the benefit of dealing with a safer product downstream and there is also evidence here that a formaldehyde treated feed is not significantly more susceptible to shear than the non-treated feed; perhaps there may yet be further advantages of processing a formaldehyde treated feed. However, extent of inactivation when working with purified JEV would first have to be measured and compared with upstream inactivation as there could be a difference in inactivation rates. Furthermore, not having inactivation as a final step prior to formulation would require additional controls of the product stream to prevent introduction of adventitious agents.

# 6 Microscale investigation of chromatography resins for JEV purification

---

Chromatography was selected for investigation as a potential alternative to sucrose gradient purification due to its ubiquitous use throughout industry and the availability of high-throughput screening (HTS) formats for resin screening and optimisation using small quantities of material. HTS of new resins and purification conditions as a replacement for a current step was an ideal starting point and provided the focus for this section of the project. However, to complement the HTS formats, adequate assays were required to be amenable to process large quantities of samples simply and effectively, therefore a certain amount of assay development and modification was also required with the objective of adapting a quantifiable JEV specific assay to HTS use.

Initial selection of resins and conditions to be screened was based on known properties of JEV alongside an appropriate buffer system at the desired pHs. The first requirement here was to identify one or two suitable resins based on maximum binding capabilities across those various conditions. Selected resins were then screened for elution conditions using the same formats and analysis techniques used during resin screening. The material used for these studies was protamine sulphate treated material (PST) in order to represent material which would be further purified using sucrose gradient centrifugation, as outlined in the generic JEV production process represented in Figure 3.3.

The ultimate aim of this section was to identify a suitable resin and conditions for studies at larger scale, which is detailed in the following chapter.

## **6.1 *PreDictor plate resin screening for binding conditions***

The JEV E-protein has a pI of 7.6 (Trent, 1977) and due to the nature of the JEV product, pHs above 9 should be avoided as these may damage the antigen (Donald Low, Valneva Biomedical Ltd., Personal communication), thus anion exchange (AEX) resins were seen as a logical starting point due to the pH range. In turn, Tris was decided upon as the buffer system because of the pH range to be explored and its regular use throughout industry. The GE PreDictor AEX screening plate offered the opportunity to screen four AEX resins and conditions in a standard 96 well plate format with high throughput screening methodology.

The first round of screening using the AEX GE PreDictor screening plates investigated the effects of loading pH (7.5, 8.0 & 8.5) and NaCl concentration (0, 20, 40 & 60 mM) on the binding capabilities of four resins (Capto Q, Capto DEAE, Q Sepharose Fast Flow and Capto Adhere). A format of 3 pHs and 4 salt concentrations was chosen as the 3 x 4 format would fit on the 96 well plate containing the 4 resins. The 3 pHs were within the desired experimental range, as stated above. The relatively low salt concentrations were selected because the starting material, PST, was assumed to already contain some salt at that point in the process and that too high an ionic concentration, and thus conductivity, would hinder the binding of a large particle such as JEV. The feed (F) in this chapter is what was loaded onto the resin, or with what the resin was challenged, was PST diluted with appropriate amounts of tris buffer containing NaCl to achieve the desired range of pHs and NaCl concentrations as described above and in section 4.5.1.

Capto Q and Q Sepharose Fast Flow are strong anion exchangers, which maintain their charge over a large pH range unlike the Capto DEAE resin that, as a weak anion exchanger, will have a more variable ionic capacity over the same pH range. Capto Adhere is a strong anion exchange resin with multi-modal functionality, meaning that in addition to ionic interaction, hydrophobic and hydrogen bonding interactions are also



possible. The characteristics of all resins can be found in Table 6.1. The plates contained 24 wells of each type of resin with 2  $\mu\text{L}$  of DEAE and Capto Q resin and 6  $\mu\text{L}$  of Q Sepharose Fast Flow and Capto Adhere. The manufacturers stated that despite the difference in resin volumes, the binding capacities are comparable (Personal communication, Jon Baker, BioProcess Technical Support, GE Healthcare). Although this claim does not appear to be wholly supported by the binding capacities in their literature, as quoted in Table 6.1, the two resins with the larger volumes QSFF and CA do appear to have highly variable capacities depending on the test protein, in the case of QSFF, and their function, in the case of CA.

Resin	Abbreviation	Type	Bead size (nm)	Capacity with test protein
Capto Q	CQ	Strong	90	BSA (67 kDa) > 100 mg/ml
Capto diethylaminoethyl	DEAE	Weak	90	Ovalbumin (66 kDa) > 90 mg/ml
Q Sepharose Fast Flow	QSFF	Strong	90	Thyroglobulin (669 kDa) 3 mg/ml HSA (68 kDa) 120 mg/ml $\alpha$ -lactalbumin (14.3 kDa) 110 mg/ml
Capto Adhere	CA	Multimodal	75	Tested in flow-through mode 100-300 mg/mL

Table 6.1 – Resin characteristics adapted from Ion Exchange columns and Media selection guide (GE Healthcare, 2011).

Each set of conditions was run in duplicate. The protein concentration of the feed, flow-through and the wash step were each measured by BCA assay with a BSA standard curve. The amount of protein found in the wash was negligible for all resins and conditions tested. The protein concentration of the feed averaged 260  $\mu\text{g/mL}$  across the 96 wells of the feed plate, with a standard deviation of 9.7%. The resins were saturated with material, as in components of PST, to evaluate adequate loading conditions. One load challenge of 200  $\mu\text{L}$  of feed per well was sufficient, in this instance, for the 2 or 6  $\mu\text{L}$  of resin per well, which amounted to approximately 52  $\mu\text{g}$  of

protein. As stated above, the feed in this instance was PST diluted with appropriate Tris buffers containing NaCl. The amount of protein measured in the flow-through from each well was used to determine the theoretical amount of protein bound to each resin type under each set of conditions (by subtracting this from the amount of protein feed into each well). The results can be seen in Figure 6.1.

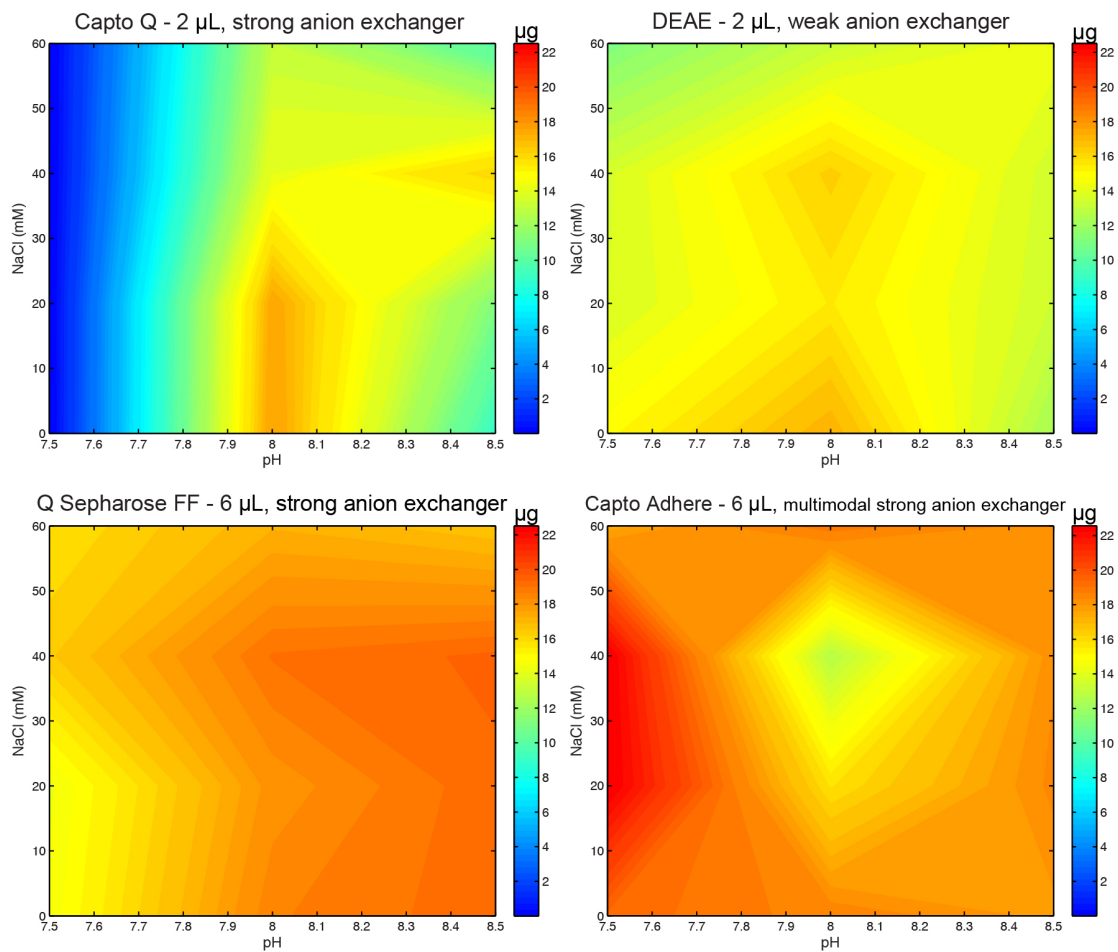


Figure 6.1 – colour contour plots demonstrating amount of protein bound to each anion exchange resin on the GE PreDictor screening plate for varying loading NaCl concentrations (0, 20, 40 and 60 mM) and pHs (7.5, 8.0 and 8.5), when challenged with PST diluted with appropriate buffer. Figures generated using Matlab R2012b (8.0.0.783).

Overall, the Q Sepharose Fast Flow (QSFF) and Capto Adhere (CA) resins bound more protein from the PST load than Capto Q (CQ) and Capto DEAE (DEAE) resins; yet each resin also demonstrated unique optimal conditions for protein binding. CQ favoured low NaCl concentration at pH 8, QSFF low NaCl with high pH, whereas CA low pH with changing NaCl concentration showing no significant impact except for at 40 mM. DEAE also displayed some variation in protein binding across the ranges observed, though appeared to favour pH 8. A possible explanation for QSFF and CA binding the most protein is that the volume of resin for each is 6  $\mu$ L per well as opposed to 2  $\mu$ L per well for CQ and DEAE. The manufacturers state that these are comparable volumes as CQ and DEAE are deemed 'high capacity' resins yet this could be for protein and not virus purification. It is feasible that other potential differences in the design space were not observed due to being below the limit of detection of the BCA assay, which is a protein concentration of approximately 20  $\mu$ g/mL. From the data it also appears that at the lowest pH investigated CQ, DEAE and QSFF, bind less protein, or in the case of CQ none at all. In contrast, with CA lower pH appears to favour protein binding. This could be an indication of Capto Adhere's multimodal functionality coming into play where anion exchange binding is poor. The BCA assay indicates total protein per sample, and while important, does not indicate the proportion of JEV binding to the resin. Consequently, the next data set needed to come from a JEV-specific assay.

A modified ELISA (mELISA) method was developed for high throughput, product specific analysis for use with PreDictor plates, whereby instead of analysing just 3 or 4 samples alongside a standard on a 96 well plate to determine antigen content, all 96 wells were used to obtain relative absorbance values for each sample. There is a sigmoidal relationship between the concentration of the JEV reference standard and absorbance in a customary sandwich JEV ELISA. In order for this different method to produce results to compare JEV binding across different resins and condition, test samples would have to be diluted to a concentration corresponding to a point within the

linear region of the absorbance/reference standard relationship. The other aspects of the JEV ELISA, coating, primary and secondary antibodies, incubation times and substrate reaction, remain unchanged. Only the sample loading onto the sheep anti-JEV coated test plate and the lack of standard and blanks are deviations from the standard protocol. Standard curves previously generated during antigen content testing of the same material determined this point in the linear region to be an absorbance value of around 2.1 (at 450 nm), a dilution of 1 to 80 with ELISA dilution buffer (1 % BSA in 1 x PBS, 0.05 % tween) was required to achieve this with the feed material. As a result, relative absorbance by ELISA was measured for the feed, flow-through and wash by diluting all samples 1:80 with ELISA dilution buffer prior to loading onto the ELISA test plates. As above, an indication of amount of JEV binding to each resin was deduced by subtracting the absorbance values of the flow-through from those of the feed from the same wells – thus the larger difference in absorbance ( $\Delta$  abs) the more JEV has been retained by the resin. The results can be seen in Figure 6.2. The absorbance values from the wash were deemed insignificant as they were in the same range as the blank values determined from testing the buffer preparation plates using the same mELISA method.

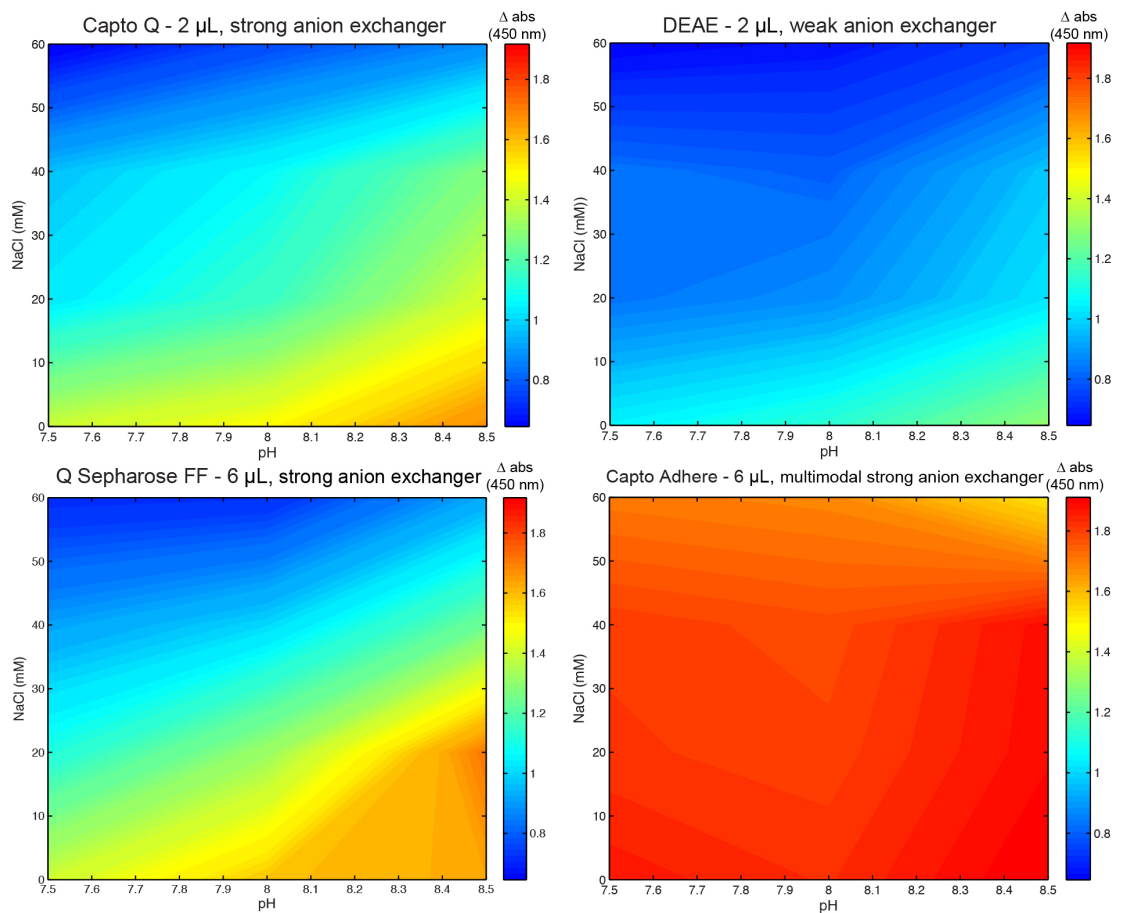


Figure 6.2 – colour contour plots showing the change in absorbance ( $\Delta \text{abs}$ ) across observed ranges of pH (7.5, 8.0 and 8.5) and NaCl concentrations (0, 20, 40 and 60 mM) for each anion exchange resin of the GE PreDictor screening plate when challenged with PST diluted with appropriate buffer.  $\Delta \text{abs}$  was elucidated from modified ELISA testing of the feed and flow-through and subtracting one from the other for each well of the resin screening plate.  $\Delta \text{abs}$  colour scale goes from least JEV binding in blue to most JEV binding in red. Figures generated using Matlab R2012b (8.0.0.783).

Overall CA bound the most JEV, consistent with the protein binding results, with DEAE binding the least, yet these two resins also displayed the least variation in binding capabilities within the observed ranges. Both of the strong anion exchangers, CQ and the QSFF, demonstrated a clear increase in JEV binding from low pH, high NaCl concentration to high pH, low NaCl concentration; with QSFF in particular having a larger window of operation for optimum JEV adherence. CA again indicated capabilities beyond anion exchange with pH and salt shown to have little effect on the amount of JEV binding to the resin.

In order to confirm the ELISA results, an SDS-PAGE gel and corresponding western blot were conducted to ensure the JEV antigen was being captured. Figure 6.3 shows a silver stained SDS-PAGE gel (A) and corresponding western blot (B) from the feed, flow-through and wash of 3 separate conditions from the screening experiment. The western blot was performed with antibodies raised against purified inactivated JEV, supplied by Valneva Scotland Ltd., therefore the appearance of bands indicates the presence of JEV in a given sample. The most prominent band occurs around 52 kDa representing the JEV envelope protein (E-protein), bands can also sometimes be observed for the capsid (C, 14 kDa) and membrane (M, 7 kDa) proteins. As seen in Figure 6.3 all feed samples contain JEV but it was not evident in the wash samples. The presence of a band in the flow-through sample indicates either non-adherence of JEV to the resin or a saturation of the resin under those conditions. The flow-through sample for the QSFF resin challenged at pH 8.5 with 0 mM NaCl is the only such sample in Figure 6.3 with no band present, confirming binding of JEV. These results are consistent with the previous analyses.

From these quantitative (Figure 6.1 and Figure 6.2) and qualitative (Figure 6.3) screening results it was concluded that the Q Sepharose FF and Capto Adhere resins were demonstrated to bind more JEV than Capto Q and DEAE. Although JEV binding results with Capto Q were comparable to Q Sepharose FF, for simplicity and practicality only two resins were selected for further studies. QSFF had a larger window

of operation than CQ and Capto Adhere appeared to bind significantly more JEV possibly due to its multimodal functionality which, as different from a simple strong anion exchanger, could offer possibilities with further investigation. Therefore the QSFF and CA resins were taken forward for small-scale binding and elution studies using the single resin PreDicator plates.



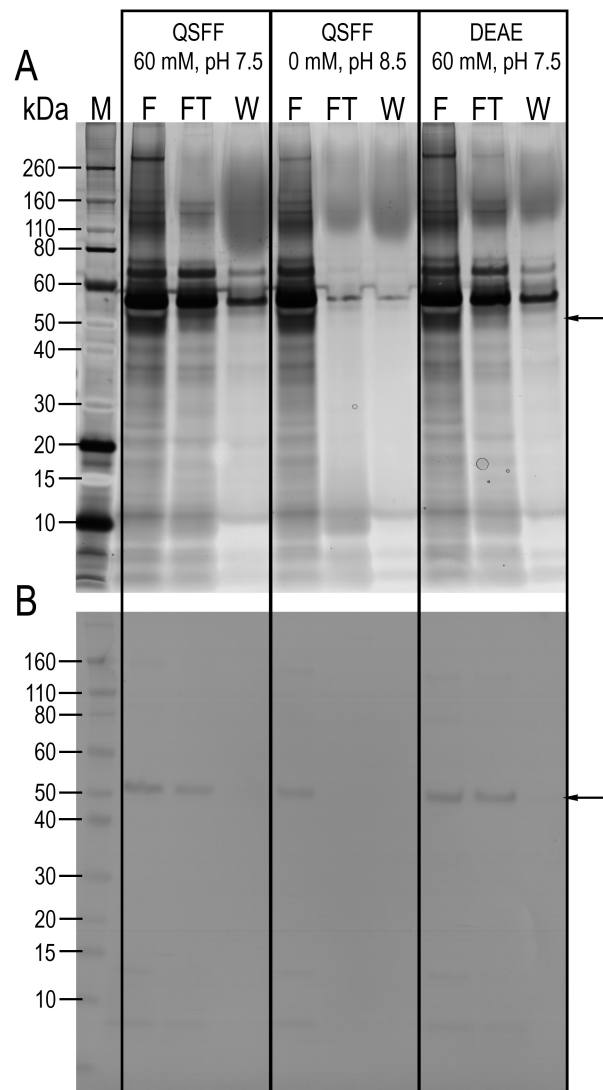


Figure 6.3 – silver stained SDS-PAGE (A) and corresponding western blot (B) analysis of selected samples from screening plate study (NaCl concentration in mM and pH). Samples loaded from stated resin and conditions are feed (F), flow-through (FT) and wash (W). Arrow indicates location of E-protein (~51 kDa) band giving positive signal in western blot for antibodies raised against JEV.

## **6.2 Elution studies on CA and QSFF single resin plates**

PreDicator plates containing only Q Sepharose FF and Cpto Adhere resins were used for binding and elution of feed material containing JEV. It was determined during screening that JEV retention on QSFF was favoured by high pH and low NaCl concentration and so, for ease of comparison, CA was assessed with these same conditions. Therefore no additional NaCl was added to the loading buffer but pH was further investigated at 8.0, 8.3 and 8.6 to observe potential effects on elution requirements and eluted product recovery. Elution from the two resins was investigated by establishing a gradient down the plate with loading buffer containing 100 to 800 mM NaCl at 100 mM increments. The 96 wells on the PreDicator plates each contained 20  $\mu$ L of resin, this was challenged with 290  $\mu$ L of feed (again, PST diluted with Tris buffers as required) and incubated for 2 hours on a shaking platform. The protein concentrations of the feeds were different for each experiment because two different batches of PST were used, the protein challenge for each well was  $54 \pm 6 \mu\text{g}$  for the QSFF plate and  $75 \pm 10 \mu\text{g}$  for the CA plate. Using all the wells on the plates and testing 3 different pHs with 8 different concentrations of NaCl for elution allowed for 4 replicates of each set of conditions.

Figure 6.4 shows the total protein data obtained using the BCA assay from these experiments. Figure 6.4.A indicates a slight increase in the amount of protein bound to QSFF compared with that bound to CA at pHs 8.0, 8.3 and 8.6, with increasing pH not shown to have a significant effect within this range. Figure 6.4.B shows the concentration of protein in the feed, flow-through and eluted fractions of increasing NaCl concentration for QSFF. The protein content of the wash steps and elution of protein from CA was below the limit of detection (LOD) of the BCA assay, this could be further evidence of CA's multimodal functionality and therefore just increasing NaCl concentration may not be the required elution strategy. This data also suggests that, for all pHs, protein elution begins and incrementally increases with 100 mM NaCl yet remains relatively unchanged after 400 mM NaCl. However, the BCA results imply a

discrepancy between protein loaded onto the resin in the feed (F) and that which flowed-through without binding (FT) and which bound but subsequently eluted (E); as in theory  $F = FT + E$ . From Figure 6.4.B it was estimated that the protein unaccounted for is 10  $\mu\text{g}$  as an approximate average across all pHs. It is possible that this is still bound to the resin with 800 mM NaCl not sufficient to elute. This may also be due in part to the use of the BCA assay at the lower end of its sensitivity; the focus on protein concentrations within such a small window towards the base of the assay's standard curve will inherently make the calculated results significantly more variable and prone to being masked by the intercept and subtraction of blanks – a contributing factor to the lack of data for the washes and eluted fractions of the CA resin.

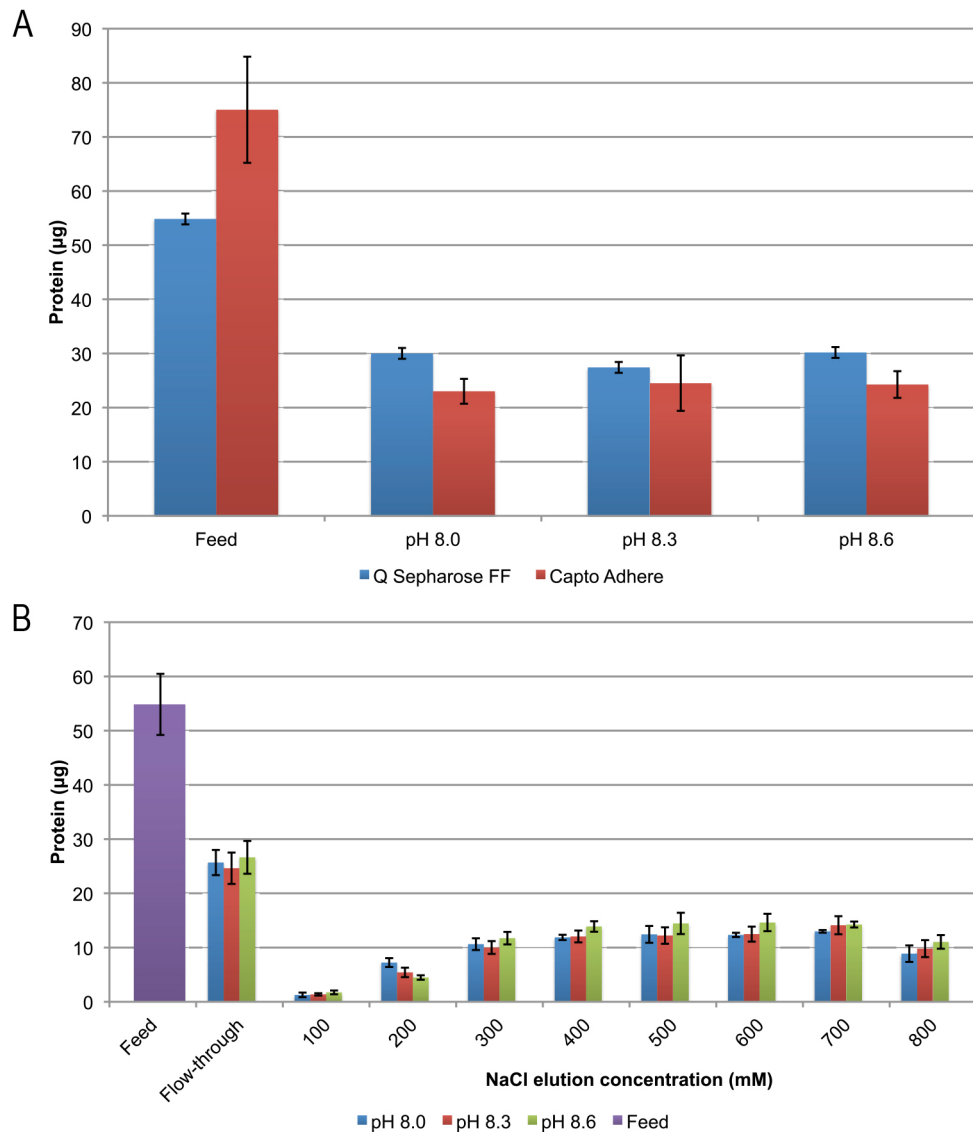


Figure 6.4 – total protein data obtained from QSFF and CA single resin plates challenged with PST diluted with appropriate buffer. Comparison of protein bound to each resin at different pHs (A). Protein content of eluted fractions for QSFF (B), washes and CA eluted protein content were below the limit of detection. Error bars based on standard deviation of analytical samples as follows: Feed in A and B, n=96; pHs in A, n=32; flow-throughs in B each pH n=32; NaCl elution concentrations in B each pH, n=4.

Figure 6.5 shows the mELISA results for the load and elute of the QSFF (A) and CA (B). The dilutions required to bring the data within range of the mELISA were 1 to 100 for the QSFF experiment and 1 to 4 for the CA experiment. Overall this data indicates that JEV bound to CA is not eluted with NaCl up to a concentration of 800 mM, unlike with QSFF which shows some JEV eluting with 100 mM NaCl increasing up to 500 mM NaCl at which point increasing NaCl has no further significant effect. The effect of increasing pH was negligible with CA and appeared to slightly promote JEV binding and elution on QSFF. This data is consistent with the BCA data in suggesting that material bound to QSFF is more easily eluted than with CA.

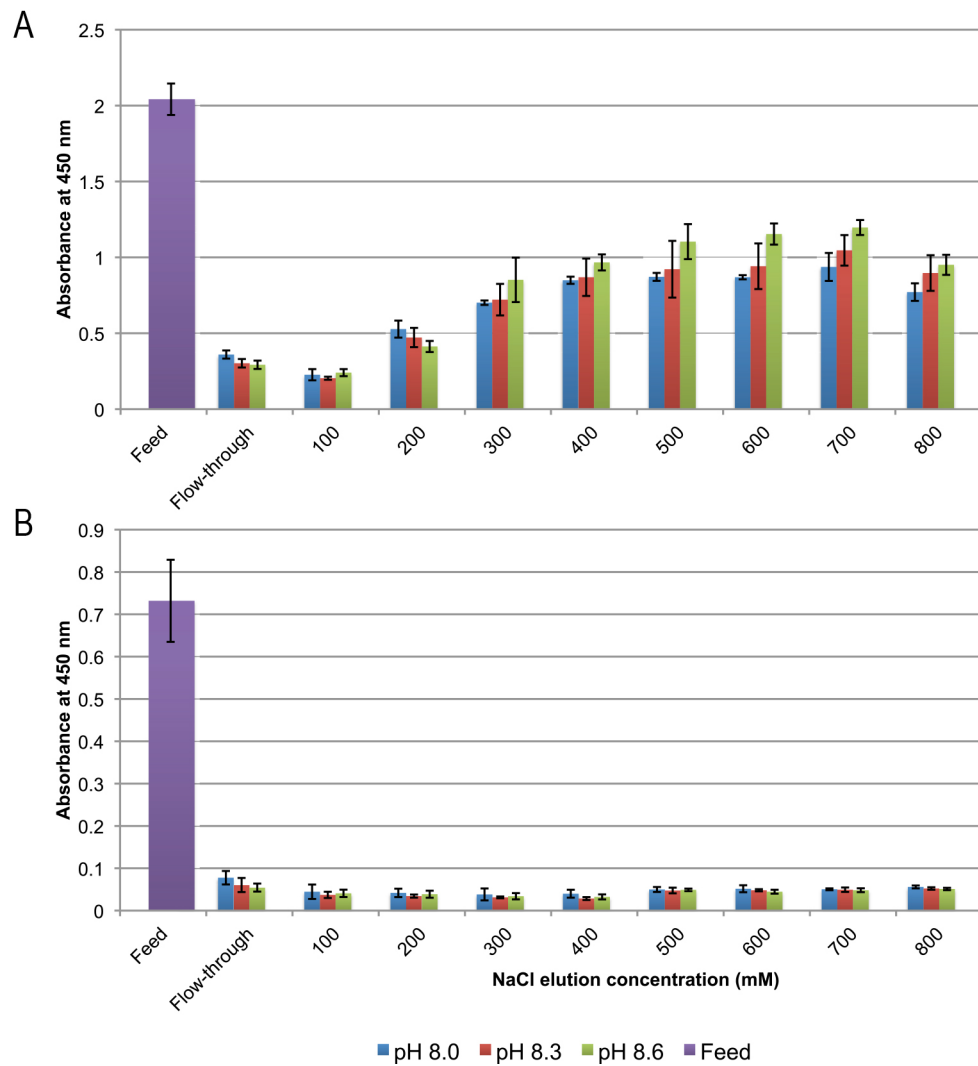


Figure 6.5 – modified ELISA absorbance data for the load and elute fractions of Q Sepharose FF (A) and Canto Adhere (B) single resin plates challenged with PST diluted with appropriate buffer. Error bars based on standard deviation of analytical samples as follows: Feed in A and B, n=96; flow-throughs in A and B each pH n=32; NaCl elution concentrations in A and B each pH, n=4.

Figure 6.6 shows a silver stained SDS-PAGE analysis of the load and elute from pH 8.6 of QSFF, with the feed, flow-through and wash samples all taken from the same corresponding well. The staining pattern of the elution fractions corroborates the BCA results in Figure 6.4.B, with no staining observed from the wash sample and some protein eluted with 200 mM NaCl which increases with 300 mM NaCl where it plateaus with no obvious further increases in band intensity. The BCA data also shows flow-through concentrations for pH 8.6 to be around 92 µg/mL and for the 200 mM NaCl elution at the same pH to be around 22 µg/mL. However no staining is evident from the flow-through sample loaded onto the gel in Figure 6.6 despite the protein concentration being reported as higher than that of the 200 mM eluted fraction where staining is evident. A possible explanation is that the protein concentration determined is derived primarily from the leftover protamine sulphate added to the process material in the previous step to remove host cell DNA from the concentrated harvest material. Protamine sulphate (PS) is a highly cationic peptide of approximately 5.1 kDa. The nature of this impurity, that of being significantly positively charged, will dictate that it does not bind to an anion exchange resin under the pH conditions investigated and should therefore be found in the flow-through. In terms of staining, the amino acid sequence of PS indicates that it is not a peptide amenable to the reduction of silver ions required by this assay for protein visualisation (Rabilloud, 1990), lacking as it does the following residues: Asp, Glu, His, Cys, Met (assuming cleavage of initiator methionine) and Lys (Moir et al., 1988). Consequently it can be assumed that protamine sulphate passes into the flow-through, where it is picked up by the BCA assay, but is not visualised with silver staining.

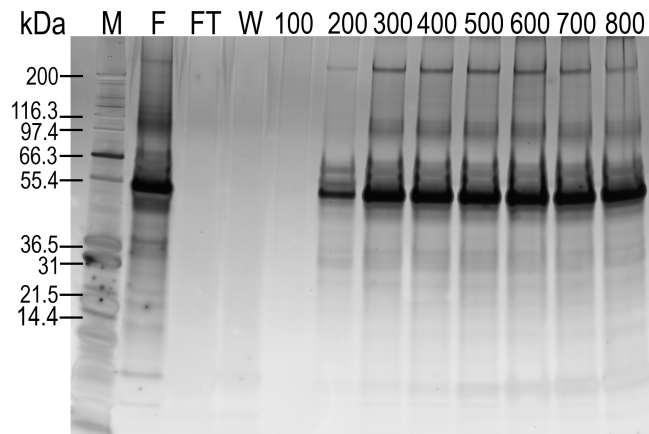


Figure 6.6 – SDS-PAGE analysis of fractions from load and elute of Q Sepharose Fast Flow single resin plate at pH 8.6. Lanes loaded as follows: Novex Mark 12 protein unstained protein standard (M), feed (F), flow-through (FT), wash (W) and NaCl elution concentration (100 – 800 mM). F, FT, W and 100 mM samples were all taken from the same corresponding well.



From this investigation it was decided to take forward Q Sepharose FF a resin for studies at a larger scale as it performed more favourably than Capto Adhere in terms of JEV recovery in eluted fractions.

### **6.3 *Microscale investigation discussion***

#### **6.3.1 Choosing Q Sepharose FF**

Overall the small-scale studies for binding and elution of PST JEV process material on micro-titre plates performed as expected. The weak anion exchanger Capto DEAE demonstrated the least desirable loading results during screening and the multi-modal Capto Adhere resin displayed the greatest affinity for binding material under all observed conditions yet the subsequent elution strategy failed in retrieving any JEV. More desirable operating windows for loading pH and NaCl and were elucidated for Capto Q and Q Sepharose Fast Flow, most probably due to being strong anion exchangers.

It is likely that QSFF and CA bound the most protein due to having 6  $\mu\text{L}$  of resin per well unlike CQ and DEAE that had 2  $\mu\text{L}$ , despite the manufacturers assertion that the latter two resins have a higher capacity and the two sets are comparable. Such a characteristic could be true for specific protein purification (e.g. monoclonal antibodies) but unlikely for virus purification as the product is too large to pass through the pores in the resin beads thus only their surface is available for ionic interaction and exchange conferring a distinct binding advantage with a larger volume of resin due to having access to a greater surface area.

Capto Adhere is a high capacity multi-modal resin designed to be operated in flow-through mode for the capture of impurities, such as viruses (GE Healthcare Life Sciences, 2012). The results show that CA functions in this respect with high capacity for protein binding and capture of JEV from the feed. The data also shows that JEV is not recovered with NaCl elution concentrations of up to 800 mM, which is why the resin

was not taken forward for larger-scale investigations. However, this could indicate an alternative mode of binding other than anion exchange as pH and NaCl concentration did not appear to affect JEV binding under the observed conditions. Perhaps the multimodal functionality of Capto Adhere came into full effect with strong hydrophobic interaction and/or hydrogen bonding having taken place instead of or as well as anion exchange.

Q Sepharose Fast Flow has previously been shown to capture enveloped viruses (Connell-Crowley et al., 2013; Strauss et al., 2009a) with the primary binding mechanism proven to be through electrostatic interaction with the charged functional group, in this case quaternary ammonium (Strauss et al., 2009b). Therefore the performance of the two strong anion exchange resins, Capto Q and QSFF, showing satisfactory levels of JEV binding with high pH and low NaCl in the screening experiment was as expected – a more highly charged resin charge (due to pH) with fewer competing ions (lower NaCl concentration). Although somewhat marginal, possible reasoning for QSFF demonstrating a more favorable operating window over CQ (Figure 6.2), apart from the larger volume of resin, could be found in the differences in the matrix structure between the two resins. Although the average bead diameter is the same (90 µm, Table 6.1), QSFF has ligands attached directly to the surface of the cross-linked agarose matrix, whereas CQ uses dextran surface extenders on an agarose matrix with a higher-level of cross-linking and porosity (Pezzini et al., 2009). These structural characteristics make CQ a popular choice for rapid (high flow rate) purification of lower molecular weight proteins through greater rigidity and higher binding capacities yet the increased ligand density could limit binding of large biomolecules, such as JEV.

### **6.3.2 HTS JEV process development and assays**

Although useful for obtaining qualitative data, SDS-PAGE and Western Blotting are not suited to high throughput processing of samples. It is necessary to be more practical

and use the quantitative methods to decide which samples to run using these other methods, as was done in this work.

Silver staining of SDS-PAGE gels is a highly sensitive technique, reportedly about 100 times more sensitive than with a Coomassie stain (Rabilloud, 1990), able to visualize bands containing low nanogram levels of protein (Chevallet et al., 2006). For chromatography process development it is useful in being able to compare relative purity of the feed and subsequent fractions. With this study the technique demonstrates banding predominantly in the region of ~56 kDa (Figure 6.3.A and Figure 6.6), this was initially assumed to be the JEV E-protein yet western blot analysis of the same fractions using antibodies raised against JEV give a signal at ~51 kDa (Figure 6.3.B), slightly below the expected value and not part of the principal band shown in the gel. Amino acid sequence analysis of the JEV E-protein returns a value of 53.8 kDa – a value which could easily be visualised as either of the other two values on a gel once a certain degree of assay error is factored into interpretation of the band location relative to the protein standard ladder. A possible explanation for the 50 to 56 kDa region of anomaly may again be found with the high concentration of protamine sulphate added in the previous step. Perhaps the highly cationic, ~5 kDa, PS binds to the JEV E-protein in such a fashion that the antibody epitopes on domain III of the protein (Lin and Wu, 2003) are inaccessible for antibody binding – thus increasing the molecular weight from ~51 to ~56 kDa yet interfering with the western blot by steric hindrance. However, this is unlikely, as unless the PS binds covalently to the E-protein then it is assumed the denaturing effect of SDS-PAGE sample preparation process would separate the two proteins.

The BCA assay is a simple total protein assay that can be adapted for use in HTS in a micro-plate format, where the BSA standard curve has linearity range of 20 to 2000 µg/mL (Thermo Scientific, 2010). Within these experiments the protein concentrations measured were rarely above 800 µg/mL and most often well below 100 µg/mL, particularly with the eluted fractions. Although within range of the linearity and as stated

above, the focus on such a small window of operation at the lower end of the assay's sensitivity engendered results more susceptible to variation and baseline fluctuations (background/blank readings). It is estimated that more optimal operating conditions would be achieved with the BCA assay with higher feed titres to make better use of the of the assay's linearity range with all samples.

The selectivity, sensitivity and high-throughput applicability of the modified ELISA provided a valuable perspective in deciding the resin with which to proceed. Yet, this new method is subjective to each individual experiment and the reagents used, as the standard curve's linear region, in terms of range of absorbance values, must be determined to elucidate the starting dilution. Two different batches of feed material and two different lots of the primary antibody were used in the screening study and the QSFF single resin experiment compared with the CA single resin plate. An immediately evident difference is the absorbance value of the feed (Figure 6.5 A and B), indicating a lower JEV titre in the batch or a primary antibody with a lower affinity for the virus, or both, in the CA experiment over the QSFF.

Previous studies involving high-throughput screening of chromatography resins for specific virus capture used quantitative PCR (qPCR) to determine log reduction values (LRV) of virus (Connell-Crowley et al., 2013; Strauss et al., 2009b). Although specific and fairly accurate, this method would not give an indication of product quality or antigen yields over the course of the step as is required when the virus is the purification target and not an impurity to be removed.

The BCA and ELISA assays are both fundamentally colorimetric assays and so can be adapted for HTS, as with the mELISA. The shift from using reference standards, blanks and controls to reliance on purely relative absorbance values may seem bold, and, to a certain extent, crude, but judged acceptable within the constraints of each individual design space. That is to say, with reference to the example above, the subjectivity of such methods needs to be taken into account in cross-experimental comparison.

Furthermore, the range of commercially available, colorimetric, microplate compatible assays would enable screening of resins and conditions for a broad range of attributes, for example dsDNA quantification with the Quan-iT™ PicoGreen® assay (Life Technologies), quicker and easier. Protein concentration could also be read directly in a U.V. transparent microplate, as has been noted in previous HTS studies (Sanaie et al., 2012).

The GE PreDictor plate format is a simple and relatively easy to use starting point for process development intending to incorporate ion exchange chromatography.

However, the plates are more ideally suited to automated platforms; having a robotic system perform the buffer preparation and all steps (loading, washing and elution) would likely reduce error and improve consistency. An optimal scenario would be to incorporate assays with high-throughput potential (e.g. BCA, ELISA) into the process development flow, with sampling, reagent mixing, incubation, testing etc... executed *in situ* alongside experimentation creating a complete chromatography screening platform. Such a setup could be made simpler, and therefore more feasible, with the use of colorimetric assays in relative absorbance format without the need for standard curves, as stated above.

### 6.3.3 **Microscale investigation summary**

These experiments successfully used a high-throughput approach to screen anion exchange resins for optimal JEV binding and elution conditions. The development of a JEV specific high-throughput assay in the modified ELISA was invaluable in this effort. A greater degree of accuracy and consistency could have been achieved with the use of an automated platform, future work should look to include such technology alongside relative absorbance assays, as suggested, to maximise throughput, data obtained and reproducibility.

# 7 Chromatography scale-up of Japanese Encephalitis virus capture and elute

---

Although sucrose gradient purification is well established for purifying viruses, it is also variable, labour intensive and not amenable to scale-up. Chromatography is well-established across the pharmaceutical and biopharmaceutical sectors, even in vaccine production and so the decision was made to investigate the possibility of purifying JEV using this technique.

The previous chapter detailed the high-throughput screening of 4 different anion exchange resins with different conditions of a Tris buffer for the capture and elution of JEV from protamine sulphate treated concentrated harvest material. Q Sepharose FF (QSFF) was deemed the best performing resin in the microplate format and taken forward for investigation using a 1 mL packed column run on an AKTA purification system. The successful purification of JEV at this scale will depend on maintaining the mass transfer levels observed during screening for effective bind and elute and building on the recovery rates with novel optimisation. Product integrity and purity were initially key markers for progress evaluated using the same techniques as with the screening study but with the Western blot playing a more central role to identify JEV in individual fractions. An assessment is made of the effectiveness of methodology transfer from batch binding microplate experiments and the feasibility of further scale-up.

## **7.1 Initial Scale-up**

Following the previous studies investigating binding and elution conditions it was decided to scale-up the investigation to a 1 mL Q Sepharose Fast Flow pre-packed

column (GE) run on an AKTA Purifier 100. The starting material was protamine sulphate treated concentrated JEV harvest material, PST, see Figure 3.3 for location in a typical JEV production process. This PST was buffer exchanged into 50 mM tris pH 8.6 (the loading buffer) with 20 mL Vivaspin tubes with a molecular weight cut-off (MWCO) of 50 kDa, to create the feed, and loaded onto the column with an injection loop at a flow-rate of 1 mL/min. The initial AKTA stepwise method was comprised of a 10 column volume (CV) post load wash with loading buffer, a 20 CV 2<sup>nd</sup> post load wash with 200 mM NaCl, elution with 400 mM NaCl and a post elution wash with 1 M NaCl (all buffers were also 50 mM tris pH 8.6). The rationale behind including a 200 mM NaCl post load wash was to separate some of the process impurities from the product elution fraction at 400 mM NaCl.

Figure 7.1.A shows the chromatogram from a load and stepwise elution of protamine sulphate treated JEV process material (PST) using the buffer exchange and conditions stated above, and the resulting silver stained SDS-PAGE gels of selected fractions in Figure 7.1.B and C. As before, the JEV E-protein was assumed to be the ~55 kDa band seen in the start material (lane SM, Figure 7.1.C pre-buffer exchange) and the feed (lane F) which is bound and eluted with 400 mM NaCl and can be seen at a relatively higher concentration and purity in lanes 10 to 12 in Figure 7.1.C. The difference in SM and F on the gel relates to the buffer exchange performed in the Vivaspin tubes, whereby some smaller <50 kDa) proteins are lost due to passing through the membrane and further product losses, possibly as a result of aggregation and membrane fouling. In this instance, the 10 mL of SM had a protein concentration of 931 µg/mL, which was reduced to 259 µg/mL in the 19 mL of F, this equates to a protein loss of 47% during Vivaspin mediated buffer exchange. This is evident with the staining in Figure 7.1.C as F appears as a diluted form of SM.

From the gels it also appears that little protein attributable to JEV can be found in the flow-through or the post elution wash. Furthermore, the protein bands observed in the post load wash seem to be impurities and/or degraded and aggregated JEV-E protein

bands within the 45 to 70 kDa region. Based on this qualitative data set, the addition of the 2<sup>nd</sup> 200 mM NaCl post load wash serves its intended purpose to remove bound impurities from the column prior to the product elution with 400 mM NaCl, thus validating the chosen method.



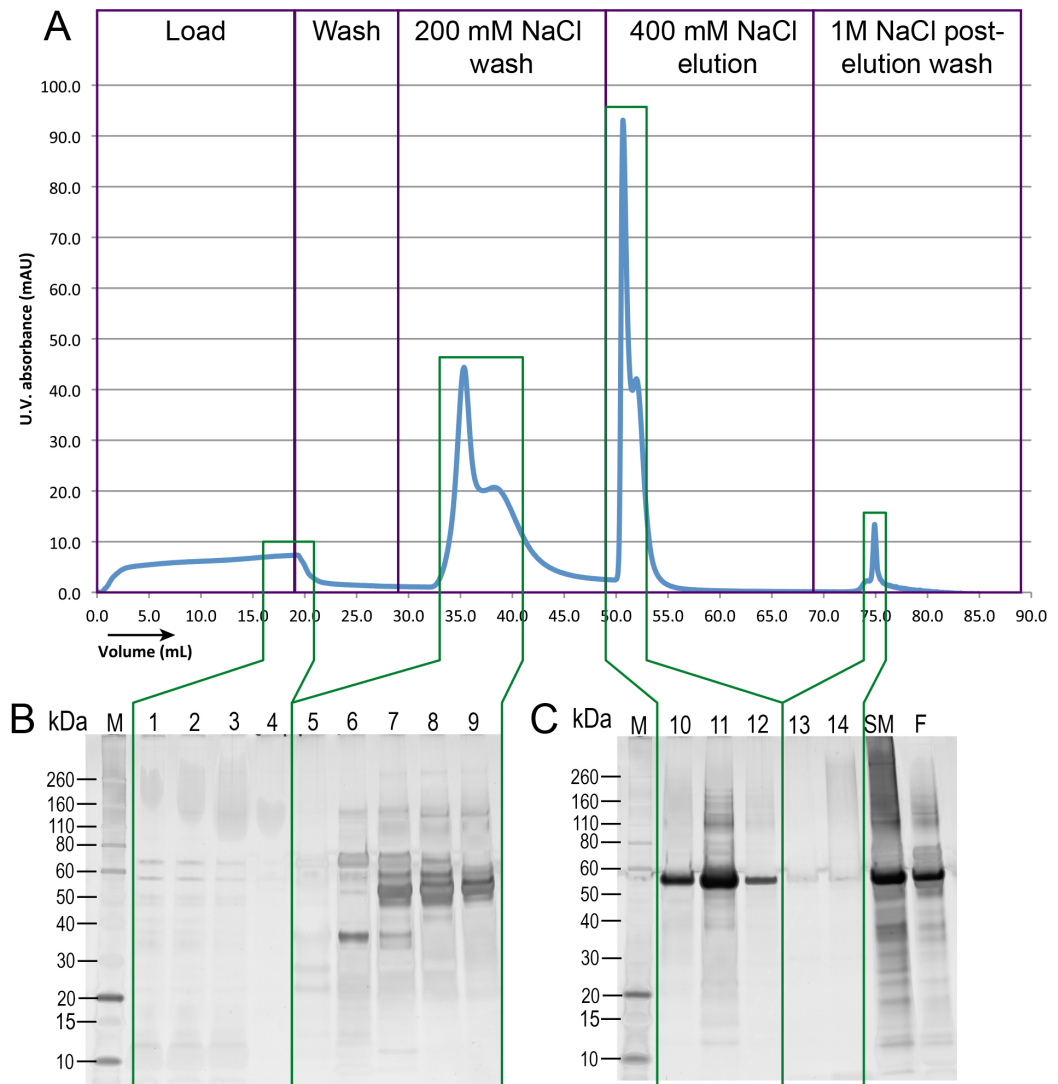


Figure 7.1 – PST JEV process material buffer exchanged into 50 mM Tris pH 8.6 loaded onto 1 mL Q Sepharose FF pre-packed column, equilibrated with the same buffer, at 1 mL/min. Chromatogram of U.V. absorbance against volume (A) and corresponding silver stained SDS-PAGE analysis of selected fractions (B and C) where M = Novex Sharp unstained protein standard, SM = start material (pre-buffer exchange) and F = feed. All buffers steps shown in A also included 50 mM Tris pH 8.6.

However, quantitative data analysis presents an entirely different picture. Figure 7.2.A and Figure 7.2.B show the total protein and antigen content by BCA assay and ELISA, of the feed and the elution pool for this particular AKTA run. Significant losses are evident as only 5.7% protein and 7.1 % antigen loaded onto the column is recovered according to these results. To a certain extent, some protein losses might be attributed to Protamine Sulphate not binding to the resin under these conditions and not being visualised with silver staining, as stated in the previous chapter. Although it is more likely that most of the PS would have been lost during the buffer exchange as it is small enough to pass through the membrane MWCO of 50 kDa and therefore would not have contributed to the protein content of the feed. It would be more reasonable to then assume that most of the JEV loaded onto the column either does not bind to the column and thus should be present in the flow-through, or does bind but is eluted with the 200 mM NaCl wash, or perhaps a combination of the two effects is being witnessed. Yet despite some protein being accounted for in the load and washes, one would still expect a significant proportion to be found in the eluted fractions, judging by the elution peak height in Figure 7.1.A and intensity of the bands observed in lanes 10-12 of Figure 7.1.C, though according to the BCA and ELISA data, this is not the case. The bands observed at 55 kDa in lanes 10-12 of Figure 7.1.C do not seem to be the JEV E protein band, though the molecular weight is in keeping with the literature value of the JEV E-protein. Thus, the poor antigen yield in the elution could be due to either JEV not being in the eluted fraction, through non-binding or being washed off with 200 mM NaCl (the wash was not assayed at this stage), or the ELISA antibodies not binding to the virus, through steric hindrance of and/or damage to the antigenic binding sites.

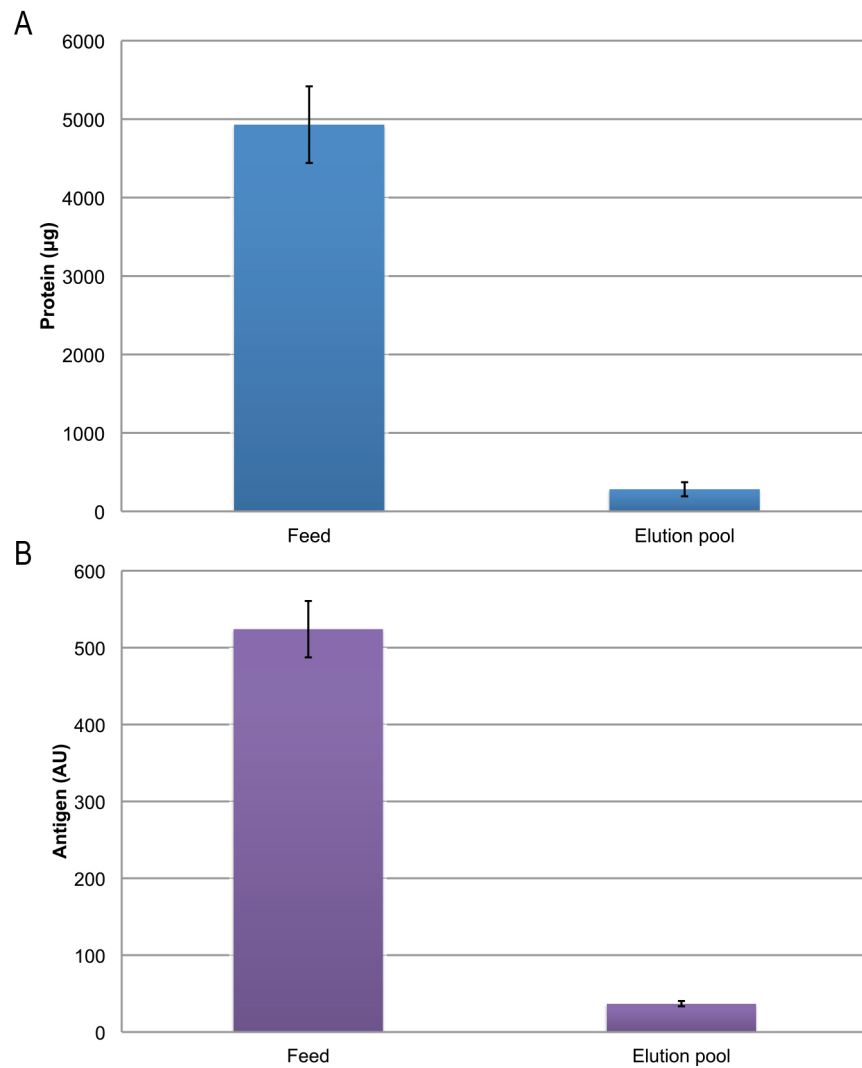


Figure 7.2 – Protein (A) and antigen (B) content of feed and elution pool relating to the AKTA run in Figure 7.1, the elution pool specifically relates to lanes 10-12 in Figure 7.1.C. The error bars arise from the standard deviation between analytical samples, n=3.

## **7.2 Antigen Monitoring using Western Blots**

Despite the qualitative and quantitative data sets being at odds, it was nevertheless clear that this initial AKTA method was unsuitable for JEV purification in its current format. The protein content discrepancies could be overlooked, to a certain extent, owing to previous concerns with the BCA assay being used to measure samples at the lower end of its sensitivity as protein levels below the LOD of the microplate format BCA assay can still be visualised by silver staining of SDS-PAGE gels. However the antigen recovery was a more pertinent issue; the results suggested that if JEV was binding to the QSFF resin at this scale the eluted product was unrecognisable to the antibodies used in the ELISA. This could be due to process damage caused by contact with the charged or conditions within the column. The next step was therefore to determine if JEV was binding under these conditions and if so, alter the conditions so that interaction with the resin over prolonged periods would not adversely affect product recovery, as suggested by some literature in the form of protein spreading on hydrophobic interaction resin (Haimer et al., 2007).

Data from two further AKTA runs is given in Figure 7.3 and Figure 7.4; in each case the pH was reduced from 8.6 to 8.3 and attempts were made to reduce the contact time of JEV with the resin by reducing the volume of feed loaded onto the column and the number of column volumes used for the washes. In the case of the run represented by Figure 7.4, the 2<sup>nd</sup> post load wash with 200 mM NaCl was removed altogether. Western blots were also performed alongside SDS-PAGE analysis to track JEV over the course of the step.

Figure 7.3 shows the results of a repeated AKTA run using the same conditions as in Figure 7.1, only this time Western blots have been included as part of the analysis. Additionally, a reduced load is used in order to minimise any background on the gels and blots (5 mL of 108 µg/mL). Unfortunately, due to the low protein concentration of the feed all subsequent samples were below the LOD for standard BCA analysis. The

feed sample (lane F, Figure 7.3.C and E) displayed the strongest immuno-signal at ~55 kDa, representing the JEV envelope protein (E), followed by the capsid (C, ~14 kDa) and membrane (M, ~7 kDa) proteins. As mentioned in the previous chapter, the sheep anti-JEV antibody used in the ELISAs and Western blots is raised against purified inactivated JEV therefore bands representing other structural proteins can show up on Western blots. There was also a visible band just above 160 kDa, which could correspond to trimerised envelope protein, possibly indicating aggregation of the protein monomer.

The most striking result from this run was the complete lack of banding in the Western blot of the 400 mM NaCl eluted fractions (Figure 7.3.E) despite the clear banding observed in the SDS-PAGE (Figure 7.3.C). It would seem that the strong 55 kDa banding seen in lanes 10-13 in Figure 7.3.C do not correspond to the JEV E-protein as identified by Western blot. Conversely, Western blot signals are observed in samples which give fainter bands after being silver stained on SDS-PAGE gels, this is particularly evident with the flow-through (Figure 7.3.B and D, lane 1), and slightly less so in the post load wash (Figure 7.3.D), with very faint Western blot bands observed at ~55 kDa and just above ~160 kDa, similar to those found in the feed. The diluted elution pool sample was included in case the 400 mM NaCl in the elution buffer was somehow damaging the antigen or interfering with the assay – a sample from the elution pool was immediately taken and diluted 1:1 with PBS. No change was noticed.

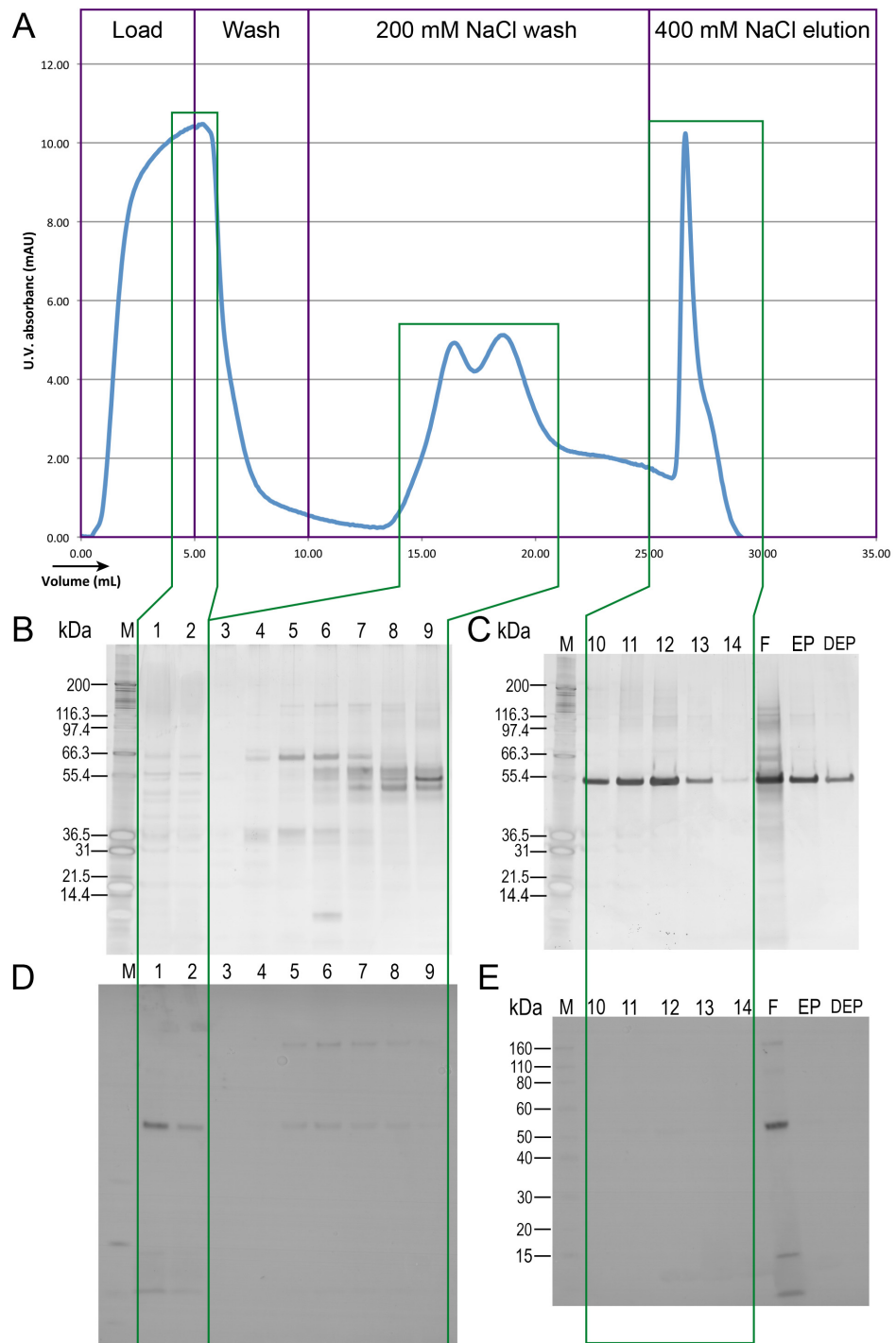


Figure 7.3 – PST JEV process material buffer exchanged into 50 mM Tris pH 8.3 loaded onto 1 mL Q Sepharose FF pre-packed column, equilibrated with the same buffer, at 1 mL/min. Chromatogram of U.V. absorbance against volume (A) and corresponding silver stained SDS-PAGE analysis (B and C) and Western blots (D and E) of selected fractions where M = Mark 12 unstained protein standard (B and C) or Novex Sharp pre-stained protein standard (E), F = feed, EP = elution pool and DEP = diluted elution pool. All buffers steps shown in A also included 50 mM Tris pH 8.3.

### ***7.3 Consequence of removing the second wash step***

A similar run was performed again with the same conditions except the load volume was also reduced compared with the first run, from 19 to 7 mL as the feed concentration was increased to 305 µg/ml, resulting in four times as much protein being loaded onto the column than the run described in Figure 7.3. Additionally, the 200 mM NaCl wash step was removed; the resulting chromatogram (A), SDS-PAGE gel (B) and Western blot (C) can be seen in Figure 7.4. The amount of material eluted off the column compared to the load is the most evident difference in the U.V. absorbance compared with the previous run. The resin appears to have correctly taken the wide load peak and concentrated the protein into a sharp, tightly defined elution peak almost 16 times the height of the original load peak (Figure 7.4.A). Figure 7.4.B indicates that the strong 55 kDa band seen in the Feed and Starting Material is concentrated and eluted in lanes 5-8, however this does not correlate with the Western blot in Figure 7.4.C. No Western blot bands were evident from the elution samples of the same size as those found in the feed and start material (Figure 7.4.C) regardless of the significant silver stained bands in the same samples above (Figure 7.4.B). The only Western blot bands observed that could be attributed to the JEV E-protein monomers are those in the feed, start material and flow-through; and as with the previous run, a larger protein is seen in the eluted fractions, with an extremely faint band at ~55 kDa in lane 5. The removal of the 200 mM NaCl second wash step had no noticeable effect; therefore prolonged interaction of material with the resin is unlikely to be the cause of the unexpected antibody binding patterns.

These two AKTA runs further cast doubt on the effectiveness of the method for the binding and elution of JEV to a QSFF resin, backing up the data in Figure 7.1 and Figure 7.2. According to the Western blots, the desired product seemed to not bind to the resin, appearing only in the feed and flow-through, and what small amount of product did appear to interact with resin and elute, was aggregated or trimerised to approximately 160kDa. Both feed samples (Figure 7.3.E and Figure 7.4.C lanes F and

SM) imply that some aggregation occurs prior to loading, yet also some aggregation could have occurred to the virus proteins on interface with the resin or during elution.



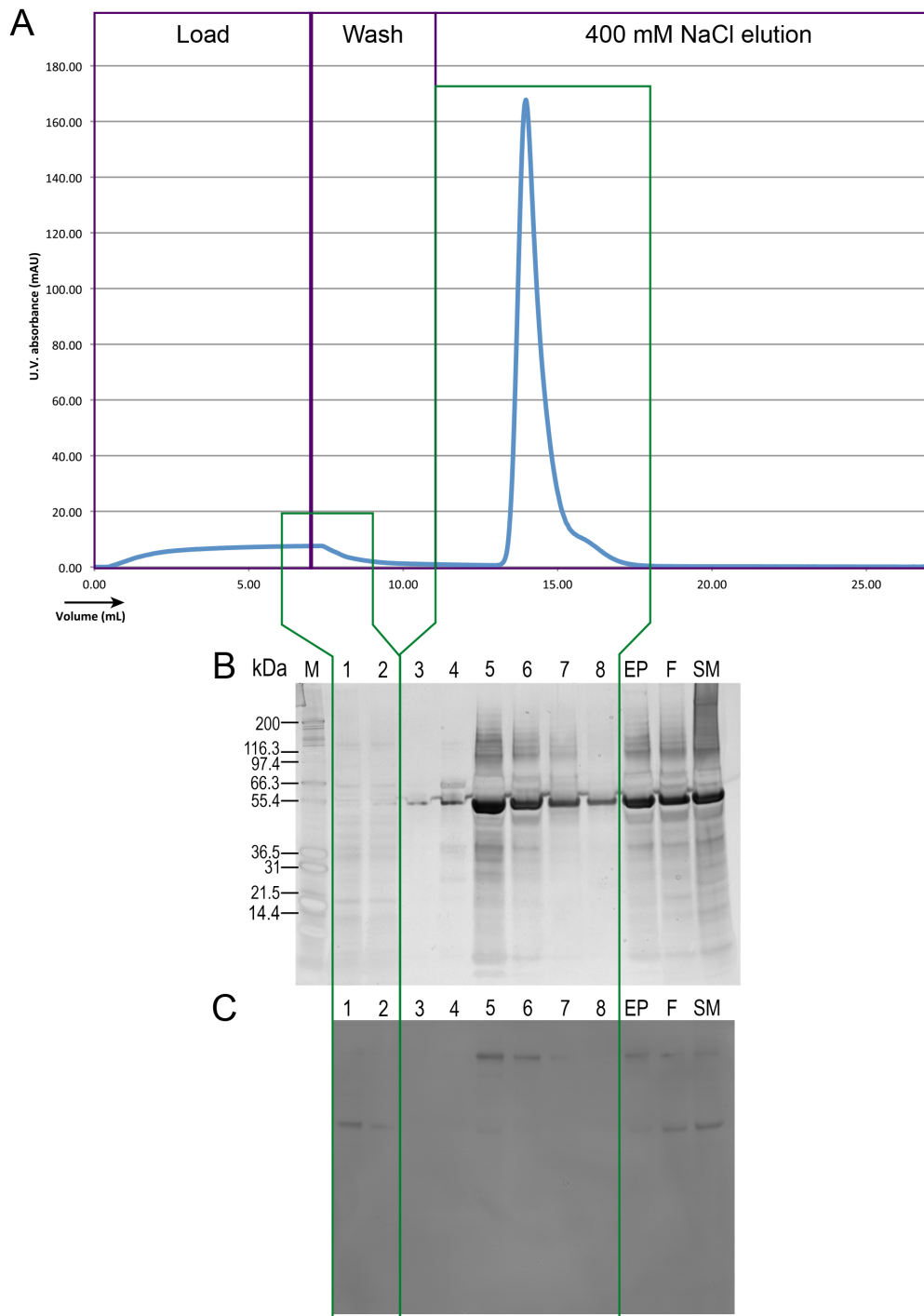


Figure 7.4 – PST JEV process material buffer exchanged into 50 mM Tris pH 8.3 loaded onto 1 mL Q Sepharose FF pre-packed column, equilibrated with the same buffer, at 1 mL/min. Chromatogram of U.V. absorbance against volume (A) and corresponding silver stained SDS-PAGE analysis (B) and Western blot (C) of selected fractions where M = Mark 12 unstained protein standard, EP = elution pool, F = feed, and SM = start material. All buffers steps shown in A also included 50 mM Tris pH 8.3

## **7.4 The impact of cross-linking the virus with formaldehyde treatment**

At this stage it was thought that perhaps the integrity of the JEV particles was being compromised when interacting with the QSFF resin; envelope protein possibly dissociating and aggregating, and the intact virions damaged to such an extent that the antigenic epitopes were unrecognisable to the antibodies which were raised against JEV – envelope protein and not giving a positive Western result. This method exposed the virus to forces not experienced during resin screening – such as shear forces of fluid flow in a pressurised system. It was conceivable that these forces, in addition to the electrostatic forces of binding to the resin, were having a detrimental effect on the virus and its surface antigens.

In an attempt to preserve the structure and antigen binding sites of JEV in the feed, and using knowledge gained from previous work (Chapter 5.1), some of the feed (PST buffered exchanged into 50 mM Tris pH 8.3, as usual) was treated with 0.02% v/v formaldehyde in the presence of 1% w/v glycine for 1 week at 4°C. It was intended that the effect of the formaldehyde would be to cross link proteins in the virus envelope thereby helping to mitigate any process damage induced during the chromatography step. The glycine, in turn, would minimise antigen losses due to the presence of the formaldehyde, as described previously. This treated material was run under the same conditions as the two previous runs, at pH 8.3, with the 200 mM NaCl second wash and compared against some non formaldehyde - glycine treated feed. The loading volumes were 5 mL for both formaldehyde treated (FT) and non-treated (NT) feeds. Figure 7.5 shows the U.V absorbance spectra of both runs (A) as well as SDS-PAGE (B and D) and Western blot analysis (C and E) of selected fractions.

The chromatogram shows that more FT material is loaded and eluted from the column than NT material – there is a 49% difference in total peak area (load, washes and elution) in FT over NT. Some variation in the amount of U.V. observable protein

between the two samples is to be expected with the buffer exchange process and the formaldehyde inactivation, but this is a significant difference. U.V. is absorbed in proteins predominantly by tryptophan and tyrosine residues (Aitken and Learmonth, 1996) and 1 % w/v glycine has been shown to not affect the U.V. absorbance of an AKTA run under the same conditions with 1 mg/mL BSA (see Appendix 10.13). Furthermore the nature of the inactivation step (with 0.02% v/v formaldehyde) should ensure very limited microorganism growth over the course the week spent at 4°C. Although this was not explicitly tested, in other instances where material was treated with formaldehyde and subsequently tested for infectivity on Vero cell monolayers, sample contamination was not found to be a problem (except in isolated cases where other factors were blamed for contamination). Therefore an increase in the amount of measurable material can be ruled out, thus if not an increase in the treated feed then perhaps a decrease in the non-treated feed, as formaldehyde treated feed is probably more stable than non-treated feed due to the cross-linking effects reducing protein degradation.

The protein content of the feeds were measured by BCA as follows: NT = 305 µg/mL and FT = 1589 µg/mL. These values are in line with the observed U.V. absorbance trace from the chromatogram, as commented on above, however there are two issues to consider with these results. The BCA assay specifically detects peptide bonds, being based on the reduction of  $\text{Cu}^{2+}$  to  $\text{Cu}^{1+}$  by protein in an alkaline medium, this reaction requires at least tripeptides. One might ask if the presence of formaldehyde and glycine could artificially increase the observed protein concentration with this method due to the cross-linking effect of formaldehyde and the binding of glycine to protein due to formaldehyde. The answer is no because formaldehyde does not induce the formation of more peptide bonds (Metz et al., 2004). Furthermore, despite being a single amino acid, glycine interferes with this assay at a concentration of 1 M (Smith et al., 1985). 1% glycine is equivalent to approximately 125 mM and has been shown to return a value below the expected protein concentration (Appendix Figure 10.7). Therefore the

FT protein concentration value, as it in this case being measured in the presence of 1 % w/v glycine, could be being reported lower than its true value. However, this interference is measured without prior incubation with formaldehyde, this incubation will decrease the available free glycine in solution as the formaldehyde induces it to bind to protein therefore at the point of measurement less will be available to interfere with the assay reagents.

Overall it follows that the BCA measurement of the NT and FT feeds can be assumed to be comparable and that the difference in the amount of measurable protein being loaded and eluted during the AKTA run could be attributed to degradation of material in the non-formaldehyde treated feed.

The SDS-PAGE and Western blot banding patterns observed in Figure 7.5.B, C, D and E correlate with those previously observed. Formaldehyde treatment had no effect in terms of acquiring JEV in the desired eluted fraction. However, ELISA data from both runs, seen in Table 7.1, shows that antigen recovery rates for the flow-throughs are 59.5% and 80.7% for the non-treated and formaldehyde treated material, respectively. Definitive evidence that, contrary to the screening results, very little JEV is binding and eluting from the resin under these conditions. It also appears that there is a protein, very similar in size to the JEV E-protein, in the eluted fraction and possibly the feed of all test material which binds to the resin but does not give positive results using either product specific assay, the Western blot or ELISA.

	<b>Non-treated feed</b>	<b>Formaldehyde and glycine treated feed</b>
Feed (AU)	409.9 ±70.6	562.9 ±25.9
Flow-through pool (AU)	243.8 ±19.2	454.2 ±14.2
Recovery (%)	<b>59.5</b> ±12.6	<b>80.7</b> ±3.9

Table 7.1 – Antigen content and recovery data based on ELISA for treated and non-treated feed. Error based on standard deviation within ELISA assay.

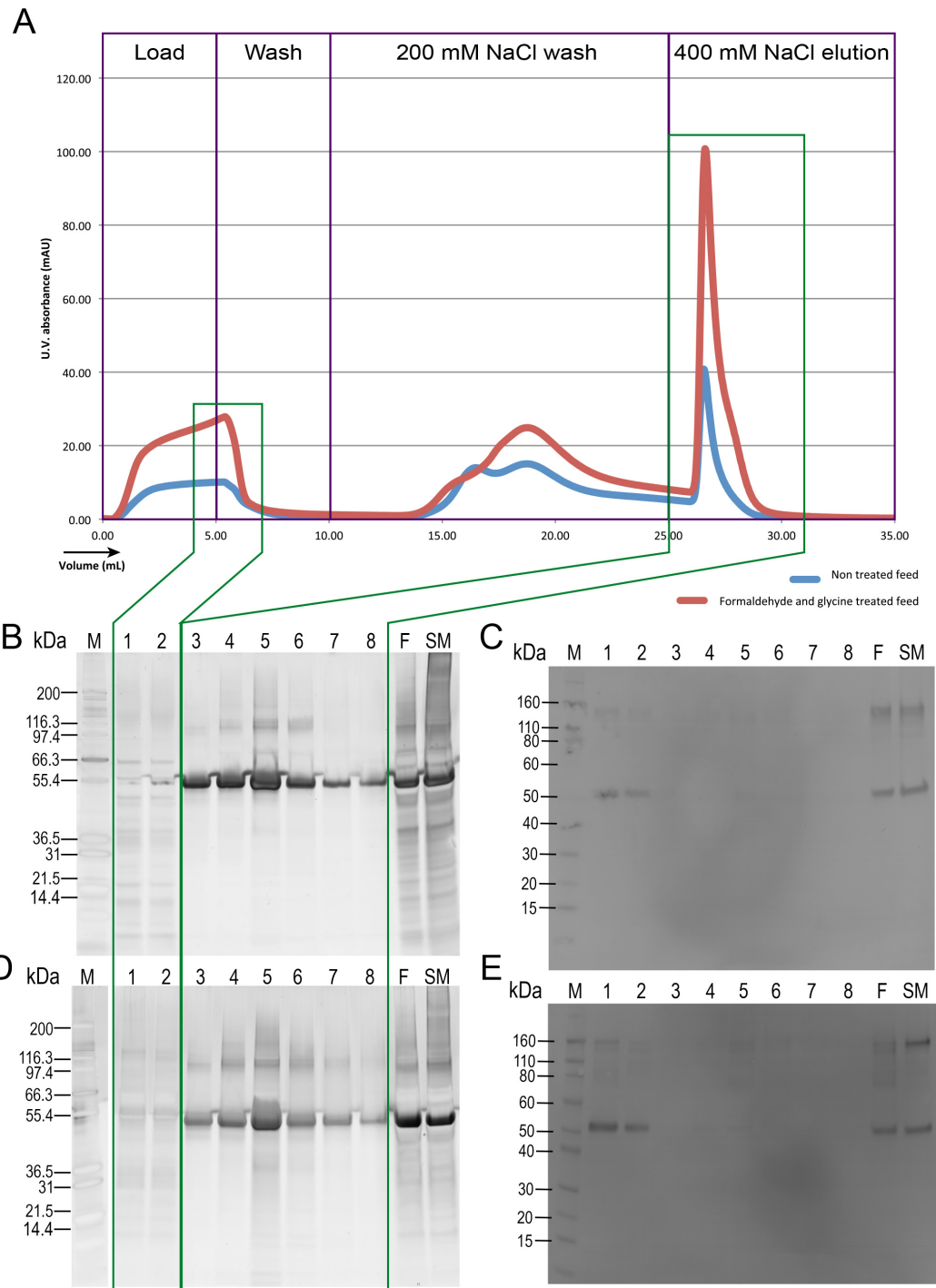


Figure 7.5 – U.V absorbance of non-treated PST feed and formaldehyde and glycine treated PST feed loaded onto 1 mL Q Sepharose FF (A) with corresponding silver stained SDS-PAGE analysis (B and D) and Western blots (C and E) of selected fractions where M = Mark 12 unstained protein standard (B and D) or Novex Sharp pre-stained protein standard (C and E), F = feed, and SM = start material. Non-treated fractions can be seen in B and C with formaldehyde and glycine treated fractions in D and E. All buffers steps shown in A also included 50 mM Tris pH 8.3.

## **7.5 Flow-through mode operation and pre-treatment**

### ***optimisation***

Clearly the bind and elute method was not suitable for JEV purification at this scale. Yet favourable antigen recovery rates were recorded in the flow-through, therefore it was decided to test the flow-through mode further, also comparing non-treated and formaldehyde treated feeds, and to dispense with the capture mode. With the second wash becoming redundant, it was removed. For this experiment, the formaldehyde treatment of the feeds was slightly different. Protamine sulphate treated JEV process material was removed from -80 °C storage, glycine was added to a concentration of 0.5 % and formaldehyde to 0.02% the mixture was then incubated at 20°C for 96 hours until quenching with sodium metabisulphite. This reduced the process exposure time and brought the glycine concentration down to a level less likely to interfere with assays without significant compromise to inactivation potential and recovery rates. It was also decided to remove the buffer exchange using centrifuge filter tubes as significant product losses were consistently observed. To create the feeds with the correct pH, the treated and non-treated PST material were diluted 1 in 3 with loading buffer (50 mM tris pH 8.3), in the same fashion as with the screening study; the feeds were each pH tested prior to loading.

One of these comparative AKTA runs is shown in Figure 7.6, in this instance the U.V. traces off the column were very similar with the NT feed giving just an 8.7% larger peak area than the FT feed, a significantly smaller difference than previously observed. However the banding patterns on both the SDS-PAGE gels (Figure 7.6.B and D) and the Western blots (Figure 7.6.C and E) are significantly different than previously observed. From the gels it appears that the FT material contained much less protein than the NT material, despite the U.V. traces being similar and the BCA results stating that the FT feed concentration was 705 µg/mL and the NT feed 428 µg/mL, in theory therefore more protein should have been loaded onto the column. Furthermore only extremely faint bands appear on the FT Western blot (Figure 7.6.E), compared with the

highly visible bands appearing in each lane with the NT material. ELISA analysis of the feeds yielded NT = 17.8 AU/mL and FT = 9.2 AU/mL, some antigen loss is expected during formaldehyde inactivation and with this batch of material of a particularly low titres it is possible that the FT material was below the LOD for the Western blot. Of perhaps greater interest is the visualisation of Western blot bands in the eluted fractions of the non-treated material (Figure 7.6.C), this was not observed in any previous AKTA runs. Possible reasons could be a larger load providing a longer residence time of the feed with the column, in turn providing greater scope for interaction or it could be a result of removing the buffer exchange step.

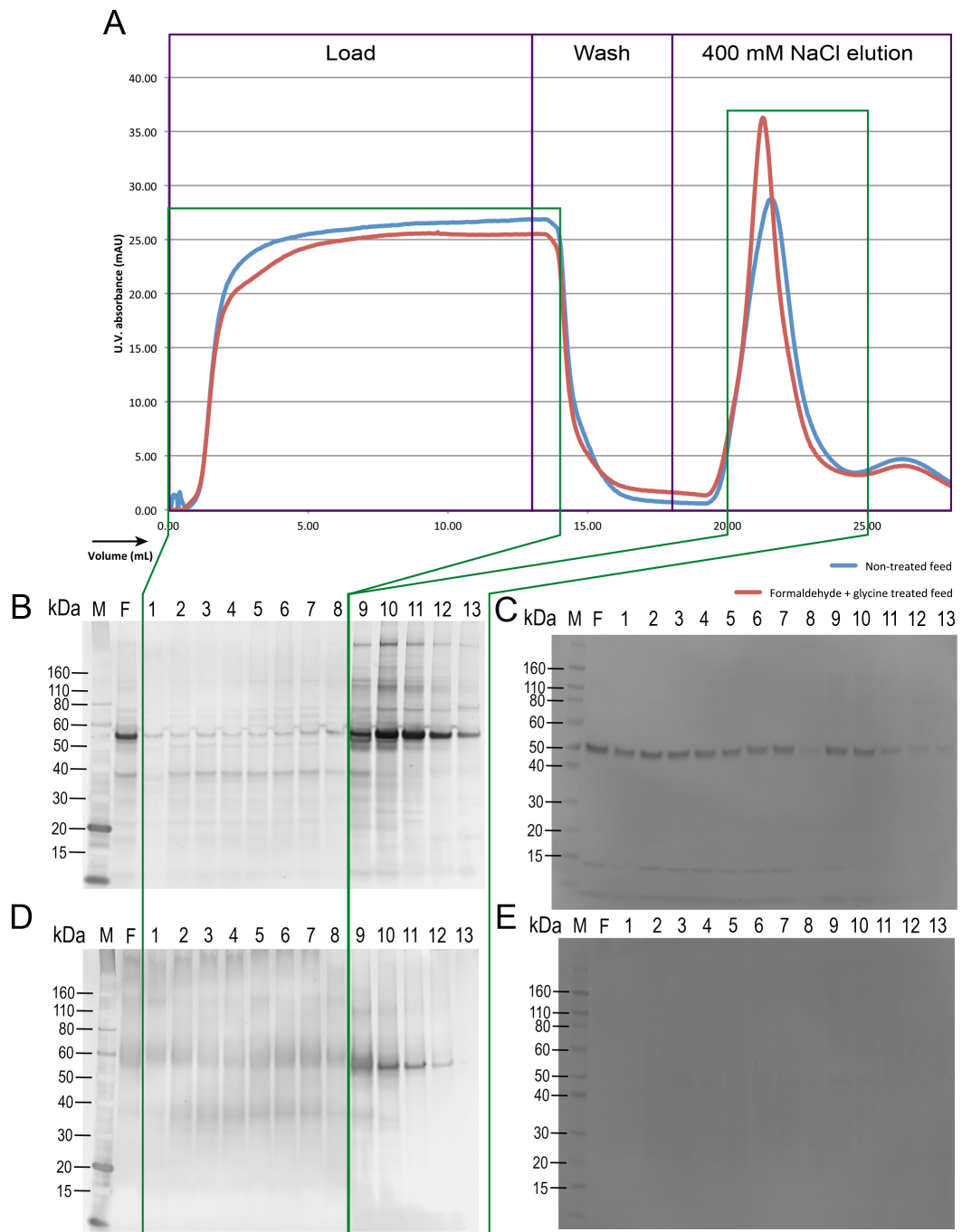


Figure 7.6 - U.V absorbance of non-treated PST feed and formaldehyde and glycine treated feed applied to a 1 mL Q Sepharose FF at 1ml/min equilibrated with 50 mM Tris pH 8.3 (A) with corresponding silver stained SDS-PAGE analysis (B and D) and Western blots (C and E) of selected fractions where M = Novex Sharp unstained (B and D) or pre-stained (C and E) protein standard and F = feed. Non-treated fractions can be seen in B and C with formaldehyde and glycine treated fractions in D and E. All buffer steps in A also contained 50 mM Tris pH 8.3.



However, one lingering consistency between all comparisons of AKTA runs of non-treated and formaldehyde and glycine treated feed is the average 20% increase in antigen recovery after flow-through mode chromatography with formaldehyde treated material. Figure 7.7 shows cumulative recovery rates for all runs where treated and non-treated feeds were compared (6 in total, 3 of each), therefore based on quantitative results, for favourable JEV antigen recovery with chromatographic purification, the bind and elute method should be abandoned in favour of a flow-through method with formaldehyde and glycine treated feed. This in contrast to the qualitative results in Figure 7.6.C, which suggest that non-treatment of the feed yields better flow-through collection of JEV antigen.

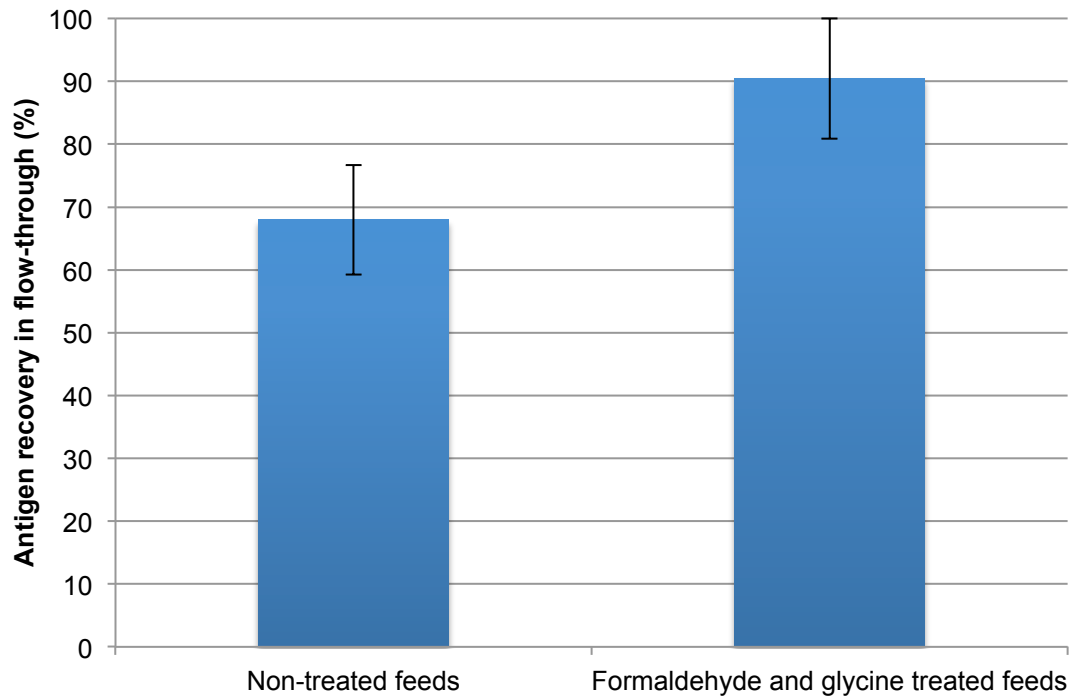


Figure 7.7 – Average JEV antigen recovery from flow-through chromatography mode of non-treated feeds and PST feeds pre-treated with formaldehyde and glycine and applied to a 1 mL Q Sepharose FF pre-packed column at 1 mL/mL for 6 different AKTA chromatography runs. Loading, equilibration and wash buffer was 50 mM Tris pH 8.3. Error bars represent standard deviation between results from separate chromatography runs, n=3.

## **7.6 Scale-up discussion**

### **7.6.1 From plates to the column**

The most striking finding of this scale-up work was the contrast in results when compared to the smaller scale bind and elute screening (Chapter 6). Based on antigen recovery, bind and elute was severely limited with the 1 mL Q Sepharose FF column. The intrinsic differences of column flow and hydrodynamic properties in the packed bed over the batch binding experiments could go some way to explaining these results. Assuming that the virus particles are too large to pass into the resin beads then mass-transfer by ionic adsorption onto the surface of the resin beads should be the limiting factor to successful binding. This type of limiting factor, external mass-transfer, is described by one study as being extremely difficult to achieve the same results when transferring between plate and column formats due to the differences in hydrodynamic conditions surrounding the resin particles (Łacki, 2012). In essence, with the plate format, as the feed is being incubated with resin slurry on an agitated platform, the resin is in effect suspended in the feed (the resin to feed ratio was approximately 1:14) as opposed to the packed column format where the feed moves around the immobile resin – here lie the fundamental differences in hydrodynamic properties which could account for the differences observed when scaling up the purification of JEV from the PreDicator plates to the 1 mL column. Contact time between feed and resin needs also to be taken into account: 2 hours on an agitated platform for the plate format and columns were loaded at 1 mL/min for each AKTA run, none of which exceeded 15 minutes. Thus, we have significant changes in two fundamental conditions, the hydrodynamic flow of the target around the resin and residence time. Yet, for a previous study these were not seen as obstacles and indeed they obtained comparable results when scaling up from HTS plate formats to columns when developing a chromatography method for the capture of a virus (Connell-Crowley et al., 2013). Although admittedly the aim of this study was virus removal, and therefore the authors were unconcerned amount maintaining virus structure, they were able to successfully

demonstrate virus binding to QSFF. Another study also significantly reduced residence time when switching to a packed column from a plate format, though this one had the benefit of intra-particle mass transfer, as the target was a glycosylated protein able to penetrate within the resin, thus changing the limiting factor to internal mass-transfer (Sanaie et al., 2012). Ultimately, for JEV purification the method transfer from batch binding plates to a column format was unsuccessful, unlike with the virus capture study mentioned above. One hypothesis could simply be the residence time – some resin binding was observed with the final AKTA run described above (Figure 7.6.C, lanes 9-13), which was one of the experimental AKTA runs with a longer contact time, totalling 13 minutes. This is a theory that could be tested with a reduced flow-rate during loading, though still at odds with the literature. Another theory, with the screening method on the plates, could be the incubation period on the agitating platform disrupting the virus to such an extent that the envelope proteins became separated and were able to migrate into the resin beads for binding and subsequent elution as the JEV E-protein is not required to be part of the whole virus to be picked up by the corresponding antibodies during analysis with Western blots and ELISA. The final, and arguably the simplest, theory to be put forward is that there simply was not enough JEV in the feed that was applied to the column in each attempt. This fact along with the difference in contact time colluded to produce different results at different scales – the increased contact time at microscale compensated for the relatively low concentration of JEV.

These results point towards significant limitations of such high-throughput process development techniques for products of this nature: large biomolecules at relatively low concentrations in the crude harvest feed streams.

### **7.6.2 JEV stability, binding and interaction**

The stability of JEV has been brought into question previously with this project and was the principle reasoning for pre-treating the feed with formaldehyde and glycine prior to loading onto the column. The consistent 20% increase in antigen recovery observed

when comparing treated with non-treated feeds could be due to increased stability of the virus particles. The stresses experienced during flow-through chromatography could have been less likely to degrade and damage the virus due to the envelope protein having been cross-linked by the formaldehyde, resulting in higher recovery rates. However, due to the method now being flow-through, it could be simply be that less of the virus is binding to the column and thus passing straight through, the formaldehyde and glycine treatment having altered the virus' surface chemistry to such an extent that the overall charge of the virus changes, compared to the non-treated feed, so less binds to the Q Sepharose FF resin under those conditions. Such alterations could be due to the lone action of the formaldehyde on JEV or the action of formaldehyde binding glycine and/or the principle contaminant, residual protamine sulphate, to the virus envelope. Formaldehyde has been shown to bind proteins to glycine and other molecules (Metz et al., 2004; Metz et al., 2005; Metz et al., 2006). Glycine is not a highly charged molecule and previous studies have shown that the zeta potential of JEV harvest material treated with formaldehyde in the presence of glycine does not significantly change (see Chapter 5.1). As previously stated in Chapter 6, protamine sulphate is a highly charged cationic peptide which will not bind to an anion exchange resin under these conditions. Therefore the possibility exists that formaldehyde induced binding of PS to JEV surface proteins could cause the overall charge on the virus particle to become less negative and therefore not bind to the anion exchange resin thus improving flow-through recovery. Repeating the experiments with purified JEV could test this theory. Formaldehyde induced binding of protamine sulphate to all proteins in solution could also explain the limited staining of the gels in Figure 7.5.D and Figure 7.6.D when compared with their non-treated counter parts (Figure 7.5.A and Figure 7.6.A), as silver ions do not bind to protamine sulphate (discussed in section 6.2).

### 7.6.3 The eluted protein

Having discussed the contents of the flow-through and the apparent non-adherence of JEV to the resin, the focus should now switch to what did adhere to the resin and was subsequently eluted with 400 mM NaCl. All AKTA runs (including those not shown) had a significant peak with said elution, fractions of which produced a distinct band at approximately 55 kDa when run on polyacrylamide gel with either silver or Coomassie staining. As discussed in Chapter 6, the JEV E-protein amino acid sequence is 500 residues long and calculated to be 53.8 kDa, Western blot analysis highlights a protein at ~52 kDa which correlates with positive control samples at Valneva Scotland Ltd. (Livingston, U.K.) who supplied the virus stock and the antibodies (D. Low, Valneva Scotland Ltd., personal communication). The eluted protein did not give an immunosignal and so was twice excised, digested and outsourced (to the UCL Wolfson Institute, London U.K.) for LC-MS identification but the analysis was inconclusive in both instances due to a weak signal and no fragments were detected. Subsequently, the same eluted bands were excised from further AKTA runs and outsourced (to Alta Bioscience, Birmingham, U.K.) for amino acid sequencing, first for 5 residues then 10 residues but again the signal was too weak for conclusive results (see Appendix 10.14). Various combinations of the short sequences obtained were still analysed using numerous BLAST searches with online resources, but no significant hits for *Flavivirus* or *Chlorocebus* (the host cell genus) proteins were made. Some searches yielded results where the top results were partial hits for proteins belonging to large families (ABC transporters, dehydrogenases...) suggesting contamination of material or samples, but ultimately the protein concentration in the excised gel samples was too low for reliable identification using either of these methods. At this point, it is not conclusively possible to say if this protein is a contaminant or a process related impurity, one of the most obvious contaminants would be bovine serum albumin (BSA). BSA is used in many assays as a standard or stabiliser and is present in the serum used to supplement growth media during cell expansion. However this band is too

small to be BSA (= 66.5 kDa) and slightly too large to be E-protein, unless the theory raised in Chapter 6.3 is again brought to the fore, that this is somehow an interaction of the JEV E-protein and protamine sulphate which inhibits antibody binding. This would give the protein the approximate size as seen by the band yet still be small enough to diffuse into the resin beads, but would be at odds with the theory above, hypothesising such an interaction to prevent anion exchange binding to the resin under these conditions due to the cationic properties of protamine sulphate.

#### 7.6.4 Bound versus unbound

With regard to protein binding, a retrospective analysis of 14 AKTA chromatography runs showed that the proportion of material in the feed which bound to resin and that which flowed-through was impacted on by storage of the feed after buffer exchange. Significant product losses were noticed when using the 50 kDa MWCO Vivaspin tubes to change the buffer of the protamine sulphate treated JEV process material (the start material, SM) into the Tris loading buffer at the required pH, therefore the decision was taken to simply dilute the SM with loading buffer instead to achieve the correct pH. However, after buffer exchange the feed was sometimes stored at 4°C overnight increasing the pH of the Tris buffer to approximately 8.9; this was not measured but the *pKa* of Tris will increase by 0.03 per 1°C degree decrease in temperature (El-Harakany et al., 1984). This did not occur with feed which was merely diluted and when the U.V. spectra of the AKTA runs of the two types of feed were compared, the results showed that feed stored overnight in Tris buffer, prior to being used in an experiment and applied to column, had proportionally more material bind to the resin. Figure 7.1.A, Figure 7.4.A and Figure 7.5.A are examples of AKTA runs in which the feed was exposed to higher pH due to low temperature storage, Figure 7.3.A and Figure 7.6.A are examples of those which were not, the elution peaks in the former set are clearly much larger relative to the loading peaks than in the latter. Figure 7.8 shows the average ratios of bound to unbound material for the two types of feeds, those stored overnight in Tris (pH >8.3) and those not (maintained at original pH of 8.3). The ratios

were determined by dividing the total U.V. peak area for the eluted material (including 2<sup>nd</sup> wash step, where applicable) by the total peak for the load. The figure clearly illustrates that feed exposed to higher pHs overnight binds on average more than 12 times a higher proportion of material to the resin than feed diluted with loading buffer.



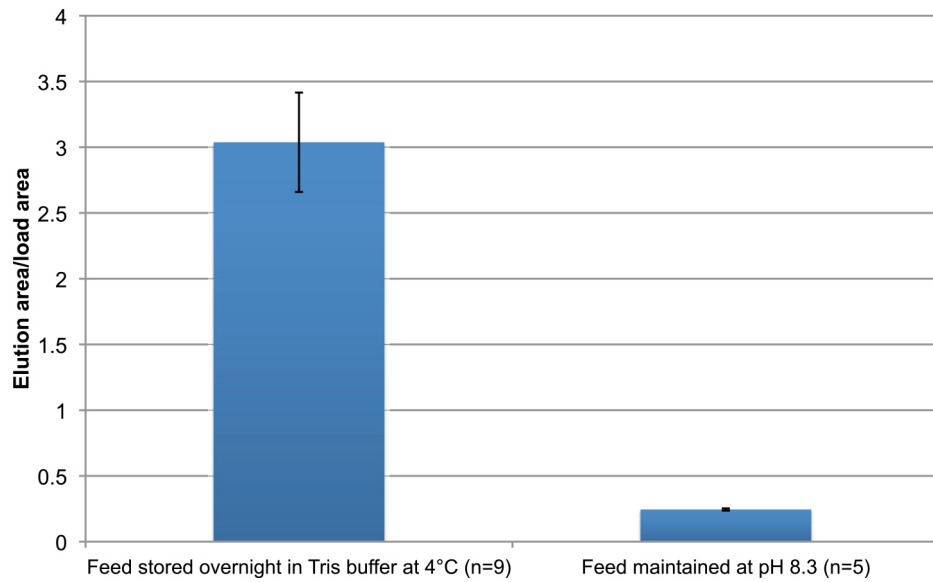


Figure 7.8 – Average ratios of bound to unbound peak areas (elution peak area over loading peak area) of AKTA runs from feeds which were stored overnight in Tris loading buffer at 4°C and feed maintained at pH 8.3. Feeds generated from PST JEV process material by either buffer exchanging into or diluting with the Tris buffer in use for a particular experiment.

Two, not necessarily mutually exclusive, theories will be put forward to help explain this behaviour. The first and most obvious is that the material in the feed was carrying more charge due its exposure to a higher pH – the feed components became more negatively charged. One may expect the pH of the solution to have fallen back to the prepared value as the temperature rises to an ambient level but perhaps the molecules within remained with a greater overall charge than they had prior to the drop in temperature. A second theory, which could work in addition to the increased charge on the molecules, is that the pH increase could also have destabilised the virus, unfolding the various proteins from each other and the lipid envelope allowing for them to penetrate the resin to bind and elute. If that were the case then formaldehyde treated JEV should mitigate this pH induced degradation, which is in fact what is suggested above when discussing the results of the AKTA run represented by Figure 7.5, where formaldehyde treated feed appears more stable. Another observation, possibly related to stability, is the appearance of potentially trimeric forms of JEV E-protein in the feeds stored in Tris buffer at 4°C overnight after buffer exchange (lanes, F and SM in Figure 7.4.C and Figure 7.5.C and E) and slightly less visibly in feed which underwent buffer exchange (Figure 7.3.C, lane F) but not in diluted feeds (Figure 7.6. C and E, lane F). The buffer exchange step itself could have somehow caused these bands to appear by damaging or dissociating the JEV particles in the feed or it could be due to a change in pH. This larger protein, identified as JEV E-protein by the Western blots, is seen in the elution fraction in Figure 7.4.C, lanes 4 and 6, though also much less so in Figure 7.3.D. It appears to bind to the resin and elutes with 200 and 400 mM NaCl, it is unlikely to be aggregated JEV because the band is consistently the size of trimerised E-protein, which would still be able to diffuse into the resin for bind and elute, unlike large aggregated virions. Furthermore, virus aggregation events are very unlikely to hold together during SDS-PAGE sample preparation, as proteins are denatured to their secondary structures. These larger forms of E-protein were not observed with the diluted feeds not exposed to fluctuations in pH. *Flavivirus* E-proteins have been shown to trimerise with decreases in pH as part of virus maturation and receptor mediated

endocytosis (Lindenbach et al., 2007; Mukhopadhyay et al., 2005), and although no such behaviour has been reported to date with increases in pH, it does demonstrate the inherent sensitivity of the protein to changes in pH. Perhaps changes in pH caused the virus to degrade and then the trimers to be formed, or the virus degraded and the shift in pH caused the trimers to form. Either way, this is further evidence of JEV instability.

### **7.6.5 Scale-up summary**

The results highlight the severe limitations when switching from high-throughput microplate based process development to a column format for virus purification for systems where differences in hydrodynamic properties have significant impact due to the nature of the product as large biomolecule compared to the smaller protein products for which they are originally designed. Indeed this is a difficult process to characterise with many different variables. Process development work of this nature should probably initially be performed with purified product before using process material, so that one may understand how it reacts to each operation without the interference of impurities or contaminants.

A consideration for future process development would be to avoid using a Tris based buffer as, should process hold steps be required, the fluctuations in pH due to temperature could destabilise the product. The stability of JEV has consistently proven to be a concern yet there is evidence herein that formaldehyde treatment can mitigate losses due to instability and processing. The continued scale-up of this method would be contingent on significant improvements in characterisation of the process components and their interactions. Based on initial results it is suggested to further explore the potential for flow-through mode chromatography, based on the qualitative data in Figure 7.6 prior embarking on pre-treatment solely for chromatography development.

# 8 Conclusions and Future work

---

## 8.1 Conclusions

### 8.1.1 JEV processing

The project established a scale down method that allowed a typical whole virus Japanese Encephalitis vaccine production process to be explored down to the microwell level. This successfully led to a certain level of characterisation of the formaldehyde inactivation step, by coupling the investigation at small scale to Design of Experiments based screening of conditions. This also allowed for the identification of significant factors linked to infectivity, antigen recovery and aggregation and the extent to which they impacted. The overriding significant factors were temperature, time and formaldehyde concentration and their potential impact on product losses through aggregation has been highlighted.

Glycine should be seriously considered for inclusion into any JEV inactivation steps using formaldehyde, having consistently shown to improve antigen recovery rates. Evidence was also presented to argue for preferentially inactivating JEV at the concentrated harvest stage. Furthermore, should scale-up of the commercial processes be considered, it has been shown that JEV harvest material could withstand considerable increase in the shear forces to which it is may be exposed.

In terms of the purification, although initially showing promising results for bind and elute the performance of Q Sepharose FF altered significantly on scale-up with having to switch to operating in flow-through mode which appeared to show promising results, and though there is still plenty of more work to be done, this has increased overall understanding of processing potential. The benefits observed by pre-treating the feed

with formaldehyde and glycine could say more about the stability of JEV than suitability of the method developed. Indeed, JEV stability was a constant issue throughout the project as can be seen in the sensitivity to pH (Chapter 7.6) and the significant drops in antigen content and infectivity of control samples (Chapter 5.1.3).

Only one type of chromatography was investigated in this work when it is likely that more than one type of chromatography step will have to be implemented to achieve the same level of purity as sucrose gradient purification. Therefore, despite the limits of density gradient purification in terms of scalability and labour intensive processing, this work underlines the useful simplicity of that technique when seeking to purify products of this type. However this also suggests that production of JEV and potentially other similar products are limited in terms of scale without significant capital investment in additional equipment and labour.

### **8.1.2 Process development using small scale high-throughput techniques**

Small-scale process development is undoubtedly cheaper than at larger scale. Yet unless adequate assays are in place to accurately support and maintain such development, high-throughput small-scale analysis becomes self-limiting. The development of the modified ELISA method provided a specific and sensitive tool for such development by making minor changes to a routine assay. It is certainly possible to use other established assays in this way – using their relative as opposed to absolute capabilities and maximising limited resources such as antibodies and standards (see below and section 6.3.2).

As stated, one of the main limitations of sucrose gradient purification, and thus reason for investigation, was scalability. Ironically, in the search for a scalable alternative the methods used were not shown to be themselves amenable to scale-up for this class of product.

### **8.1.3 Retrospective process characterisation and development**

With retrospective characterisation of pre-existing vaccine manufacturing processes, one is locked into all the established production and purification strategies along with the associated analytics. This limits the scope of potential improvements in terms of changes that can be made to manufacturing processes and in even broader terms challenge the vaccine product itself. Perhaps a Vero cell derived inactivated whole virus vaccine is not the most efficient or effective product to combat the spread of Japanese Encephalitis – other potential products are suggested below. Although a benefit of having production processes already established is that reference material should be readily available. Indeed, from this work it could be argued that any such process development should be performed with purified product first to elucidate how the product itself should react in the different environments to which it is exposed.

## **8.2 Future work**

### **8.2.1 Further JEV process investigation**

The benefit of including glycine in formaldehyde JEV inactivation needs to be proven at larger scale. Furthermore, although touched on in this work, it was never completely established whether changing the location of the formaldehyde inactivation step would have a quantifiable benefit on process yield. This could link in to further stability studies of JEV through-out the process and determine fully whether purifying a cross-linked virus particle is easier or gains higher recoveries than would otherwise be observed.

The extent of formaldehyde induced cross-linking could also be investigated in relation to virus stability, possibly using circular dichroism and heat to monitor the shift from tertiary to secondary structures. Or a highly sensitive particle sizing techniques, beyond DLS and NTA, such as atomic force microscopy or transmission electron microscopy, could be used to investigate whether the cross-linking effect causes the virus particles to contract, and if so by how much relative to the conditions and additives used for inactivation.

The screening plates failed to predict behaviour on scale-up to column resins, possibly due to the differences in hydrodynamic conditions between the two formats, as stated in Chapter 7.6. The theory states there should be some form of charge relationship between the resin and the virus and this appeared to be observed in the microwell format though perhaps the differences in hydrodynamic conditions allow for other forces to come into play. The results from the Capto Adhere at least allow that this is a possibility. Only anion exchange resins were tested at this small scale but cation and hydrophobic interaction resins are also available. Moreover, to investigate the possible mass transfer issue, different monolith media and membrane adsorbers are also now available at this scale for high-throughput investigation. Further to this, batch-binding experiments could also be investigated at larger scale as this would reduce the stresses on the product.

As stated above, many of the questions surrounding this work could be answered if much of it was repeated with purified JEV. This would focus observed effects solely on JEV, such as the interaction or lack thereof with the chromatography media, which could then be compared against results such as these from crude process material.

The microscale methodologies used here could be coupled with other high-throughput methodologies at a similar scale, with a view to incorporating upstream development of cell proliferation and viral titres at harvest with, as touched on in Section 6.3.2, colorimetric (or similar) microplate based process analytics within a fully automated system. This would form a complete microscale process development platform with minimum operator input generating significant amounts of data. For example, different upstream culture conditions could be investigated in sequence with different purification conditions, or even technologies. In parallel, the relevant process information could be acquired *in situ*, characterising the developments as they unfold by simplifying assays such as BCA total protein, Picogreen and ELISA. This simplification would involve just using their absorbance (or otherwise) attribute, without standards or blanks, accruing relative, as opposed to absolute, quantitative data – which is for the most part what is

required at this scale to make decision on which routes to investigate at larger scale. Indeed, reference material (or pre-purified product) and blanks could be included within this development process stream.

With protamine sulphate identified as the most significant and visible process impurity perhaps different DNAses could be investigated for removing host cell DNA instead. As JEV is an RNA virus it should not be affected. However, perhaps RNAses could also be investigated as potential JEV inactivating agents.

### **8.2.2 Impurity characterisation**

The 56 kDa protein band observed throughout the chromatography investigation is a mystery. It appears to be an uncharacterisable process impurity structurally unrelated to JEV, as no antibody binding was evident. Understanding, or at the least identifying, this protein and where it came from could lead to increasing yields further, for example if it is identified as some form of degraded or damaged product perhaps it can be elucidated how where it occurred. Or, should it turn out to be a process related impurity perhaps certain production materials would need to be re-evaluated.

### **8.2.3 Other processes and the future vaccines**

Clearly beyond the scope of this work, though it would be interesting to attempt to apply what was found here to other virus purification and inactivation processes. Particularly viruses of a more labile disposition – would increased robustness due to cross-linking be more evident, or even possible?

The Japanese Encephalitis virus, as with many such whole virus vaccine products, is clearly a difficult product to handle and monitor. So while for this type of vaccine this is a good start for process development, understanding and characterisation, this is just scratching the surface.

Perhaps then the key to more successful vaccine products lies in changing their nature – moving away from fragile whole viruses to more robust products. Such vaccines



should be able to withstand not only their large-scale manufacture but also the rigours of global product supply without the need for a cold-chain to the point of care. This is a longstanding issue with all medicines, not just vaccines. Yet with vaccines the solutions could be simpler than with, say, a therapeutic protein for which activity must be preserved. The antigens which provide future immunity do not have activity, just their structure must be preserved, and not even in its entirety as part of the whole pathogen. For example, once identified potential immunogens could be immobilised onto stable more stable supports, such as gold nanoparticles, to elicit an immune response. Such a study as already been performed with *Flavivirus* E-protein in mice (Niikura et al., 2013), but as previously stated in section 3.2.3, subunit vaccines do not perform well outside of animal models for JE vaccines. Overall then, it could be argued that the vaccines products need to improve before the processes.

## 9 References

---

- Aitken A, Learmonth M. 1996. Protein determination by UV absorption. In: Walker, JM, editor. *protein Protoc. Handb.* Humana Press, pp. 3–6.  
[http://link.springer.com/protocol/10.1007/978-1-60327-259-9\\_1](http://link.springer.com/protocol/10.1007/978-1-60327-259-9_1).
- Aizawa C, Hasegawa S, Chih-Yuan C, Yoshioka I. 1980. Large-scale purification of Japanese encephalitis virus from infected mouse brain for preparation of vaccine. *Appl. Environ. Microbiol.* **39**:54–7.  
<http://www.pubmedcentral.nih.gov/articlerender.fcgi?artid=291283&tool=pmcentrez&rendertype=abstract>.
- Andreadis ST, Roth CM, Le Doux JM, Morgan JR, Yarmush ML. 1999. Large-scale processing of recombinant retroviruses for gene therapy. *Biotechnol. Prog.* **15**:1–11. <http://www.ncbi.nlm.nih.gov/pubmed/9933508>.
- Bachmann MF, Kündig TM, Kalberer CP, Hengartner H, Zinkernagel RM. 1993. Formalin inactivation of vesicular stomatitis virus impairs T-cell- but not T-help-independent B-cell responses. *J. Virol.* **67**:3917–22.  
<http://www.pubmedcentral.nih.gov/articlerender.fcgi?artid=237758&tool=pmcentrez&rendertype=abstract>.
- Barteling S, Vreeswijk J. 1991. Developments in foot-and-mouth disease vaccines. *Vaccine* **9**:75–88. <http://linkinghub.elsevier.com/retrieve/pii/0264410X91902614>.
- Barteling S, Woortmeyer R. 1984. Formaldehyde inactivation of foot-and-mouth disease virus. Conditions for the preparation of safe vaccine. *Arch. Virol.* **80**:103–117. <http://www.springerlink.com/index/H428077X51640706.pdf>.

- Beasley DWC, Lewthwaite P, Solomon T. 2008. Current use and development of vaccines for Japanese encephalitis. *Expert Opin. Biol. Ther.* **8**:95–106.  
<http://www.ncbi.nlm.nih.gov/pubmed/18081539>.
- Bergander T, Nilsson-Välímáa K, Oberg K, Lacki KM. 2008. High-throughput process development: determination of dynamic binding capacity using microtiter filter plates filled with chromatography resin. *Biotechnol. Prog.* **24**:632–9.  
<http://www.ncbi.nlm.nih.gov/pubmed/18454563>.
- Besra L, Liu M. 2007. A review on fundamentals and applications of electrophoretic deposition (EPD). *Prog. Mater. Sci.* **52**:1–61.  
<http://dx.doi.org/10.1016/j.pmatsci.2006.07.001>.
- Böttiger M, Lycke E, Melen B, Wrangé G. 1958. Inactivation of poliomyelitis virus by formaldehyde; incubation time in tissue culture of formalin treated virus. *Arch. Gesamte Virusforsch.* **8**:259–66. <http://www.ncbi.nlm.nih.gov/pubmed/13821990>.
- Boychyn M, Yim SSS, Bulmer M, More J, Bracewell DG, Hoare M. 2004. Performance prediction of industrial centrifuges using scale-down models. *Bioprocess Biosyst. Eng.* **26**:385–91. <http://www.ncbi.nlm.nih.gov/pubmed/14566553>.
- Boychyn M, Yim SSS., Ayazi Shamlou P, Bulmer M, More J, Hoare M. 2001. Characterization of flow intensity in continuous centrifuges for the development of laboratory mimics. *Chem. Eng. Sci.* **56**:4759–4770.  
<http://www.sciencedirect.com/science/article/pii/S0009250901001397>.
- Brown F. 2001. Inactivation of viruses by aziridines. *Vaccine* **20**:322–7.  
<http://www.ncbi.nlm.nih.gov/pubmed/11672893>.
- Burden CS, Jin J, Podgornik A, Bracewell DG. 2012. A monolith purification process for virus-like particles from yeast homogenate. *J. Chromatogr. B* **880**:82–89.  
<http://linkinghub.elsevier.com/retrieve/pii/S1570023211007422>.

- Burgess RR, Jendrisak JJ. 1975. Procedure for the rapid, large-scale purification of *Escherichia coli* DNA-dependent RNA polymerase involving polymin P precipitation and DNA-cellulose chromatography. *Biochemistry* **14**:4634–4638. <http://pubs.acs.org/doi/abs/10.1021/bi00692a011>.
- Cardoso AI, Beauverger P, Gerlier D, Wild TF, Rabourdin-Combe C. 1995. Formaldehyde inactivation of measles virus abolishes CD46-dependent presentation of nucleoprotein to murine class I-restricted CTLs but not to class II-restricted helper T cells. *Virology* **212**:255–258. <http://linkinghub.elsevier.com/retrieve/pii/S0042682285714791>.
- Chambers TJ, Hahn CS, Galler R, Rice CM. 1990. Flavivirus genome organization, expression, and replication. *Annu. Rev. Microbiol.* **44**:649–88. <http://www.ncbi.nlm.nih.gov/pubmed/2174669>.
- Chevallet M, Luche S, Rabilloud T. 2006. Silver staining of proteins in polyacrylamide gels. *Nat. Protoc.* **1**:1852–8. <http://www.pubmedcentral.nih.gov/articlerender.fcgi?artid=1971133&tool=pmcentrez&rendertype=abstract>.
- Chhatre S, Titchener-Hooker NJ. 2009. Review: Microscale methods for high-throughput chromatography development in the pharmaceutical industry. *J. Chem. Technol. Biotechnol.* **84**:927–940. <http://doi.wiley.com/10.1002/jctb.2125>.
- Coffman JL, Kramarczyk JF, Kelley BD. 2008. High-throughput screening of chromatographic separations: I. Method development and column modeling. *Biotechnol. Bioeng.* **100**:605–18. <http://www.ncbi.nlm.nih.gov/pubmed/18496874>.
- Connell-Crowley L, Larimore EA, Gillespie R. 2013. Using high throughput screening to define virus clearance by chromatography resins. *Biotechnol. Bioeng.* n/a–n/a. <http://dx.doi.org/10.1002/bit.24869>.

- Crooks AJ, Lee JM, Dowsett AB, Stephenson JR. 1990. Purification and analysis of infectious virions and native non-structural antigens from cells infected with tick-borne encephalitis virus. *J. Chromatogr.* **502**:59–68.  
<http://www.ncbi.nlm.nih.gov/pubmed/2157727>.
- Darnell MER, Subbarao K, Feinstone SM, Taylor DR. 2004. Inactivation of the coronavirus that induces severe acute respiratory syndrome, SARS-CoV. *J. Virol. Methods* **121**:85–91. <http://www.ncbi.nlm.nih.gov/pubmed/15350737>.
- Darwish M, Hammon W. 1966. Studies on Japanese B encephalitis virus vaccines from tissue culture. VI. Development of a hamster kidney tissue culture inactivated vaccine for man. 2. The characteristics of inactivation of an attenuated strain of OCT-541. *J. Immunol. (Baltimore, Md. 1950)* **96**:806.  
<http://www.ncbi.nlm.nih.gov/pubmed/4288022>.
- Davies JT. 1987. A physical interpretation of drop sizes in homogenizers and agitated tanks, including the dispersion of viscous oils. *Chem. Eng. Sci.* **42**:1671–1676.  
[http://dx.doi.org/10.1016/0009-2509\(87\)80172-0](http://dx.doi.org/10.1016/0009-2509(87)80172-0).
- Downing LA, Bernstein JM, Walter A. 1992. Active respiratory syncytial virus purified by ion-exchange chromatography: characterization of binding and elution requirements. *J. Virol. Methods* **38**:215–28.  
<http://www.ncbi.nlm.nih.gov/pubmed/1517352>.
- El-Harakany A, Abdel Halim, F. M, Barakat, O. A. 1984. Dissociation constants and related thermodynamic quantities of the protonated acid form of tris-(hydroxymethyl)-aminomethane in mixtures of 2-methoxyethanol and. *J. Electroanal. Chem.* **162**:285–305.  
<http://www.sciencedirect.com/science/article/pii/S0022072884801710>.

- Erlanger TE, Weiss S, Keiser J, Utzinger J, Wiedenmayer K. 2009. Past, Present, and Future of Japanese Encephalitis. *Emerg. Infect. Dis.* **15**:1–7.  
<http://www.pubmedcentral.nih.gov/articlerender.fcgi?artid=2660690&tool=pmcentrez&rendertype=abstract>.
- Ferreira-Torres C, Micheletti M, Lye GJ. 2005. Microscale process evaluation of recombinant biocatalyst libraries: application to Baeyer-Villiger monooxygenase catalysed lactone synthesis. *Bioprocess Biosyst. Eng.* **28**:83–93.  
<http://www.ncbi.nlm.nih.gov/pubmed/16208497>.
- Filipe V, Hawe A, Jiskoot W. 2010. Critical evaluation of Nanoparticle Tracking Analysis (NTA) by NanoSight for the measurement of nanoparticles and protein aggregates. *Pharm. Res.* **27**:796–810.  
<http://www.pubmedcentral.nih.gov/articlerender.fcgi?artid=2852530&tool=pmcentrez&rendertype=abstract>.
- Fraenkel-Conrat H, Mecham DK. 1949. The reaction of formaldehyde with proteins; demonstration of intermolecular cross-linking by means of osmotic pressure measurements. *J. Biol. Chem.* **177**:477–486.  
<http://www.ncbi.nlm.nih.gov/pubmed/18107450>.
- Frazatti-Gallina NM, Mourão-Fuches RM, Paoli RL, Silva MLN, Miyaki C, Valentini E, Raw I, Higashi HG. 2004. Vero-cell rabies vaccine produced using serum-free medium. *Vaccine* **23**:511–7. <http://www.ncbi.nlm.nih.gov/pubmed/15530700>.
- Furesz J. 2006. Developments in the production and quality control of poliovirus vaccines -- historical perspectives. *Biologicals* **34**:87–90.  
<http://www.ncbi.nlm.nih.gov/pubmed/16621594>.

- Galdiero F. 1979. Adenovirus aggregation and preservation in extracellular environment. *Arch. Virol.* **59**:99–105.  
<http://link.springer.com/10.1007/BF01317899>.
- GE Healthcare LS. 2011. Ion exchange columns and media Selection guide - Ion Exchange Media. GE Healthcare, Life Sciences.
- GE Healthcare Life Sciences. 2012. Capto™ adhere. *Instr.* 28-9064-05 AC.
- Gupta RK, Misra CN, Gupta VK, Saxena SN. 1991. An efficient method for production of purified inactivated Japanese encephalitis vaccine from mouse brains. *Vaccine* **9**:865–7. <http://www.ncbi.nlm.nih.gov/pubmed/1811372>.
- Guy HM, McCloskey L, Lye GJ, Mitrophanous KA, Mukhopadhyay TK. 2013. Characterization of lentiviral vector production using microwell suspension cultures of HEK293T-derived producer cells. *Hum. Gene Ther. Methods* **24**:125–39. <http://online.liebertpub.com/doi/abs/10.1089/hgtb.2012.200>.
- Hagen AJ, Oliver CN, Sitrin RD. 1996. Optimization of poly(ethylene glycol) precipitation of hepatitis A virus used to prepare VAQTA, a highly purified inactivated vaccine. *Biotechnol. Prog.* **12**:406–12.  
<http://www.ncbi.nlm.nih.gov/pubmed/8652125>.
- Hahn R. 2012. Methods for characterization of biochromatography media. *J. Sep. Sci.* **35**:3001–32. <http://www.ncbi.nlm.nih.gov/pubmed/23111926>.
- Haimer E, Tscheliessnig A, Hahn R, Jungbauer A. 2007. Hydrophobic interaction chromatography of proteins IV. Kinetics of protein spreading. *J. Chromatogr. A* **1139**:84–94. <http://www.ncbi.nlm.nih.gov/pubmed/17116304>.

- Halstead SB, Thomas SJ. 2010. Japanese encephalitis: new options for active immunization. *Clin. Infect. Dis.* **50**:1155–64.  
<http://www.ncbi.nlm.nih.gov/pubmed/20218889>.
- Hopps HE, Bernheim BC, Nisalak A, Tjio JH, Smadel JE. 1963. Biologic characteristics of a continuous kidney cell line derived from the African green monkey. *J. Immunol.* **91**:416. <http://www.jimmunol.org/content/91/3/416.short>.
- Hutchinson N, Bingham N. 2006. Shear stress analysis of mammalian cell suspensions for prediction of industrial centrifugation and its verification. *Biotechnol. Bioeng.*  
<http://onlinelibrary.wiley.com/doi/10.1002/bit.21029/abstract>.
- Islam RS, Tisi D, Levy MS, Lye GJ, Experimental S. 2007. Framework for the rapid optimization of soluble protein expression in *Escherichia coli* combining microscale experiments and statistical experimental design. *Biotechnol. Prog.* **23**:785–93. <http://www.ncbi.nlm.nih.gov/pubmed/17592858>.
- Jakubik JJ, Vicik SM, Tannatt MM, Kelley BD. 2004. West Nile Virus inactivation by the solvent/detergent steps of the second and third generation manufacturing processes for B-domain deleted recombinant factor VIII. *Haemophilia* **10**:69–74.  
<http://www.ncbi.nlm.nih.gov/pubmed/14962223>.
- Josefsberg JO, Buckland B. 2012. Vaccine process technology. *Biotechnol. Bioeng.* **109**:1443–60. <http://www.ncbi.nlm.nih.gov/pubmed/22407777>.
- Jungbauer A, Hahn R. 2004. Monoliths for fast bioseparation and bioconversion and their applications in biotechnology. *J. Sep. Sci.* **27**:767–778.  
<http://doi.wiley.com/10.1002/jssc.200401812>.
- Jungbauer A, Hahn R. 2008. Polymethacrylate monoliths for preparative and industrial separation of biomolecular assemblies. *J. Chromatogr. A* **1184**:62–79.  
<http://www.ncbi.nlm.nih.gov/pubmed/18241874>.



- Kelley BD, Switzer M, Bastek P, Kramarczyk JF, Molnar K, Yu T, Coffman J. 2008. High-throughput screening of chromatographic separations: IV. Ion-exchange. *Biotechnol. Bioeng.* **100**:950–63. <http://www.ncbi.nlm.nih.gov/pubmed/18551530>.
- Kistner O, Barrett PN, Mundt W, Reiter M, Schober-Bendixen S, Dorner F. 1998. Development of a mammalian cell (Vero) derived candidate influenza virus vaccine. *Vaccine* **16**:960–8. <http://www.ncbi.nlm.nih.gov/pubmed/9682344>.
- Kumar AAP, Rao YUB, Joseph ALW, Mani KR, Swaminathan K. 2002. Process standardization for optimal virus recovery and removal of substrate DNA and bovine serum proteins in Vero cell-derived rabies vaccine. *J. Biosci. Bioeng.* **94**:375–83. <http://www.ncbi.nlm.nih.gov/pubmed/16233321>.
- Łącki KM. 2012. High-throughput process development of chromatography steps: advantages and limitations of different formats used. *Biotechnol. J.* **7**:1192–202. <http://www.ncbi.nlm.nih.gov/pubmed/22745056>.
- Lambert DM, Pons MW, Mbuy GN, Dorsch-Hasler K. 1980. Nucleic acids of respiratory syncytial virus. *J. Virol.* **36**:837–46. <http://www.pubmedcentral.nih.gov/articlerender.fcgi?artid=353711&tool=pmcentrez&rendertype=abstract>.
- Lang J, Cetre JC, Picot N, Lanta M, Briantais P, Vital S, Le Mener V, Lutsch C, Rotivel Y. 1998. Immunogenicity and safety in adults of a new chromatographically purified Vero-cell rabies vaccine (CPRV): a randomized, double-blind trial with purified Vero-cell rabies vaccine (PVRV). *Biologicals* **26**:299–308. <http://www.ncbi.nlm.nih.gov/pubmed/10403033>.
- Levy MSM, Ciccolini LLAS, Yim SSSS, Tsai JT, Titchener-Hooker N, Ayazi Shamlou P, Dunnill P. 1999. The effects of material properties and fluid flow intensity on

plasmid DNA recovery during cell lysis. *Chem. Eng. Sci.* **54**:3171–3178.  
<http://www.sciencedirect.com/science/article/pii/S0009250998003583>.

Lin C-W, Wu S-C. 2003. A functional epitope determinant on domain III of the Japanese encephalitis virus envelope protein interacted with neutralizing-antibody combining sites. *J. Virol.* **77**:2600–2606.  
<http://jvi.asm.org/cgi/content/abstract/77/4/2600>.

Lindenbach BD, Thiel H-J, Rice CM. 2007. Flaviviridae: The Viruses and Their Replication. In: Knipe, DM, Howley, PM, editors. *Fields Virol.* 5th ed. Lippincott-Raven, pp. 1101–1152.

Liu MA. 2003. DNA vaccines: a review. *J. Intern. Med.* **253**:402–410.  
<http://doi.wiley.com/10.1046/j.1365-2796.2003.01140.x>.

Loewenstein E. 1909. Über aktive Schutzimpfung bei Tetanus durch Toxoide. *Zeitschrift für Hyg. und Infekt.* **62**:491–508.  
<http://link.springer.com/10.1007/BF02217451>.

Lyddiatt A, O'Sullivan D a. 1998. Biochemical recovery and purification of gene therapy vectors. *Curr. Opin. Biotechnol.* **9**:177–85.  
<http://www.ncbi.nlm.nih.gov/pubmed/9588005>.

Mackenzie JS, Gubler DJ, Petersen LR. 2004. Emerging flaviviruses: the spread and resurgence of Japanese encephalitis, West Nile and dengue viruses. *Nat. Med.* **10**:S98–109. <http://www.ncbi.nlm.nih.gov/pubmed/15577938>.

Metz B, Kersten G, Jong A de, Meiring H, Hove J ten, Hennink WE, Crommelin DJA, Jiskoot W. 2005. Identification of formaldehyde-induced modifications in proteins: reactions with diphtheria toxin. In: . *Struct. characterisation diphtheria toxoid*. Utrecht: Proefschrift Universiteit, pp. 139–154.

[http://www.thetruthaboutstuff.com/pdf/\(179\) Metz 2005, Identification of formaldehyde-induced modifications in proteins.pdf](http://www.thetruthaboutstuff.com/pdf/(179) Metz 2005, Identification of formaldehyde-induced modifications in proteins.pdf).

Metz B, Kersten GFA, Baart GJE, de Jong A, Meiring H, ten Hove J, van Steenbergen MJ, Hennink WE, Crommelin DJ a, Jiskoot W. 2006. Identification of formaldehyde-induced modifications in proteins: reactions with insulin. *Bioconjug. Chem.* **17**:815–22. <http://www.ncbi.nlm.nih.gov/pubmed/16704222>.

Metz B, Kersten GFA, Hoogerhout P, Brugghe HF, Timmermans HAM, de Jong A, Meiring H, ten Hove J, Hennink WE, Crommelin DJA, Jiskoot W. 2004. Identification of formaldehyde-induced modifications in proteins: reactions with model peptides. *J. Biol. Chem.* **279**:6235–43. <http://www.ncbi.nlm.nih.gov/pubmed/14638685>.

Micheletti M, Lye GJ. 2006. Microscale bioprocess optimisation. *Curr. Opin. Biotechnol.* **17**:611–8. <http://www.ncbi.nlm.nih.gov/pubmed/17084609>.

Moir RD, Centre HS, Dixon GH. 1988. Characterization of a Protamine Gene from the Chum Salmon. *J. Mol. Evol.* **27**:8–16.

Montgomery DC. 2009. Two-Level Fractional Factorial Designs. In: . *Des. Anal. Exp.* 7th ed., pp. 289–359.

Morenweiser R. 2005. Downstream processing of viral vectors and vaccines. *Gene Ther.* **12 Suppl 1**:S103–10. <http://www.ncbi.nlm.nih.gov/pubmed/16231042>.

Mukhopadhyay S, Kuhn RJ, Rossmann MG. 2005. A structural perspective of the flavivirus life cycle. *Nat. Rev. Microbiol.* **3**:13–22. <http://www.ncbi.nlm.nih.gov/pubmed/15608696>.

Niikura K, Matsunaga T, Suzuki T, Kobayashi S, Yamaguchi H, Orba Y, Kawaguchi A, Hasegawa H, Kajino K, Ninomiya T, Ijiro K, Sawa H. 2013. Gold nanoparticles as

a vaccine platform: influence of size and shape on immunological responses in vitro and in vivo. *ACS Nano* **7**:3926–38.

<http://pubs.acs.org/doi/pdf/10.1021/nn3057005>.

Okuda K, Ito K, Miyake K, Morita M, Ogonuki M. 1975. Purification of Japanese encephalitis virus vaccine by zonal centrifugation. *J. Clin. Microbiol.* **1**:96–101.  
<http://www.pubmedcentral.nih.gov/articlerender.fcgi?artid=274950&tool=pmcentrez&rendertype=abstract>.

Opitz L, Lehmann S, Reichl U, Wolff MW. 2009. Sulfated membrane adsorbers for economic pseudo-affinity capture of influenza virus particles. *Biotechnol. Bioeng.* **103**:1144–54. <http://www.ncbi.nlm.nih.gov/pubmed/19449393>.

Opitz L, Lehmann S, Zimmermann A, Reichl U, Wolff MW. 2007. Impact of adsorbents selection on capture efficiency of cell culture derived human influenza viruses **131**:309–317.

Perez O, Paolazzi CC. 1997. Production methods for rabies vaccine. *J. Ind. Microbiol. Biotechnol.* **18**:340–347. <http://link.springer.com/10.1038/sj.jim.2900391>.

Pezzini J, Cabanne C, Santarelli X. 2009. Comparative study of strong anion exchangers: structure-related chromatographic performances. *J. Chromatogr. B. Analyt. Technol. Biomed. Life Sci.* **877**:2443–50.  
<http://www.ncbi.nlm.nih.gov/pubmed/19617007>.

Plesner AM, Arlien-Søborg P, Herring M. 1998. Neurological complications to vaccination against Japanese encephalitis. *Eur. J. Neurol.* **5**:479–485.  
<http://onlinelibrary.wiley.com/doi/10.1046/j.1468-1331.1998.550479.x/abstract>.

Poláková I, Pokorná D, Dušková M, Šmahel M. 2010. DNA vaccine against human papillomavirus type 16: Modifications of the E6 oncogene. *Vaccine* **28**:1506–1513.  
<http://www.sciencedirect.com/science/article/pii/S0264410X09018726>.

- Prem Kumar AA, Mani KR, Palaniappan C, Bhau LNR, Swaminathan K. 2005. Purification, potency and immunogenicity analysis of Vero cell culture-derived rabies vaccine: a comparative study of single-step column chromatography and zonal centrifuge purification. *Microbes Infect.* **7**:1110–6.  
<http://www.ncbi.nlm.nih.gov/pubmed/16046167>.
- Provost PJ, Hughes J V, Miller WJ, Giesa P a, Banker FS, Emini E a. 1986. An inactivated hepatitis A viral vaccine of cell culture origin. *J. Med. Virol.* **19**:23–31.  
<http://www.ncbi.nlm.nih.gov/pubmed/3009703>.
- Putnak R, Barvir DA, Burrous JM, Dubois DR, D'Andrea VM, Hoke CH, Sadoff JC, Eckels KH. 1996. Development of a purified, inactivated, dengue-2 virus vaccine prototype in Vero cells: immunogenicity and protection in mice and rhesus monkeys. *J. Infect. Dis.* **174**:1176–84.  
<http://www.ncbi.nlm.nih.gov/pubmed/8940206>.
- Pyo Hong S, Yoo WD, Putnak R, Srivastava AK, Eckels KH, Chung YJ, Mo Rho H, Kim S. 2001. Preparation of a purified, inactivated Japanese encephalitis (JE) virus vaccine in Vero cells. *Biotechnol. Lett.* **23**:1565–1573.  
<http://www.springerlink.com/index/rv5573868155t3uu.pdf>.
- Rabilloud T. 1990. Mechanisms of protein silver staining in polyacrylamide gels: a 10-year synthesis. *Electrophoresis* **11**:785–94.  
<http://www.ncbi.nlm.nih.gov/pubmed/1706657>.
- Race E, Stein C a, Wigg MD, Baksh a, Addawe M, Frezza P, Oxford JS. 1995. A multistep procedure for the chemical inactivation of human immunodeficiency virus for use as an experimental vaccine. *Vaccine* **13**:1567–75.  
<http://www.ncbi.nlm.nih.gov/pubmed/8578844>.

- Saha K, Lin YC, Wong PK. 1994. A simple method for obtaining highly viable virus from culture supernatant. *J. Virol. Methods* **46**:349–52.  
<http://www.ncbi.nlm.nih.gov/pubmed/8006113>.
- Sanaie N, Cecchini D, Pieracci J. 2012. Applying high-throughput methods to develop a purification process for a highly glycosylated protein. *Biotechnol. J.* **7**:1242–55.  
<http://www.ncbi.nlm.nih.gov/pubmed/22899660>.
- Simizu B, Abe S, Yamamoto H, Tano Y, Ota Y, Miyazawa M, Horie H, Satoh K, Wakabayashi K. 2006. Development of inactivated poliovirus vaccine derived from Sabin strains. *Biologicals* **34**:151–4.  
<http://www.ncbi.nlm.nih.gov/pubmed/16679028>.
- Smith P, Krohn R, Hermanson G. 1985. Measurement of Protein Using Bicinchoninic Acid. *Anal. ...* **85**:76–85.  
<http://www.sciencedirect.com/science/article/pii/0003269785904427>.
- Sofer G. 2003. Virus Inactivation in the 1990s — and into the 21st Century. *Biopharm Int.*
- Solomon T. 2000. Neurological aspects of tropical disease: Japanese encephalitis. *J. Neurol. Neurosurg. Psychiatry* **68**:405–415.  
<http://jnnp.bmj.com/cgi/doi/10.1136/jnnp.68.4.405>.
- Srivastava a K, Putnak JR, Lee SH, Hong SP, Moon SB, Barvir D a, Zhao B, Olson R a, Kim SO, Yoo WD, Towle a C, Vaughn DW, Innis BL, Eckels KH. 2001. A purified inactivated Japanese encephalitis virus vaccine made in Vero cells. *Vaccine* **19**:4557–65. <http://www.ncbi.nlm.nih.gov/pubmed/12569794>.
- Stiasny K, Heinz FX. 2006. Flavivirus membrane fusion. *J. Gen. Virol.* **87**:2755–66.  
<http://www.ncbi.nlm.nih.gov/pubmed/16963734>.

- Strauss DM, Lute S, Brorson K, Blank GS, Chen Q, Yang B. 2009a. Removal of Endogenous Retrovirus-Like Particles from CHO-Cell Derived Products Using Q Sepharose Fast Flow Chromatography. *Biotechnol. Prog.* **25**:1194–1197. <http://onlinelibrary.wiley.com/doi/10.1002/btpr.249/full>.
- Strauss DM, Lute S, Tebaykina Z, Frey DD, Ho C, Blank GS, Brorson K, Chen Q, Yang B. 2009b. Understanding the mechanism of virus removal by Q sepharose Fast Flow chromatography during the purification of CHO-cell derived biotherapeutics. *Biotechnol. Bioeng.* **104**:371–80. <http://www.ncbi.nlm.nih.gov/pubmed/19575414>.
- Stüve O, Eagar TN, Frohman EM, Cravens PD. 2007. DNA plasmid vaccination for multiple sclerosis. *Arch. Neurol.* **64**:1385–6. <http://archneur.jamanetwork.com/article.aspx?articleid=794531>.
- Sugawara K, Nishiyama K, Ishikawa Y, Abe M, Sonoda K, Komatsu K, Horikawa Y, Takeda K, Honda T, Kuzuhara S, Kino Y, Mizokami H, Mizuno K, Oka T, Honda K. 2002. Development of Vero cell-derived inactivated Japanese encephalitis vaccine. *Biol. J. Int. Assoc. Biol. Stand.* **30**:303–314. <http://linkinghub.elsevier.com/retrieve/pii/S1045105602903453>.
- Sumiyoshi H, Mori C, Fuke I, Morita K, Kuhara S, Kondou J, Kikuchi Y, Nagamatu H, Igarashi a. 1987. Complete nucleotide sequence of the Japanese encephalitis virus genome RNA. *Virology* **161**:497–510. <http://www.ncbi.nlm.nih.gov/pubmed/3686827>.
- Suzuki K, Ando T. 1972. Studies on protamines. XVII. The complete amino acid sequence of clupeine YI. *J. Biochem.* **72**:1433–46. <http://www.ncbi.nlm.nih.gov/pubmed/4664741>.
- Tait a S, Aucamp JP, Bugeon A, Hoare M. 2009. Ultra scale-down prediction using microwell technology of the industrial scale clarification characteristics by

centrifugation of mammalian cell broths. *Biotechnol. Bioeng.* **104**:321–31.

<http://www.ncbi.nlm.nih.gov/pubmed/19507199>.

Thermo Scientific. 2010. Thermo Scientific Pierce Protein Assay Technical Handbook  
Version 2. 1602063 12/10.

Todd D, Creelan JL, Mackie DP, Rixon F, McNulty MS. 1990. Purification and  
biochemical characterization of chicken anaemia agent. *J. Gen. Virol.* **71 ( Pt  
4)**:819–23. <http://www.ncbi.nlm.nih.gov/pubmed/2109040>.

Toriniwa H, Komiya T. 2007. Japanese encephalitis virus production in Vero cells with  
serum-free medium using a novel oscillating bioreactor. *Biologicals* **35**:221–6.  
<http://www.ncbi.nlm.nih.gov/pubmed/17400474>.

Toriniwa H, Komiya T. 2008. Long-term stability of Vero cell-derived inactivated  
Japanese encephalitis vaccine prepared using serum-free medium. *Vaccine*  
**26**:3680–9. <http://www.ncbi.nlm.nih.gov/pubmed/18534722>.

Trent DW. 1977. Antigenic characterization of flavivirus structural proteins separated by  
isoelectric focusing. *J. Virol.* **22**:608–18.  
<http://www.pubmedcentral.nih.gov/articlerender.fcgi?artid=515759&tool=pmcentrez&rendertype=abstract>.

Wang Y, Ouyang F. 1999. Bead-to-bead transfer of Vero cells in microcarrier culture.  
*Cytotechnology* **31**:221–4. <http://www.ncbi.nlm.nih.gov/pubmed/19003145>.

Warren J, Smadel J, Rasmussen A. 1948. The antibody response in human beings  
inoculated with Japanese encephalitis vaccine, chick embryo type. *J. Immunol.*  
(*Baltimore, Md.* 1950) **58**:211. <http://www.ncbi.nlm.nih.gov/pubmed/18905195>.



- Wenger MD, DePhillips P, Bracewell DG. 2008. A microscale yeast cell disruption technique for integrated process development strategies. *Biotechnol. Prog.* **24**:606–14. <http://www.ncbi.nlm.nih.gov/pubmed/18410155>.
- Wenger MD, Dephillips P, Price CE, Bracewell DG. 2007. An automated microscale chromatographic purification of virus-like particles as a strategy for process development. *Biotechnol. Appl. Biochem.* **47**:131–9. <http://www.ncbi.nlm.nih.gov/pubmed/17311568>.
- Van Wezel a L, van Steenis G, van der Marel P, Osterhaus a D. 2009. Inactivated poliovirus vaccine: current production methods and new developments. *Rev. Infect. Dis.* **6 Suppl 2**:S335–40. <http://www.ncbi.nlm.nih.gov/pubmed/6429814>.
- WHO. 2006. Weekly epidemiological record. *orton.catie.ac.cr* 34/35 ed. Geneva: World Health Organisation Geneva, CH. Vol. 2004. <http://orton.catie.ac.cr/cgi-bin/wxis.exe/?IsisScript=KARDEX.xis&method=post&formato=2&cantidad=1&expresion=mfn=003687>.
- Wolff MW, Siewert C, Hansen SP, Faber R, Reichl U. 2010. Purification of cell culture-derived modified vaccinia ankara virus by pseudo-affinity membrane adsorbers and hydrophobic interaction chromatography. *Biotechnol. Bioeng.* **107**:312–20. <http://www.ncbi.nlm.nih.gov/pubmed/20506129>.

# 10 Appendix

## 10.1 Cell passage data

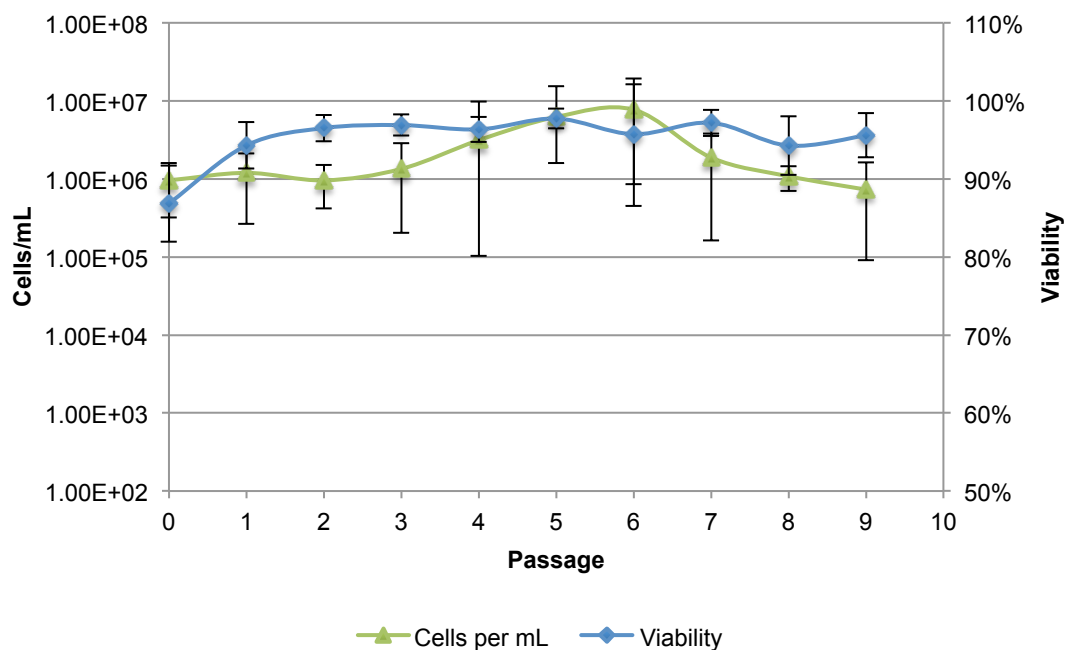


Figure 10.1 – Accumulated passage data for Vero cells grown at laboratory scale in T150 tissue culture flasks with L-glutamine, serum and antimycotic supplemented media. Error bars are based on standard deviation of results, where it was impossible to show negative error on the log scale of the primary axis (for passages 3 to 7 and 9), the minimum measured cells/mL value was used. N number for each passage (P): P0 =15, P1 = 14, P2 = 12, P3 = 9, P4 = 9, P5 = 5, P6 = 3. P7 = 4, P8 = 3, P9 = 2.

## 10.2 Viral harvest titres

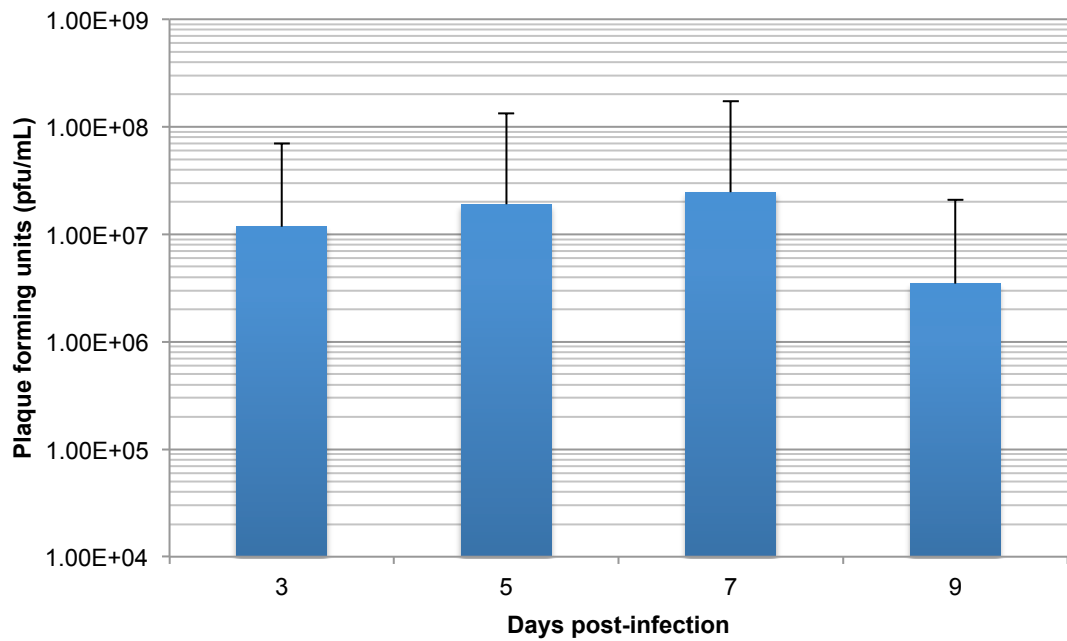


Figure 10.2 – Average plaque assay derived viral titres for each of the four harvest points at 3, 5, 7 and 9 days post infection of the Vero cell cultures at laboratory-scale production of JEV. Error bars based on standard deviation thus only maximum error can be plotted on a logarithmic scale, n=5.

### 10.3 Example batch process analytics

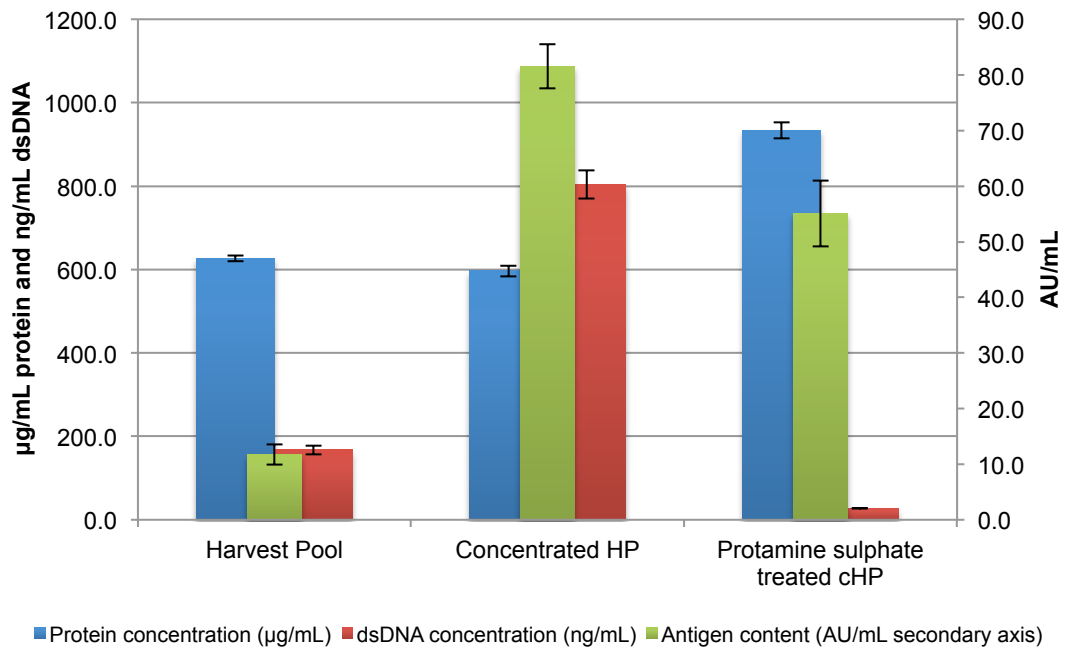


Figure 10.3 – Process analytics for a batch after pooling the harvest (HP), concentrating the harvest (cHP) and treating it with protamine sulphate to remove hcDNA. The antigen content data overlaps the total protein and dsDNA data because it is plotted on the secondary axis.

Error bars are of standard deviation of samples within their respective assays (n=3).

## 10.4 Typical BCA assay standard curve generated with BSA

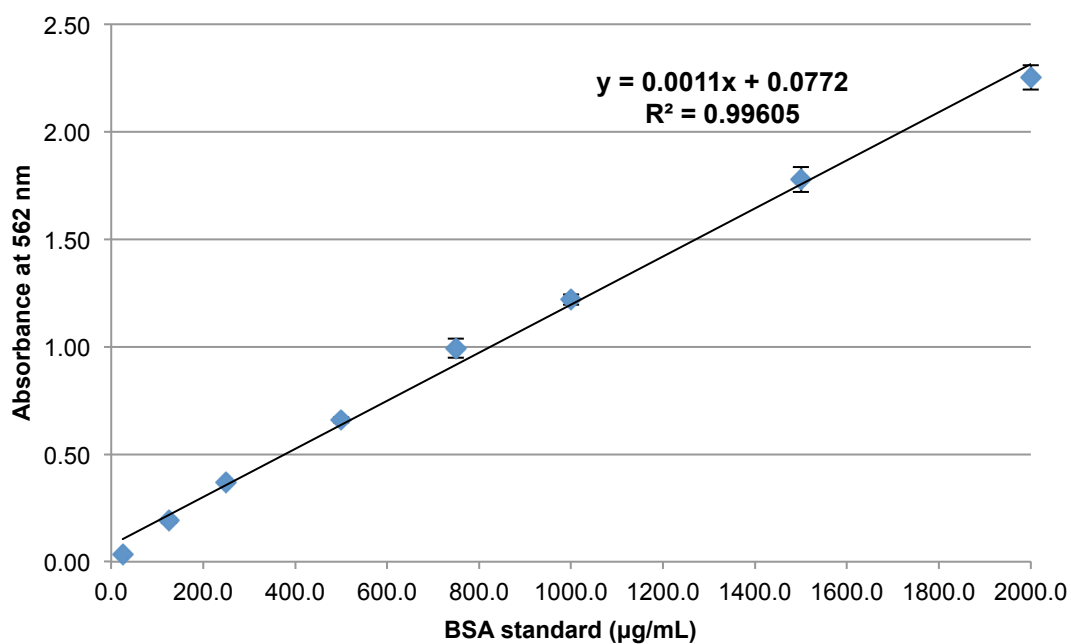


Figure 10.4 – BCA assay standard curve generated with bovine serum albumin (BSA). Error bars represent standard deviation of absorbance reading for dilution of the BSA reference standard, n=4.

## 10.5 Typical Quant-iT PicoGreen standard curve with dsDNAs

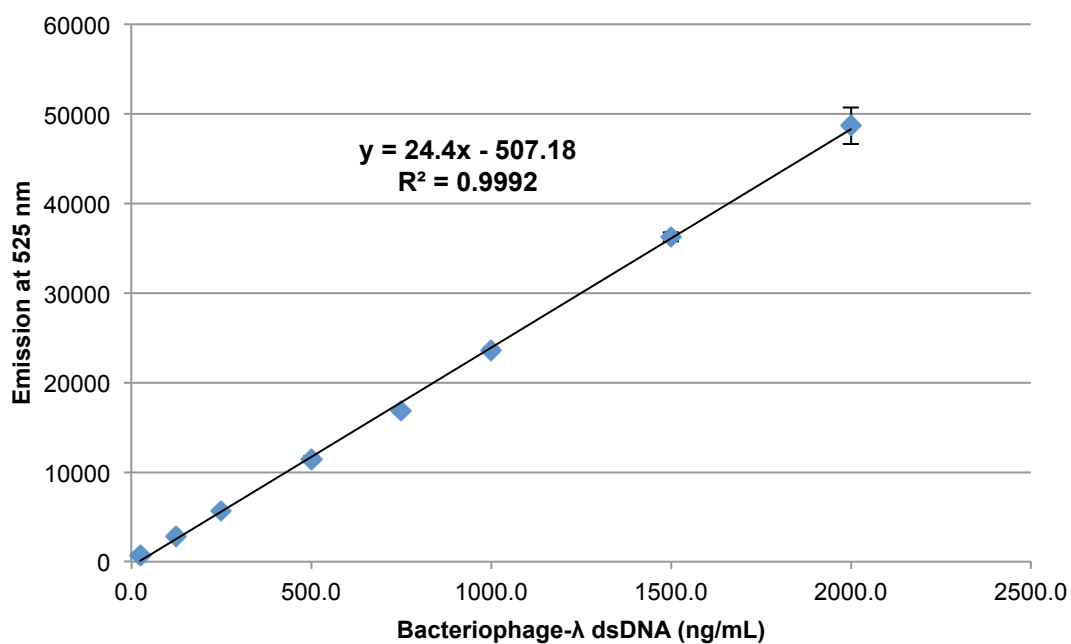
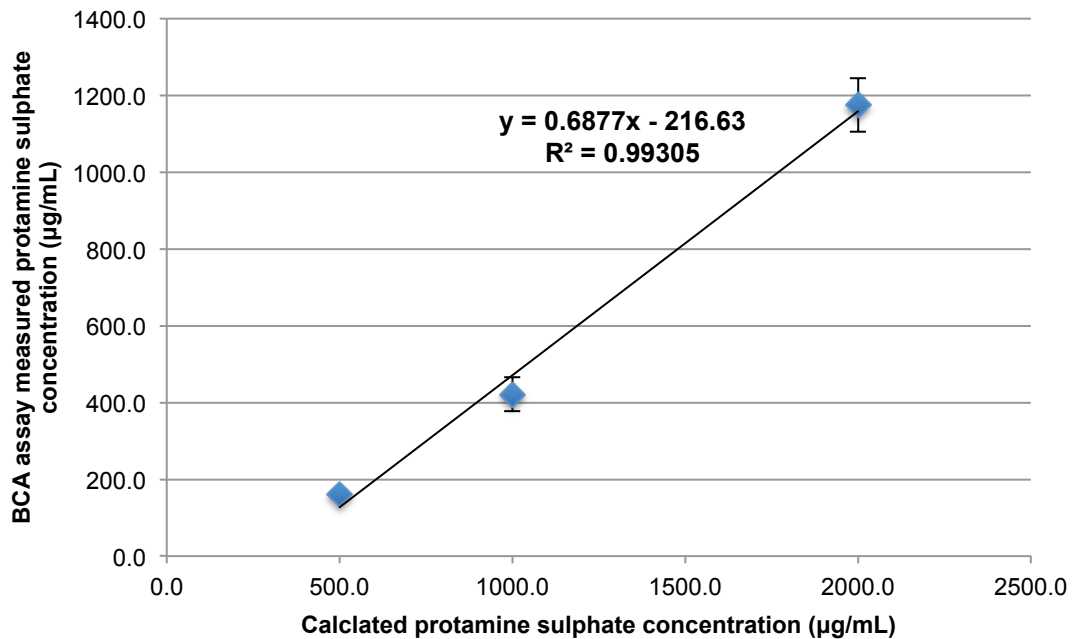
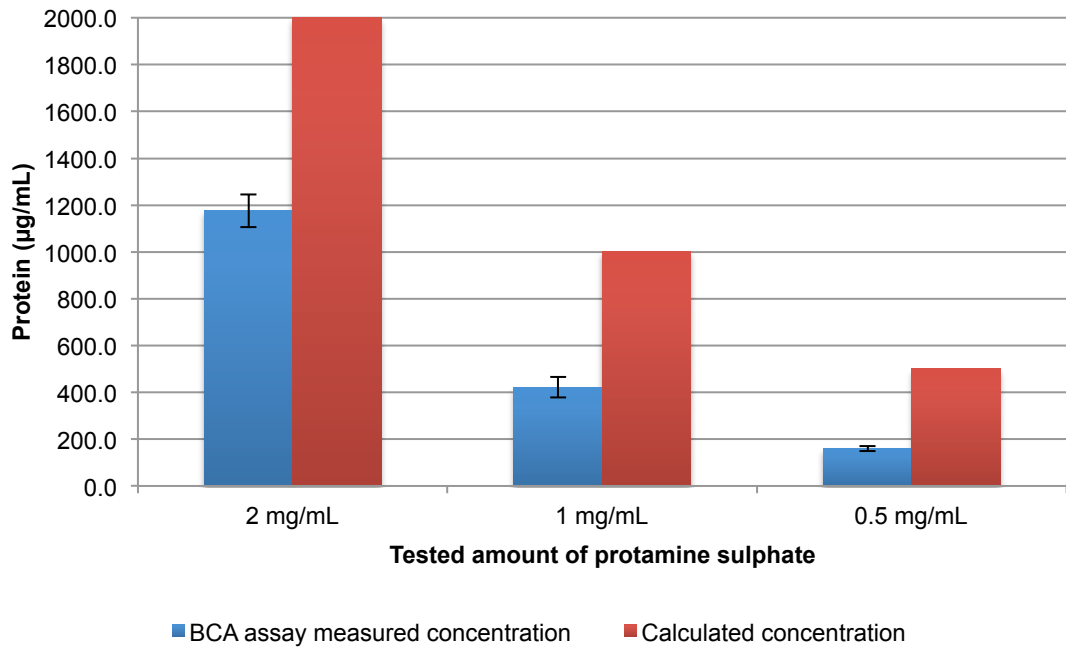


Figure 10.5 – Quant-iT PicoGreen assay standard curve generated with the supplied bacteriophage-λ DNA. Excited at 483 nm and read at 525 nm, the error bars represent the standard deviation of measured emissions for each dilutions of the reference standard, n=3.

## 10.6 Protamine sulphate measured by BCA assay

These two graphs show the difference between calculated (by weighing out) and BCA assay measured protamine sulphate concentration. The measured value is >50% lower than the calculated value, the difference also increased the smaller the amount of PS.



## 10.7 Design summary for fractional 2-level factorial on purified

### JEV from DX8

Design Summary												
File Version	8.0.1.0	Runs	36									
Study Type	Factorial	Blocks	No Blocks									
Design Type	2 Level Factorial	4										
Center Points												
Design Model	Reduced 3FI	Build Time (ms)	4.61									
Factor	Name	Units	Type	Subtype	Minimum	Maximum	Coded	Values	Mean	Std. Dev.		
A	Formaldehyde concentration	%	Numeric	Continuous	0.02	0.04	FALSE	1.000=0.04	0.03	0.01		
B	pH		Numeric	Continuous	7	9	FALSE	1.000=9.00	8	0.94		
C	Temperature	C	Numeric	Continuous	22	35	FALSE	1.000=35.00	28.5	6.13		
D	Glycine	%	Numeric	Continuous	0.05	0.5	FALSE	1.000=0.50	0.28	0.21		
E	Lysine	%	Numeric	Continuous	0.05	0.5	FALSE	1.000=0.50	0.28	0.21		
F	Sorbitol	%	Numeric	Continuous	0.1	1	FALSE	1.000=1.00	0.55	0.42		
G	Glycerol	%	Numeric	Continuous	0.1	1	FALSE	1.000=1.00	0.55	0.42		
H	PEG	%	Numeric	Continuous	0.1	1	FALSE	1.000=1.00	0.55	0.42		
Response	Name	Units	Obs	Analysis	Minimum	Maximum	Mean	Std. Dev.	Ratio	Trans	Model	
Y1	antigen	IU/mL	36	Factorial	0.01	0.63	0.150159	0.15514	63	None	R2FI	



## 10.8 Design evaluation for fractional 2-level factorial on purified

### JEV from DX8

Use your mouse to right click on individual cells for definitions.

8 Factors: A, B, C, D, E, F, G, H

Design Matrix Evaluation for Factorial Reduced 3FI Model

Factorial Effects Aliases

[Est. Terms] Aliased Terms

[Intercept] = Intercept

[A] = A + BCF + BDG

[B] = B + ACF + ADG

[C] = C + ABF + DFG

[D] = D + ABG + CFG

[E] = E

[F] = F + ABC + CDG

[G] = G + ABD + CDF

[H] = H

[AB] = AB + CF + DG

[AC] = AC + BF + EGH

[AD] = AD + BG + EFH

[AE] = AE + CGH + DFH

[AF] = AF + BC + DEH

[AG] = AG + BD + CEH

[AH] = AH + CEG + DEF

[BE] = BE + CDH + FGH

[BH] = BH + CDE + EFG

[CD] = CD + FG + BEH

[CE] = CE + AGH + BDH

[CG] = CG + DF + AEH

[CH] = CH + AEG + BDE

[DE] = DE + AFH + BCH

[DH] = DH + AEF + BCE

[EF] = EF + ADH + BGH

[EG] = EG + ACH + BFH

[EH] = EH + ACG + ADF + BCD + BFG

[FH] = FH + ADE + BEG

[GH] = GH + ACE + BEF

[ABE] = ABE + CEF + DEG

[ABH] = ABH + CFH + DGH

[ACD] = ACD + AFG + BCG + BDF

Design Matrix Evaluation Performed Omitting Aliased Terms

Aliases are calculated based on your response selection,  
taking into account missing datapoints, if necessary.  
Watch for aliases among terms you need to estimate.

Factorial Effects Defining Contrast

I = ABCF = ABDG = CDFG = ACEGH = ADEFH = BCDEH = BEFGH

Defining Contrast Word Lengths

	1	2	3	4	5	6	7
	0	0	0	3	4	0	0
	8						
	0						

Degrees of Freedom for Evaluation

Model 31

Residuals	4
Lack Of Fit	1
Pure Error	3
Corr Total	35

A recommendation is a minimum of 3 lack of fit df and 4 df for pure error.

This ensures a valid lack of fit test.

Fewer df will lead to a test that may not detect lack of fit.

Power at 5 % alpha level to detect signal/noise ratios of

Term	StdErr**	VIF	Ri-Squared	0.5 Std. Dev.	1 Std. Dev.	2 Std. Dev.
A	0.18	1	0	19.50%	57.20%	98.40%
B	0.18	1	0	19.50%	57.20%	98.40%
C	0.18	1	0	19.50%	57.20%	98.40%
D	0.18	1	0	19.50%	57.20%	98.40%
E	0.18	1	0	19.50%	57.20%	98.40%
F	0.18	1	0	19.50%	57.20%	98.40%
G	0.18	1	0	19.50%	57.20%	98.40%
H	0.18	1	0	19.50%	57.20%	98.40%
AB	0.18	1	0	19.50%	57.20%	98.40%
AC	0.18	1	0	19.50%	57.20%	98.40%
AD	0.18	1	0	19.50%	57.20%	98.40%
AE	0.18	1	0	19.50%	57.20%	98.40%
AF	0.18	1	0	19.50%	57.20%	98.40%
AG	0.18	1	0	19.50%	57.20%	98.40%
AH	0.18	1	0	19.50%	57.20%	98.40%
BE	0.18	1	0	19.50%	57.20%	98.40%
BH	0.18	1	0	19.50%	57.20%	98.40%
CD	0.18	1	0	19.50%	57.20%	98.40%
CE	0.18	1	0	19.50%	57.20%	98.40%
CG	0.18	1	0	19.50%	57.20%	98.40%
CH	0.18	1	0	19.50%	57.20%	98.40%
DE	0.18	1	0	19.50%	57.20%	98.40%
DH	0.18	1	0	19.50%	57.20%	98.40%
EF	0.18	1	0	19.50%	57.20%	98.40%
EG	0.18	1	0	19.50%	57.20%	98.40%
EH	0.18	1	0	19.50%	57.20%	98.40%
FH	0.18	1	0	19.50%	57.20%	98.40%
GH	0.18	1	0	19.50%	57.20%	98.40%
ABE	0.18	1	0	19.50%	57.20%	98.40%
ABH	0.18	1	0	19.50%	57.20%	98.40%
ACD	0.18	1	0	19.50%	57.20%	98.40%

\*\*Basis Std. Dev. = 1.0

Standard errors should be similar within type of coefficient. Smaller is better.

Ideal VIF is 1.0. VIFs above 10 are cause for alarm, indicating coefficients are poorly estimated due to multicollinearity.

Ideal Ri-squared is 0.0. High Ri-squared means terms are correlated with each other, possibly leading to poor models.

Power should be approximately 80% for the effect you want to detect.

Be sure to set the Model (on previous screen) to be an estimate of the terms you expect to be significant.

Measures Derived From the  $(X'X)^{-1}$  Matrix

Std	Leverage	Point Type
1	0.9965	Factorial
2	0.9965	Factorial
3	0.9965	Factorial
4	0.9965	Factorial

5	0.9965	Factorial
6	0.9965	Factorial
7	0.9965	Factorial
8	0.9965	Factorial
9	0.9965	Factorial
10	0.9965	Factorial
11	0.9965	Factorial
12	0.9965	Factorial
13	0.9965	Factorial
14	0.9965	Factorial
15	0.9965	Factorial
16	0.9965	Factorial
17	0.9965	Factorial
18	0.9965	Factorial
19	0.9965	Factorial
20	0.9965	Factorial
21	0.9965	Factorial
22	0.9965	Factorial
23	0.9965	Factorial
24	0.9965	Factorial
25	0.9965	Factorial
26	0.9965	Factorial
27	0.9965	Factorial
28	0.9965	Factorial
29	0.9965	Factorial
30	0.9965	Factorial
31	0.9965	Factorial
32	0.9965	Factorial
33	0.0278	Center
34	0.0278	Center
35	0.0278	Center
36	0.0278	Center

Average = 0.8889

Watch for leverages close to 1.0. Consider replicating these points or make sure they are run very carefully.

## **10.9 Conditions and antigen data for fractional 2-level factorial on purified JEV from DX8**

Std	Run	Factor 1 A:Formalder %	Factor 2 B:pH	Factor 3 C:Temp °C	Factor 4 D:Glycine %	Factor 5 E:Lysine %	Factor 6 F:Sorbitol %	Factor 7 G:Glycerol %	Factor 8 H:PEG %	Response 1 Antigen AU/mL
30	1	0.04	7	35	0.5	0.5	0.1	0.1	0.1	0.04
24	2	0.04	9	35	0.05	0.5	1	0.1	0.1	0.08
14	3	0.04	7	35	0.5	0.05	0.1	0.1	1	0.02
8	4	0.04	9	35	0.05	0.05	1	0.1	1	0.09
27	5	0.02	9	22	0.5	0.5	1	0.1	0.1	0.29
23	6	0.02	9	35	0.05	0.5	0.1	1	0.1	0.08
11	7	0.02	9	22	0.5	0.05	1	0.1	1	0.25
29	8	0.02	7	35	0.5	0.5	1	1	0.1	0.63
15	9	0.02	9	35	0.5	0.05	0.1	0.1	0.1	0.15
6	10	0.04	7	35	0.05	0.05	0.1	1	0.1	0.01
26	11	0.04	7	22	0.5	0.5	1	0.1	1	0.04
16	12	0.04	9	35	0.5	0.05	1	1	0.1	0.23
35	13	0.03	8	28.5	0.275	0.275	0.55	0.55	0.55	0.043
31	14	0.02	9	35	0.5	0.5	0.1	0.1	1	0.3
20	15	0.04	9	22	0.05	0.5	0.1	0.1	1	0.09
4	16	0.04	9	22	0.05	0.05	0.1	0.1	0.1	0.09
13	17	0.02	7	35	0.5	0.05	1	1	1	0.63
5	18	0.02	7	35	0.05	0.05	1	0.1	0.1	0.16
18	19	0.04	7	22	0.05	0.5	1	1	0.1	0.01
28	20	0.04	9	22	0.5	0.5	0.1	1	0.1	0.2
3	21	0.02	9	22	0.05	0.05	1	1	0.1	0.1
34	22	0.03	8	28.5	0.275	0.275	0.55	0.55	0.55	0.03
19	23	0.02	9	22	0.05	0.5	1	1	1	0.12
17	24	0.02	7	22	0.05	0.5	0.1	0.1	0.1	0.1
21	25	0.02	7	35	0.05	0.5	1	0.1	1	0.13
36	26	0.03	8	28.5	0.275	0.275	0.55	0.55	0.55	0.03
33	27	0.03	8	28.5	0.275	0.275	0.55	0.55	0.55	0.04
9	28	0.02	7	22	0.5	0.05	0.1	1	0.1	0.32
32	29	0.04	9	35	0.5	0.5	1	1	1	0.23
1	30	0.02	7	22	0.05	0.05	0.1	0.1	1	0.13
7	31	0.02	9	35	0.05	0.05	0.1	1	1	0.11
12	32	0.04	9	22	0.5	0.05	0.1	1	1	0.15
2	33	0.04	7	22	0.05	0.05	1	1	1	0.01
22	34	0.04	7	35	0.05	0.5	0.1	1	1	0.01
25	35	0.02	7	22	0.5	0.5	0.1	1	1	0.42
10	36	0.04	7	22	0.5	0.05	1	0.1	0.1	0.04

# 10.10DX8 design summary for inactivation of harvest material

## Design Summary

File Version 8.0.7.1  
 Study Type Factorial  
 Design Type 2 Level Factorial  
 Center Points 4  
 Design Model Reduced 3FI  
 Runs 20  
 Blocks No Blocks  
 Build Time (ms) 2.32963

Factor	Name	Units	Type	Subtype	Minimum	Maximum	Coded	Values	Mean	Std. Dev.
A	Time	hours	Numeric	Continuous	24	96	-1.000=24.00	1.000=96.00	60	32.20
B	pH		Numeric	Continuous	7	9	-1.000=7.00	1.000=9.00	8	0.89
C	Temperature	deg C	Numeric	Continuous	4	37	-1.000=4.00	1.000=37.00	20.5	14.76
D	Formaldehyde conc	%	Numeric	Continuous	0.01	0.05	-1.000=0.01	1.000=0.05	0.03	0.02
E	Sorbitol	%	Numeric	Continuous	0.1	1	-1.000=0.10	1.000=1.00	0.55	0.40
F	Glycine	%	Numeric	Continuous	0.1	1	-1.000=0.10	1.000=1.00	0.55	0.40

Response	Name	Units	Obs	Analysis	Minimum	Maximum	Mean	Std. Dev.	Ratio	Trans	Model
Y1	NS % in class 35-60 nm	%	19	Factorial	3.70	8.19	5.76	1.10	2.21	None	No model chosen
Y2	Antigen	ug/mL	20	Factorial	9.01	33.89	18.53	6.83	3.76	None	R2FI
Y3	Size DLS	d.nm	18	Factorial	89.56	282.80	128.72	52.40	3.16	None	R2FI
Y4	Activity	pfu/mL	20	Factorial	0	5900	416.9	1356.68	N/A	None	RMain effects
Y5	Zeta potential	mV	20	Factorial	-18.16	-10.45	-14.66	2.00	1.74	None	RMain effects
Y6	Mobility	umcm/Vs	20	Factorial	-1.42	-0.82	-1.15	0.16	1.74	None	RMain effects
Y7	Conductivity	mS/cm	20	Factorial	13.98	15.92	14.94	0.52	1.14	None	RMain effects
Y8	Sm/Lrg particle ratio		20	Factorial	0.12	0.35	0.21	0.06	2.84	None	R2FI

## 10.11DX8 design evaluation for harvest material experiment

Use your mouse to right click on individual cells for definitions.

6 Factors: A, B, C, D, E, F

Design Matrix Evaluation for Factorial Reduced 3FI Model

Factorial Effects Aliases

[Est. Terms] Aliased Terms

[Intercept] = Intercept

[A] = A + BCE + DEF

[B] = B + ACE + CDF

[C] = C + ABE + BDF

[D] = D + AEF + BCF

[E] = E + ABC + ADF

[F] = F + ADE + BCD

[AB] = AB + CE

[AC] = AC + BE

[AD] = AD + EF

[AE] = AE + BC + DF

[AF] = AF + DE

[BD] = BD + CF

[BF] = BF + CD

[ABD] = ABD + ACF + BEF + CDE

[ABF] = ABF + ACD + BDE + CEF

Design Matrix Evaluation Performed Omitting Aliased Terms

Aliases are calculated based on your response selection,  
taking into account missing datapoints, if necessary.  
Watch for aliases among terms you need to estimate.

Factorial Effects Defining Contrast

I = ABCE = ADEF = BCDF

Defining Contrast Word Lengths

1	2	3	4	5	6
0	0	0	3	0	0

Degrees of Freedom for Evaluation

Model	15
Residuals	4
Lack Of Fit	1
Pure Error	3
Corr Total	19

A recommendation is a minimum of 3 lack of fit df and 4 df for pure error.

This ensures a valid lack of fit test.

Fewer df will lead to a test that may not detect lack of fit.

Power at 5 % alpha level to detect signal/noise ratios of

Term	StdErr**	VIF	Ri-Squared	0.5 Std. Dev.	1 Std. Dev.	2 Std. Dev.
A	0.25	1	0	12.2 %	33.6 %	84.3 %
B	0.25	1	0	12.2 %	33.6 %	84.3 %
C	0.25	1	0	12.2 %	33.6 %	84.3 %
D	0.25	1	0	12.2 %	33.6 %	84.3 %
E	0.25	1	0	12.2 %	33.6 %	84.3 %
F	0.25	1	0	12.2 %	33.6 %	84.3 %
AB	0.25	1	0	12.2 %	33.6 %	84.3 %
AC	0.25	1	0	12.2 %	33.6 %	84.3 %

AD	0.25	1	0	12.2 %	33.6 %	84.3 %
AE	0.25	1	0	12.2 %	33.6 %	84.3 %
AF	0.25	1	0	12.2 %	33.6 %	84.3 %
BD	0.25	1	0	12.2 %	33.6 %	84.3 %
BF	0.25	1	0	12.2 %	33.6 %	84.3 %
ABD	0.25	1	0	12.2 %	33.6 %	84.3 %
ABF	0.25	1	0	12.2 %	33.6 %	84.3 %

\*\*Basis Std. Dev. = 1.0

Standard errors should be similar within type of coefficient. Smaller is better.

Ideal VIF is 1.0. VIFs above 10 are cause for alarm, indicating coefficients are poorly estimated due to multicollinearity.

Ideal Ri-squared is 0.0. High Ri-squared means terms are correlated with each other, possibly leading to poor models.

Power should be approximately 80% for the effect you want to detect.

Be sure to set the Model (on previous screen) to be an estimate of the terms you expect to be significant.

Measures Derived From the  $(X'X)^{-1}$  Matrix

Std	Leverage	Point Type
	1	0.9875 Factorial
	2	0.9875 Factorial
	3	0.9875 Factorial
	4	0.9875 Factorial
	5	0.9875 Factorial
	6	0.9875 Factorial
	7	0.9875 Factorial
	8	0.9875 Factorial
	9	0.9875 Factorial
	10	0.9875 Factorial
	11	0.9875 Factorial
	12	0.9875 Factorial
	13	0.9875 Factorial
	14	0.9875 Factorial
	15	0.9875 Factorial
	16	0.9875 Factorial
	17	0.05 Center
	18	0.05 Center
	19	0.05 Center
	20	0.05 Center
=	Average	0.8

Watch for leverages close to 1.0. Consider replicating these points or make sure they are run very carefully.

## 10.12 All conditions and data for fractional 2-level factorial on JEV harvest material from DX8

Std	Run	Factor 1 A:Time hours	Factor 2 B:pH	Factor 3 C:Temperature °C	Factor 4 D:Formaldehyde conc %	Factor 5 E:Sorbitol %	Factor 6 F:Glycine %	Response 1 NS % in class 35- 60 nm %	Response 2 Antigen µg/mL	Response 3 Size (DLS) d.nm	Response 4 Activity pfu/mL	Response 5 Zeta potential mV	Response 6 Mobility µmcm/Vs	Response 7 Conductivity mS/cm	Response 8 Sm/L/g particle ratio
10	1	96	7	4	0.05	1	1	5.49823	20.5772	92.62	3	-17.04	-1.3358	14.46	0.195625
18	2	60	8	20.5	0.03	0.55	0.55	4.80754	17.4295	106.6	0	-15.44	-1.2108	15.16	0.163231
5	3	24	7	37	0.01	1	1	4.42973	22.8376	115.6	0	-14.44	-1.1338	13.98	0.145742
16	4	96	9	37	0.05	1	1	6.27546	9.03596	172.5	0	-14.68	-1.1512	14.04	0.225549
4	5	96	9	4	0.01	0.1	1	4.80594	22.2103	99.95	1800	-12.54	-0.98432	15.78	0.179851
14	6	96	7	37	0.05	0.1	0.1	5.36498	9.00798	104.6	0	-16.4	-1.2846	14.86	0.203161
13	7	24	7	37	0.05	1	0.1	6.77946	11.1776	114.2	0	-15.68	-1.2288	15.34	0.245948
11	8	24	9	4	0.05	1	0.1	6.09344	18.5736	130	0	-15.74	-1.234	14.76	0.206117
12	9	96	9	4	0.05	0.1	0.1	7.60671	15.9081	99.34	0	-18.16	-1.4248	15.44	0.323387
17	10	60	8	20.5	0.03	0.55	0.55	5.33681	15.7232	132.1	0	-15.96	-1.2506	14.98	0.196305
19	11	60	8	20.5	0.03	0.55	0.55	5.18795	16.4896	102.7	0	-15.58	-1.2198	15.1	0.188948
15	12	24	9	37	0.05	0.1	1	5.2074	11.6488	136.4	0	-10.448	-0.81836	14.12	0.17899
20	13	60	8	20.5	0.03	0.55	0.55	5.83654	17.3382	112.3	0	-12.16	-0.95286	15.44	0.220723
8	14	96	9	37	0.01	1	0.1	8.1867	14.7454	282.8	0	-14.72	-1.15234	15.08	0.350148
1	15	24	7	4	0.01	0.1	0.1	6.14897	33.8933	98.62	630	-16.04	-1.2592	15.92	0.253122
7	16	24	9	37	0.01	0.1	0.1	7.22624	19.5632	114.8	0	-13.66	-1.07088	15	0.277946
9	17	24	7	4	0.05	0.1	1	5.11588	25.3851	132.2	0	-11.54	-0.90608	14.68	0.209282
3	18	24	9	4	0.01	1	1	3.69876	32.9626	89.56	5900	-11.98	-0.9401	14.86	0.123162
6	19	96	7	37	0.01	0.1	1	5.60808	13.6119	250.8	0	-15.28	-1.1976	14.78	0.195519
2	20	96	7	4	0.01	1	0.1	4.63773	22.3819	106.4	5	-15.8	-1.238	15.1	0.170069



### 10.13 BSA and glycine AKTA control runs

Figure 10.6 shows the elution profiles from three AKTA runs with a base buffer of 50 mM tris pH 8.3 on a pre-packed 1 mL Q Sepharose Fast Flow column: 5 mL each of 1% glycine, 1 mg/mL BSA and 1 mg/mL BSA with 1% glycine. These runs were performed to assess the effect of glycine on the bind and elute of BSA to the resin. As seen in Figure 10.6, 1% glycine on its own did not produce a significant U.V. absorbance profile while the profiles of 1 mg/mL BSA with and without 1 % glycine are indistinguishable from one another. Therefore 1% glycine does not affect the elution profile of BSA off QSFF under these conditions.

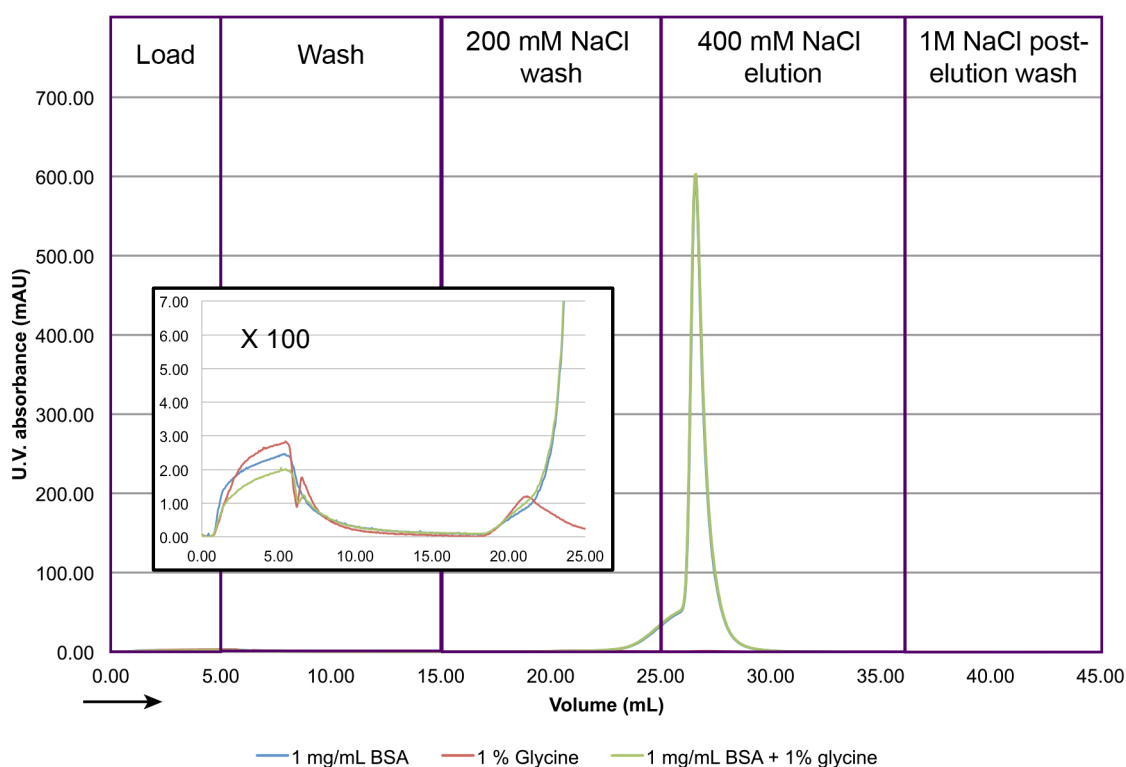


Figure 10.6 – U.V. absorbance chromatograms 5 mL each of 1 mg/mL BSA, 1% glycine and 1 mg/mL BSA with 1% glycine, all run in 50 mM tris pH 8.3 on a pre-packed 1 mL Q Sepharose Fast Flow column. 1% glycine on its own does not show any significant U.V. absorbance and when added to 1mg/mL BSA it does not change the elution profile. Insert shows the load and start of the elution peak with the absorbance scale increased 100 fold to distinguish between the U.V. traces.

To investigate the effect of 1 % glycine on the BCA assay, selected fractions from the run depicted in Figure 10.6 were analysed using the assay. 1% glycine on its own gave results below the LOD of the standard BCA assay and the results are not included with those of the 1 mg/mL BSA and the 1 mg/mL BSA + 1 % glycine shown in Figure 10.7. The load, wash and elute samples for both feeds gave the results indicating no interference from glycine with the assay. The feed samples, however, gave significantly different results with the sample containing 1 % glycine returning a value much smaller than that of the BSA only sample. This effect was reduced but still evident when sample was diluted 1:2 with PBS.

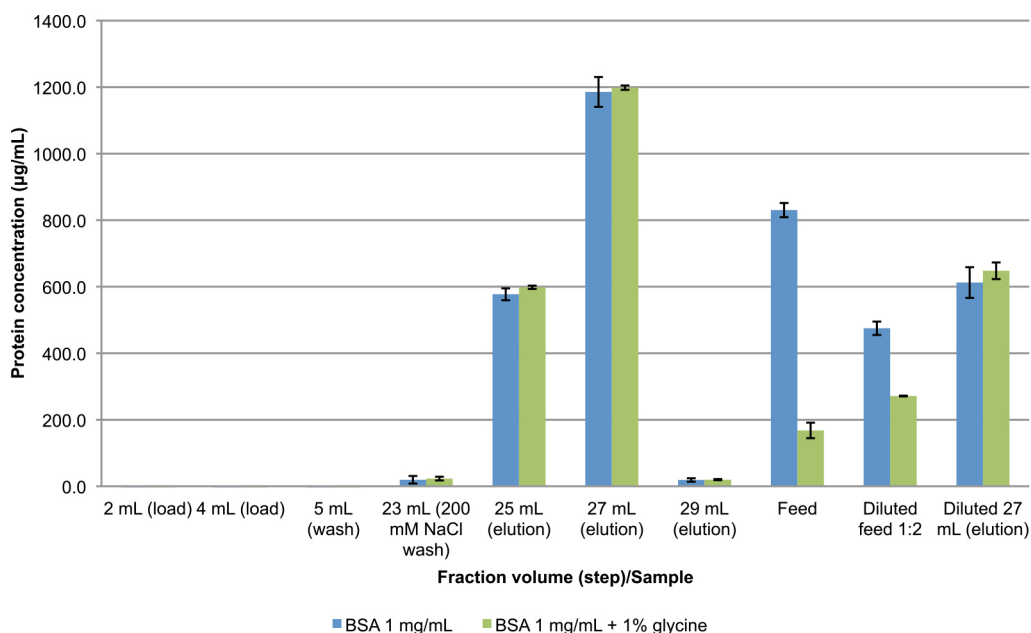
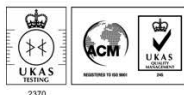


Figure 10.7 – Protein concentration determined by BCA assay relating to fractions and samples from the AKTA run described in Figure 10.6. The diluted samples were diluted with equal part PBS. Error bars are based on standard deviation of experimental samples, n=3.

## 10.14 Outsourced sequencing results

### 10.14.1 Sequencing attempt 1 - 5 amino acids



#### Protein sequence report

Created on 28-Jan-13

Alta Bioscience code: S5871

Customer sample code: Gel Slice

#### N terminus

Residue			
1	I?	M?	
2	L?		
3	L?	H?	
4	K?		
5	---		
6	E?	F?	
7			
8			
9			
10			
11			
12			
13			
14			
15			

Comments:- Extremely weak signal, results are highly inconclusive.

#### Notes on the presentation of the data:-

? = most probable assignment. - = nothing detected at this position. X = unknown component  
Where several sequences are observed, an attempt is made to arrange them in descending order of abundance at each residue. However because of difficulties inherent in the sequencing process, this should be treated as a guide only.

Reported by \_\_\_\_\_

Date \_\_\_/\_\_\_/\_\_\_

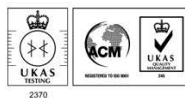
File name: S5871 M Hughson.doc

Template: Proseq15, version 4. Last modified 14<sup>th</sup> March 2012

For conditions of sale, please refer to our brochure or our website at <http://altabioscience.com/terms-and-conditions>

Figure 10.8 – Report from 1<sup>st</sup> sequencing attempt of 5 amino acid sequence results for excised ~55 kDa gel from eluted fractions of a typical AKTA run.

## 10.14.2 Sequencing attempt 2 – 10 amino acids



### Protein sequence report

Created on 18-Feb-13

Alta Bioscience code: S5886

Customer sample code: 56 kDa band

#### N terminus

Residue			
1	D		
2	T	P	
3	H	L?	
4	K	A?	
5	S		
6	E		
7	A	I	
8	A?		
9	A?		
10	R		
11			
12			
13			
14			
15			

Comments:- Extremely weak signal just readable above baseline however some results are inconclusive. Indications of a secondary component present.

#### Notes on the presentation of the data:-

? = most probable assignment. - = nothing detected at this position. X = unknown component  
Where several sequences are observed, an attempt is made to arrange them in descending order of abundance at each residue. However because of difficulties inherent in the sequencing process, this should be treated as a guide only.

Reported by \_\_\_\_\_ Date \_\_\_/\_\_\_/\_\_\_

File name: S5886 M Hughson.doc

Template: Proseq15, version 4. Last modified 14<sup>th</sup> March 2012

For conditions of sale, please refer to our brochure or our website at <http://altabioscience.com/terms-and-conditions>

Figure 10.9 – Report from 2<sup>nd</sup> sequencing attempt of 10 amino acid sequence results for excised ~55 kDa gel from eluted fractions of a typical AKTA run